UNIVERSITY OF CALIFORNIA,
IRVINE

Radiation- and Chemotherapy-Induced Cognitive Deficits: Neural-Derived Extracellular Vesicles as Translational Therapies

DISSERTATION

submitted in partial satisfaction of the requirements
for the degree of

DOCTOR OF PHILOSOPHY

in Environmental Health Sciences

University of California – Irvine

by

Sarah Mae Smith

Dissertation Committee:
Professor Charles L. Limoli, Chair
Professor Stephen C. Bondy
Professor Brian J. Cummings
Professor Peter J. Donovan
Associate Professor Masashi Kitazawa

2022

DEDICATION

For Camden, Fenway, Mara Jade, and Bobby

AND

For every patient who has struggled to receive needed healthcare

AND

For every advocate fighting so that no one will ever again have to struggle to receive needed healthcare

"At times, in medicine, you feel you are inside a colossal and impossibly complex machine whose gears will turn for you only according to their own arbitrary rhythm. The notion that human caring, the effort to do better for people, might make a difference can seem hopelessly naïve. But it isn't."
~Atul Gawande

TABLE OF CONTENTS

	Page
LIST OF FIGURES	iv
LIST OF TABLES	viii
ACKNOWLEDGEMENTS	ix
CURRICULUM VITAE	xi
ABSTRACT OF THE DISSERTATION	xvi
CHAPTER 1: INTRODUCTION AND BACKGROUND — STEM CELLS FOR THE RESOLUTION OF RADIATION INJURY TO THE BRAIN	1
CHAPTER 2: FUNCTIONAL EQUIVALENCE OF STEM CELL AND STEM CELL-DERIVED EXTRACELLULAR VESICLE TRANSPLANTATION TO REPAIR THE IRRADIATED BRAIN	11
CHAPTER 3: INITIAL RESULTS — EFFECTS OF A CLINICALLY-RELEVANT COMBINED CHEMOTHERAPY/ RADIATION PROTOCOL USING TEMOZOLOMIDE	46
CHAPTER 4: GABAERGIC EXTRACELLULAR VESICLES IMPROVE COGNITION FOLLOWING IRRADIATION, WHILE GLUTAMATERGIC EXTRACELLULAR VESICLES FAIL TO DO SO — THE NEUROBIOCHEMICAL MECHANISTIC BASIS	66
CHAPTER 5: IN A CLINICALLY-RELEVANT COMBINED CRANIAL IRRADIATION/ TEMOZOLOMIDE TREATMENT PARADIGM, GABAERGIC EXTRACELLULAR VESICLES RESTORE NEUROBEHAVIORAL FUNCTION AND NEUROTROPHIN LEVELS	96
CHAPTER 6: PROTECTIVE ADMINISTRATION OF GABAERGIC EXTRACELLULAR VESICLES BEFORE IRRADIATION PRESERVES COGNITIVE PERFORMANCE AND NEUROTROPHIC FACTOR LEVELS AFTER IRRADIATION	114
REFERENCES	130

LIST OF FIGURES

		Page
Figure 2.1	Experimental design/ graphical abstract	15
Figure 2.2	Bilateral transplantation with human neural stem cells improves cranial irradiation (IRR)-induced behavioral impairments	21
Figure 2.3	In vivo tracking of cranially grafted extracellular vesicles	23
Figure 2.4	Bilateral transplantation of human neural stem cells preserves host neuronal morphology in the dentate gyrus following irradiation	25
Figure 2.5	Unilateral transplantation of human neural stem cells (hNSCs) or hNSC-derived extracellular vesicles (EVs) protects dendritic complexity in the contralateral dentate gyrus following irradiation	27
Figure 2.6	Beneficial effects of bilateral transplantation of human neural stem cells (hNSC) on dendritic morphology in the dentate gyrus persist at four months following irradiation	29
Figure 2.7	Bilateral transplantation of human neural stem cells rescues the radiation-induced reduction in dendritic spine density in the dentate gyrus	33
Figure 2.8	Unilateral transplantation of human neural stem cell-derived extracellular vesicles modulate glial cell line-derived neurotrophic factor in the irradiated hippocampus	35
Figure 2.9	The numbers of PSD-95 puncta are increased after irradiation and were attenuated by unilateral transplantation of human neural stem cells (hNSCs) or unilateral transplantation of hNSC-derived extracellular vesicles in the contralateral hemisphere	37
Figure 2.10	Either bilateral or unilateral transplantation of human neural stem cells (hNSCs), or bilateral or unilateral transplantation of hNSC-derived extracellular vesicles ameliorates the increase in activated microglia following irradiation	41
Figure 3.1	Experimental design (athymic nude rats)	50
Figure 3.2	Spontaneous exploration data for athymic nude rats receiving a combined irradiation and temozolomide treatment paradigm, including learning and memory tasks and assays intended to assess anxiety	56
Figure 3.3	Experimental design (Fischer 344 rats)	58

LIST OF FIGURES (Continued)

		Page
Figure 3.4	Performance on spontaneous exploration tasks by Fischer rats after administration of fractionated irradiation (IRR), temozolomide (TMZ), or sham irradiation/ solvent injection (Control)	64
Figure 3.5	Percentage of time spent freezing by Fischer 344 rats receiving fractionated irradiation (IRR), intraperitoneal temozolomide (TMZ), or sham irradiation/ intraperitoneal solvent (Control) in a fear conditioning paradigm	65
Figure 4.1	Preliminary electrophysiology data in irradiated mice following the retro-orbital application of extracellular vesicles	67
Figure 4.2	Experimental design	69
Figure 4.3	Retro-orbital injection of GABAergic extracellular vesicles improves performance on the Novel Object Recognition test following fractionated irradiation	78
Figure 4.4	Performance on the Novel Place Recognition task following 26 Gy fractionated irradiation +/- retro-orbital injection of GABAergic extracellular vesicles	79
Figure 4.5	Application of GABAergic extracellular vesicles by retro-orbital injection ameliorates irradiation-induced decrements in performance on the Object in Place spontaneous exploration task	81
Figure 4.6	Fractionated irradiation (8.67 Gy x 3) reduces the number of transitions between the light and dark areas during the Light-Dark Box Test	82
Figure 4.7	Administration of glutamatergic extracellular vesicles fails to improve ability to discriminate between novelty and familiarity in Novel Object Recognition following irradiation	84
Figure 4.8	Radiation-induced decrements in performance on the Novel Place Recognition task are not mitigated by the injection of glutamatergic extracellular vesicles	85
Figure 4.9	Radiation eliminates rats' capacity to identify novelty on the Object in Place task, and this deleterious effect is not alleviated by retro-orbital injection of glutamatergic extracellular vesicles	86
Figure 4.10	Reduction in brain-derived neurotrophic factor due to fractionated irradiation improved with application of GABAergic EVs	88

LIST OF FIGURES (Continued)

Figure 4.11	Glial cell-derived neurotrophic factor (GDNF) decline due to fractionated irradiation ameliorated with application of GABAergic EVs	90
Figure 4.12	Brain-derived neurotrophic factor levels in animals receiving glutamatergic extracellular vesicles after fractionated irradiation are heightened compared to irradiated animals and similar to control levels of BDNF	92
Figure 4.13	Irradiated rats experience a significant decrease in glial cell-derived neurotrophic factor that is partially attenuated by retro-orbital injection of glutamatergic extracellular vesicles	93
Figure 4.14	Dendritic spine density in the dentate gyrus is diminished after cranial irradiation, but application of GABAergic extracellular vesicles recovers spine density	95
Figure 5.1	Experimental design	98
Figure 5.2	Fischer 344 rats display a trend towards a deficit in performance on the Novel Object Recognition task after receiving a combined TMZ+IRR treatment as compared to control animals and animals receiving GABAergic extracellular vesicles along with the TMZ+IRR, but differences are not statistically significant	106
Figure 5.3	Control two-month-old rats demonstrated superior cognitive performance on the Novel Place Recognition task relative to rats received combined temozolomide/ irradiation therapy, but those animals that also received GABAergic extracellular vesicles exhibited rescued ability to discriminate similar to that of the controls	109
Figure 5.4	Retro-orbital administration of GABAergic extracellular vesicles restored performance on an assay for anxiety-like behavior subsequent to combined temozolomide/ irradiation therapy, approximating the performance of control animals	110
Figure 5.5	Glial cell-derived neurotrophic factor in the hippocampus experiences a striking decline after the administration of a combined temozolomide/ irradiation paradigm; this drastic decrease is attenuated by the retro-orbital injections of GABAergic extracellular vesicles	112
Figure 6.1	Experimental design	117
Figure 6.2	Protective application of GABAergic extracellular vesicles by retro-orbital injection mitigates radiation-induced performance decrements on the Novel Object Recognition task	125

LIST OF FIGURES (Continued)

Figure 6.3	Pre-emptive administration of retro-orbital GABAergic extracellular vesicles prior to irradiation obliterates the inability to discriminate between novelty and familiarity on the Novel Place Recognition task	126
Figure 6.4	Reductions in brain-derived neurotrophic factor following 26 Gy fractionated irradiation are ameliorated by the protective application of GABAergic extracellular vesicles by retro-orbital injection before the doses of radiation	128
Figure 6.5	Glial cell-derived neurotrophic factor levels in the hippocampus are preserved in the irradiated brain if GABAergic extracellular treatment is applied by retro-orbital injection protectively prior to irradiation	129

LIST OF TABLES

		Page
Table 3.1	Timeline of treatments for athymic nude rats	53
Table 3.2	Timeline of treatments for TMZ and IRR cohorts of Fischer 344 rats	61
Table 4.1	Timeline of treatments for irradiation +/- GABAergic or glutamatergic extracellular vesicles	72
Table 5.1	Timeline of treatments for combined irradiation/ temozolomide paradigm to probe the impact of GABAergic extracellular vesicles	101
Table 6.1	Timeline of treatment for protective application of GABAergic extracellular vesicles prior to irradiation	120

ACKNOWLEDGEMENTS

I am deeply indebted to my advisor, Dr. Charles Limoli for his guidance, mentorship, encouragement, and patience. Dr. Limoli's dedication to his lab, to the pursuit of sound research, and to my development has been an inspiration which has helped me grow as a scientist. In addition, the Limoli lab team was instrumental in educating me and guiding me through my various studies and publication. I would like to thank Dr. Munjal Acharya, Dr. Vipan Parihar, Dr. Janet Baulch, Dr. Ron Leavitt, Dr. Nicole Chmielewski-Stivers, Dr. Deblina Dey, Ning Ru, Barrett Allen, Maria Angulo, Janelle Doyle, Al Anoud Daoud Baddour, Kashvi Ranjan, Amber Syage, Robert Krattli, Lauren Apodaca, Liping Yu, and especially Erich Giedzinski for their advice, guidance, and friendship.

Thank you to my dissertation committee, Dr. Stephen C. Bondy, Dr. Brian J. Cummings, Dr. Peter J. Donovan, and Dr. Masashi Kitazawa for your patience and your astute scientific inquiries, which vastly improved the studies enumerated in this dissertation.

I am grateful for the support from the UCI Medical Scientist Training Program which has funded my research time throughout the years and our program director Dr. Al Goldin, who is a tenacious advocate for his students. I am also thankful for Dr. Ulrike Luderer and Dr. Robert Edwards, my advisors throughout my tenure in the MSTP. My work would not have been possible without the support from T32 NS082174 (NIH Training Program in Stem Cell Translational Medicine for Neurological Disorders) and T32 GM008620 (NIGMS UCI Medical Scientist Training Program). Thank you also to Dr. Donovan and Dr. Leslie Thompson, who administered the T32 NS082174 training grant and its many fortifying activities.

I also thank Springer Nature for permission to include Chapter One of my dissertation, which was originally published in *Current Stem Cell Reports*, as well as AlphaMed Press and Wiley to include Chapter Two of my dissertation, which was originally published in *Stem Cells Translational Medicine*.

I am greatly appreciative of my colleagues and classmates in the Medical Scientist Training Program and the Environmental Health Sciences Ph.D. program, from whom I have learned immensely and who have helped propel each other to success throughout our lengthy degrees.

Lastly, I would like to thank my family and friends who have supported me through the years as I put the copious time and effort into my studies and research. I am profoundly beholden to the medical students and physicians I have met and befriended through my advocacy work, many of whom have been my collaborators and co-conspirators in some of the most important patient-focused initiatives I have undertaken. I thank Dr. Zarah Iqbal, Dr. Beth Griffiths, and Dr. Nuriel Moghavem for their insightful wisdom, their courageousness in speaking truth to power, and their sincere and deeply-held commitment to doing right by their patients, all of which I hope to emulate as a future physician. I thank Dr. Pooja Desai and Dr. Trishna Narula for being among my first friends in organized medicine, learning to navigate the advocacy landscape with me and always being there for me to this day when I need you. I am forever grateful to Dr. Hari Iyer for his indefatigable activism, his insatiable thirst for policy knowledge and willingness to teach me about what he has learned, and his sense of humor without which I would not have gotten through a strenuous year on the American Medical Association Board of Trustees. Thank you to Dr. Rachel

Ekaireb for her undaunted determination to enact patient-first policy in the face of any number of challenges, her bold candor, and her kindness. Finally, I am tremendously indebted to Dr. Helene Nepomuceno for her vision and poise, her profound compassion, and her consistent reminder that one need not be the loudest voice in the room to be the most impactful.

Thank you to my parents, Dr. James Smith, Jr., DVM and Cheryl Smith who have always been there for me when I need them. My father is one of my earliest heroes and first encouraged my foray into science and medicine as I followed him around his veterinary hospital at his heel and peppered him with questions about everything I observed. He is a model of selfless service to his patients, be they feline, canine, or otherwise. My mother has forever been my advocate and relentlessly pushes me to succeed.

Thank you to my siblings, Hannah Smith and Justin Smith, especially for being kind enough to come out to California to support me following my surgery over the past month- I don't know what I would have done without you for the past several weeks, and I'm grateful that the experience brought us closer despite the trying circumstances.

Thank you to Nana Senecal, who has been my closest confidant, my most vehement defender, and my most enthusiastic cheerleader for as long as I can remember- I am so thrilled you will be sharing this achievement with me.

A million thank yous to my partner, Dr. Christopher Libby, who has endured SO much to support me in following my dreams and who never allows me to give up.

And thank you to my writing companions Camden, Fenway, Mara Jade, and Bobby, who have kept me sane and muted my anxiety and self-doubt over the years. There is nothing better than a furry face to restore my faith in my ability to persist.

CURRICULUM VITAE – SARAH MAE SMITH

Unit 3060, 1801 East Katella Avenue • Anaheim, California 92805 • ssmith2@hs.uci.edu

EDUCATION

University of California, Irvine School of Medicine Entered August 2013
MD/ PhD Student, Medical Scientist Training Program

- Letters of Commendation in Clinical Foundations I, Genetics, and Immunology
- Electives: Examine the Painting, Examine the Patient; Global Health; Health Policy; Medical Spanish; Patient Stories, Doctor Stories; Social Medicine; Ultrasound

Johns Hopkins University, Baltimore, Maryland May 2012
Bachelor of Arts in Neuroscience (Minor in Spanish for the Professions)
Graduated with General Honors and Departmental Honors in Neuroscience

RESEARCH EXPERIENCE

PhD Dissertation Work, Laboratory of Dr. Charles Limoli March 2016 to Present
University of California, Irvine, Department of Radiation Oncology

- Exploring the cognitive effects of temozolomide, an alkylating chemotherapeutic agent, and fractionated irradiation
- Investigating the therapeutic effects of different cell types, including embryonic stem cells and induced pluripotent stem cells, and their associated exosomes on combined irradiation/chemotherapy-induced cognitive dysfunction

PhD Rotation in the Laboratory of Dr. Robert Hunt January 2016 to March 2016
University of California, Irvine, Department of Anatomy and Neurobiology

- Examined the role of CHD2, a chromatin remodeler, in epileptic encephalopathies by characterizing its expression in the brain during development and the anatomy of cells in the brain in CHD2 knockout

PhD Rotation in the Laboratory of Dr. Charles Limoli September 2015 to December 2015
University of California, Irvine, Department of Radiation Oncology

- Investigated stem cell therapies for radiation-included cognitive dysfunction

PhD Rotation in the Laboratory of Dr. Yongsheng Shi June 2014 to August 2014
University of California, Irvine, Department of Microbiology and Molecular Genetics

- Studied post-transcriptional gene regulation in stem cells and cancer, specifically the interaction between CstF50, a polyadenylation factor, and p53, the most commonly mutated tumor suppressor in cancer, using techniques such as cell culture, protein gel electrophoresis, Western blotting, and immunopurification

Laboratory of Dr. Xiaoqin Wang January 2010 to May 2013
Johns Hopkins University, Department of Biomedical Engineering

- Investigated vocal-auditory interactions in marmoset monkeys using behavioral experiments and computational analysis

Laboratory of Dr. Paul Worley October 2009 to April 2012
Johns Hopkins University, Department of Neuroscience

- Examined the role of immediate early genes in learning and memory in mouse models

PUBLICATIONS

Smith SM, Giedzinski E, Angulo MC, Lui T, Lu C, Park AL, Tang S, Martirosian V, Ru N, Chmielewski NN, Liang Y, Baulch JE, Acharya MM, Limoli CL. Functional Equivalence of Stem Cell and Stem Cell-Derived Extracellular Vesicle Transplantation to Repair the Irradiated Brain. *Stem Cells Translational Medicine*. 2020 Jan;9(1):93-105. doi: 10.1002/sctm.18-0227. Epub 2019 Sep 30. PMID: 31568685; PMCID: PMC6954724.

Smith SM, Limoli CL. Stem Cell Therapies for the Resolution of Radiation Injury to the Brain. *Current Stem Cell Reports*. 2017 Dec;3(4):342-347. doi: 10.1007/s40778-017-0105-5. Epub 2017 Oct 11. PMID: 29423356; PMCID: PMC5798632.

Parihar VK, Syage A, Flores L, Lilagan A, Allen BD, Angulo MC, Song J, Smith SM, Arechavala RJ, Giedzinski E, Limoli CL. The Cannabinoid Receptor 1 Reverse Agonist AM251 Ameliorates Radiation-Induced Cognitive Decrements. *Frontiers in Cellular Neuroscience*. 2021 Jun 28;15:668286. doi: 10.3389/fncel.2021.668286. PMID: 34262437; PMCID: PMC8273551.

HEALTHCARE POLICY

California Medical Association Board of Trustees January 2021 to Present
Healthy California for All Technical Advisory Committee March 2020 to Present

- Represents almost 3,000 medical student members on the executive body of the largest state medical society to manage the activities and affairs of the association
- Oversees policy development, legislative positioning and prioritization, distribution of finances, membership initiatives, and governance reform

American Medical Association Board of Trustees June 2019 to June 2020

- Represented 50,000 medical student members on the executive body of the largest physician organization in the nation in executing advocacy and implementing the policy created by the House of Delegates
- Determined resource allocation, established major legislative and regulatory strategy, performed governance duties, and undertook high-level strategic vision planning for the association

American Medical Association Council on Medical Service June 2017 to June 2019
Chair, Committee on Health System Reform June 2018 to June 2019

- Studied and evaluated the social and economic aspects of medical care and recommends policies on these issues to the AMA House of Delegates related to the socioeconomic factors that influence the practice of medicine
- As Chair of the Committee on Health System Reform, facilitated the Committee's discussions of its reports and presents the Committee's recommendations to the Council
- Served as one of three liaisons to the AMA's Council on Science and Public Health throughout the preparation of the Councils' joint report on aligning clinical and financial incentives for high-value care for the Interim 2018 House of Delegates

California Medical Association Council on Medical Services October 2016 to December 2020

- Studied and makes recommendations concerning medical service financing and delivery, cost and quality reporting, insurance and reimbursement, managed care, health information technology, and practice management issues
- Student member of the Council that serves as a reference committee for the CMA House of Delegates on related issues

American Medical Association Medical Student Section Delegate June 2016 to June 2017

- Represented the Medical Student Section in the AMA House of Delegates and chaired the MSS Caucus, leading a team of 54 regional delegates and alternate delegates and several state student delegates

- Transmitted resolutions authored by the Medical Student Section to the House of Delegates, responsible for overseeing the crafting and delivery of testimony in support of the MSS's position on all items of business
- Administered the MSS resolution review process and mentored student resolution authors

CALPAC Board of Directors March 2018 to October 2018; January 2015 to December 2015

- Elected to represent medical students on the Board of Directors of the California Medical Association's political action committee
- Participated in interviewing gubernatorial candidates for the 2016 election, culminating in the California Medical Association's endorsement of Gavin Newsom

AMA Medical Student Section House of Delegates Coordinating Committee Chair, July 2015 to June 2016; **Member**, July 2014 to June 2016

- Acted a policy analyst for the Medical Student Section in determining a well-informed position for the section on AMA House of Delegates resolutions based on MSS policy
- Coordinated the medical student section testimony in the AMA House of Delegates as the head of a reference committee team addressing medical practice, service, and insurance (Reference Committee J) at the 2014 AMA HOD Interim Meeting; headed the reference committee team for public health (Reference Committee D) at the 2015 AMA HOD Annual Meeting

AMA Medical Student Section Region 1 Chair June 2015 to June 2016

- Oversaw the AMA medical student sections of fifteen states, maintaining communication and collaboration among the constituent students and with other regions, and representing the region to the MSS Governing Council

Region 1 Delegate to the AMA House of Delegates January 2016 to June 2016

Region 1 Alternate Delegate to the AMA House of Delegates January 2015 to December 2015

- Elected by medical student representatives from across a region comprised of fifteen states to represent the interests of medical students in the AMA House of Delegates (HOD), participating in the policy-making process and impacting the issues upon which the AMA advocates

California Medical Association Council on Ethical, Legal, and Judicial Affairs, October 2015 to October 2016

- Responsible for studying and making recommendations concerning evolving social and philosophical trends and issues that are of immediate or long-term concern to the medical profession, with emphasis on medical ethics, bio-ethics and attendant areas for the California Medical Association

California Medical Association Reference Committee E (Quality, Ethics, and Medical Practice Issues) Member, October to December 2014

- First medical student in five years to serve on a CMA reference committee
- Deliberated with a team of physicians to offer recommendations on resolutions submitted to the CMA House of Delegates 2014 meeting pertaining to quality, ethics, and medical practice issues, considering online and in-person testimony by physicians and medical students as well as background research

AMA Medical Student Section Reference Committee Member AMA-MSS Annual 2015

- Worked as part of a team to develop recommendations on resolutions submitted to the AMA-MSS assembly for Annual 2015 based on online peer testimony and background research

AMA-MSS Region 1 Secretary June 2014 to June 2015

- Served as Region 1's Secretary, coordinating communication and organization among the region's delegations while also working on projects with the Region 1 Governing Council
- Instituted regional resolution committees to review resolutions considered at the MSS assembly at Annual 2015, to enable the region to have a well-informed position on each resolution

AMA-MSS Region 1 Meeting Co-Chair February 6th to 8th, 2015

- Planned a meeting attended by over eighty medical students from five states centered around "Engagement in the Changing Landscape of Healthcare Policy"

California Medical Association Council on Legislation February 2014 to December 2014

- Served as the medical student on the California Medical Association Council on Legislation, including an in-person meeting in March 2014 to set the organization's legislative agenda for the year, providing the students' perspective on the bills reviewed by the assembly

UC Irvine Delegate to American Medical Association- Medical Student Section and California Medical Association, October 2013 to January 2015

- Responsible for official representation of UC Irvine to the Orange County Medical Association, California Medical Association, and American Medical Association
- Attended CMA Legislative Advocacy Day in 2014 and 2015; met with California state legislators to advocate for increased graduate medical education funding, removal of the personal belief exemption for vaccination, and increased Medi-Cal reimbursements
- Lobbied at the California Democratic Party Convention in March 2014 under the auspices of the CMA to advocate against an anti-MICRA ballot measure that would increase healthcare costs and decrease access to care; returned to the CDP Convention in April 2015 to advocate for removal the personal belief exemption for vaccination

COMMUNITY SERVICE, LEADERSHIP, AND ACTIVITIES

UC Irvine Medical Initiative Against Homelessness August 2013 to June 2016

President, January 2014 to June 2015

- Actively involved in the Recuperative Care and Health Education Outreach programs, offering healthcare for members of the homeless community in Orange County and promoting healthy practices through education for homeless individuals

UC Irvine School of Medicine Oncology Interest Group September 2013 to Present

President, February 2014 to June 2015; Continuing Participant

- Planned and coordinated numerous talks for medical students from physicians spanning the field of oncology, including a pediatric oncologist, a panel of oncology fellows and residents in various specialties, and a professor of medicine who was a cancer patient

UC Irvine School of Medicine Neurosurgery Interest Group March 2014 to Present

Vice-President, March 2014 to June 2015; Continuing Participant

- Created a new interest group at UC Irvine to support medical students interested in pursuing careers in neurosurgery
- Coordinated the first annual Conference on Neurosurgical Anatomy on May 23, 2014 to expose students to neuroanatomy relevant to neurosurgical procedures and the neurosurgical field

UC Irvine School of Medicine Flying Samaritans August 2013 to Present

Trip Coordinator, December 2013 to December 2014; Continuing Volunteer

- Organized a group of medical students and Orange County physicians to travel to Valle Redondo, Mexico each month to provide free treatment to the surrounding community with an emphasis on lifestyle changes and counseling
- Participated in the healthcare delivery by taking vital signs, collecting patient histories, and presenting to the attending physicians

UC Irvine School of Medicine Academic Medicine Interest Group
Journal Club Moderator February 2014 to February 2015

- Moderator of monthly presentations and discussions of academic medical literature, hosted by a new interest group

UC Irvine Outreach Clinic September 2013 to Present
Director of Referrals and Community Relations, December 2013 to January 2015; Continuing Volunteer

- Acted as the liaison and works to establish strong relationships with community organizations and medical specialists to provide free comprehensive healthcare to the underserved and uninsured population of Orange County at the Lestonnac Clinic

International Emory Global Health Case Competition Member January 2014 to March 2014

- Chosen to represent UC Irvine at this international competition as one of two medical student members of the six-person team
- Developed a viable solution (the institution of a Civil Society Advisory Board) in response to a case prompt asking participants to re-imagine the World Health Organization

ABSTRACT OF THE DISSERTATION

Radiation- and Chemotherapy-Induced Cognitive Deficits: Neural-Derived Extracellular Vesicles as Translational Therapies

by

Sarah Mae Smith

Doctor of Philosophy in Environmental Health Sciences

University of California, Irvine, 2022

Professor Charles L. Limoli, Chair

Approximately 24,000 patients are diagnosed with brain tumors each year, which represents an estimated 166,000 people living with brain cancer as of 2015. Radiotherapy constitutes one of the principle therapies for primary and metastatic brain tumors along with chemotherapy and surgery, with roughly 200,000 patients receiving brain radiation treatment each year in the United States. One of the most common and most damaging iatrogenic effects of cancer treatment is cognitive dysfunction, including impairments in working memory, learning ability, executive function, and attention. The deleterious effects of cranial ionizing radiation exposure are exacerbated by concomitant use of chemotherapeutic agents that elevate neurotoxicity. While the mechanisms underlying radiation-induced cognitive dysfunction have not yet been elucidated, much of the underlying pathology believed to be contributory is related to decreased hippocampal neurogenesis, increased neuroinflammation, microvascular injury and alterations in neuronal structure that disrupts dendritic morphology, spine density and synaptic proteins. Stem cell-based transplantation strategies have also shown considerable promise in ameliorating the negative effects of cranial irradiation.

My initial work in the Limoli lab sought to examine the impact of bilateral and unilateral hemisphere transplantations of human neural stem cell (hNSC) and hNSC-derived extracellular

vesicles on the structural integrity of hippocampal neurons in the irradiated rodent brain, in order to ascertain the extent and range of the beneficial effects of cell-based therapies as a function of distance from the transplant site (which has important therapeutic implications for dosing and administration). We found that stem cell transplantation decreases the number of activated microglia at one month post-irradiation, signifying a reduction in neuroinflammation. In addition, grafted stem cells preserved host neuronal structure one month and four months after irradiation. Stem cell transplantation also allayed the increased expression of the major synaptic scaffolding protein PSD-95 caused by irradiation. Further, as clinical utility of stem cell transplantation strategies to offset normal tissue damage caused by irradiation may be limited by the downstream potential for teratoma formation and immune rejection, we also attempted to circumvent such caveats by evaluating the promise of using transplanted human neural stem cell-derived extracellular vesicles in place of stem cells. We showed that unilateral transplantation of both stem cells and extracellular vesicles 48 hours post-irradiation signals for the renormalization of synaptic proteins such as PSD-95 in the contralateral hippocampus, and found that unilateral transplantation has the same protective effects on neuroinflammation, dendritic morphology, and spine density as bilateral transplantation.

My later studies evaluate the impact of GABAergic neuron-derived extracellular vesicles on irradiation- and chemotherapy-associated neurocognitive deficits associated with clinically-relevant treatments, including fractionated radiation and the chemotherapeutic agent temozolomide (TMZ). We first examined whether retro-orbital injection of extracellular vesicles (EV) derived from GABAergic neurons can alleviate radiation-associated deficits in cognition at one month following treatment. GABAergic neuron-derived EVs are proposed to improve cognition after cancer therapy through providing an inhibitory impetus to compensate for irradiation- and chemotherapy-induced hippocampal hyperexcitation, as is apparent in

preliminary electrophysiology studies in irradiated animals. Our behavioral data suggests that fractionated irradiation has deleterious neurological effects as determined by performance on hippocampus-, prefrontal cortex- and amygdala-dependent behavioral tasks, and that retro-orbital injection of GABAergic EVs attenuates some of these effects and rescues cognition. Intriguingly, these benefits were not replicated with the application of glutamatergic neuron-derived EVs, which did not reverse the observed decrements in cognitive function after irradiation. In exploring the neurobiochemical basis for this rescue in cognition on neuronal morphology, synaptic integrity, and neurotrophic factors, we found that dendritic spine density in the dentate gyrus of the hippocampus is significantly reduced following irradiation, but statistically similar to controls following the application of retro-orbital GABAergic EVs. We also determined that irradiation reduced levels of neurotrophins in the hippocampus, but retro-orbital injections of GABAergic EVs ameliorated this decrease.

We built upon these studies by next exploring whether retro-orbital injection of GABAergic neuron-derived EVs can ameliorate the adverse effects associated with a systemic insult to the brain, intraperitoneal injections of the chemotherapeutic agent temozolomide (TMZ), in the context of a clinically-relevant treatment protocol also including fractionated radiation. Temozolomide is an alkylating agent that crosses the blood-brain barrier and is used primarily to treat glioblastoma. Again, several of the behavioral tasks show neurocognitive decrements following the TMZ+IRR protocol, which were improved with the GABAergic EV injections. Likewise, tissue from the hippocampi of these animals was analyzed for neurotrophic factor levels, which revealed that glial cell-derived neurotrophic factor was reduced after irradiation but improved in the GABAergic EV cohort.

Finally, we have been evaluating the optimal timecourse for delivery of GABAergic neuron-derived EVs being employed to rescue cognitive decrements associated with irradiation

by examining whether retro-orbitally injecting GABAergic neuron-derived EVs the week before the first fractionated radiation dose could result in a preemptive protective effect. We have identified that the protective paradigm of GABAergic EV application mitigates radiation-induced cognitive injury and enhances the quantity of neurotrophins in the hippocampus relative to irradiated animals.

CHAPTER ONE: INTRODUCTION AND BACKGROUND — STEM CELLS FOR THE RESOLUTION OF RADIATION INJURY TO THE BRAIN

Adapted From: Smith SM, Limoli CL. Stem Cell Therapies for the Resolution of Radiation Injury to the Brain. Current Stem Cell Reports. 2017 Dec;3(4):342-347. doi: 10.1007/s40778-017-0105-5. Epub 2017 Oct 11. PMID: 29423356; PMCID: PMC5798632.

Abstract

Transplantation of human stem cells in the irradiated brain was first shown to resolve radiation-induced cognitive dysfunction in a landmark paper by Acharya et al., appearing in PNAS in 2009. Since that time, work from the same laboratory as well as other groups have reported on the beneficial (as well as detrimental) effects of stem cell grafting after cranial radiation exposure. Improved learning and memory found many months after engraftment has since been associated with a preservation of host neuronal morphology, a suppression of neuroinflammation, improved myelination and increased cerebral blood flow. Interestingly, many (if not all) of these beneficial effects can be demonstrated by substituting stem cells with extracellular vesicles derived from human stem cells during transplantation, thereby eliminating many of the more long-standing concerns related to immunorejection and teratoma formation. Stem cell and extracellular vesicle transplantation into the irradiated brain of rodents has uncovered some unexpected benefits that hold promise for ameliorating many of adverse neurocognitive complications associated with major cancer treatments. Properly developed, such approaches may provide much needed clinical recourse to millions of cancer survivors suffering from the unintended side effects of their cancer therapies.

Introduction

Approximately 24,000 patients are diagnosed with brain tumors each year, which represents an estimated 166,000 people living with brain cancer as of 2015 [1]. Radiotherapy comprises one of the principle therapies for primary and metastatic brain tumors in addition to chemotherapy and surgery, with approximately 200,000 patients receiving brain radiation treatment each year in the United States [2]. These treatments have become increasingly effective in improving the prognosis for patients afflicted with central nervous system (CNS) cancers. As progress has been made in the early detection and treatment of cancer, survival rates have increased, with the five-year survival rate rising from 23.0% in 1975 to 33.2% in 2014 [1, 3], adding to the importance of preserving the quality of life for cancer survivors. One of the most common and most damaging iatrogenic effects of cancer treatment is cognitive dysfunction, including impairments in working memory, learning ability, executive function, and attention, with the neurocognitive sequelae typically manifesting many months to years following the cessation of treatment [4–8]. Each year, roughly 100,000 patients with brain tumors survive for at least six months, which is sufficient time for the development of radiation-induced cognitive decrements, which afflict between 50% and 90% of adults who survive at least that long with some degree of impairment [9, 10].

The deleterious effects of cranial ionizing radiation exposure are progressive, particularly in pediatric populations, and are exacerbated with increasing dose, volume of irradiated brain, and by concomitant use of chemotherapeutic agents that elevate neurotoxicity. While the precise mechanisms underlying radiation-induced cognitive dysfunction remain to be elucidated, much of the underlying pathology believed to be contributory if not causal is related to decreased hippocampal neurogenesis, increased neuroinflammation (activated microglia and pro-inflammatory cytokines), microvascular injury, and alterations in neuronal structure that disrupts

dendritic morphology, spine density and synaptic proteins [2, 9–12]. Increased oxidative stress likely plays a critical role, by perpetuating cycles of inflammation and damage that prolong the signature of radiation injury in the brain [13–15]. Pharmacologic therapies currently under investigation to either prevent or restore neurocognitive functionality after radiation treatment are limited, and include anti-inflammatory agents such as peroxisomal proliferator-activated receptor agonists, renin-angiotensin system blockers such as angiotensin-converting enzyme inhibitors and angiotensin II type 1 receptor blockers, and inhibitors of adenosine kinase [9, 16]. Stem cell-based transplantation strategies have also shown considerable promise in ameliorating the negative effects of cranial irradiation. Given the prominent role that cognitive health plays in the quality of life for survivors of brain tumors [17], continued exploration and refinement of stem cell therapies to treat radiation-induced cognitive decrements could have a profound effect on the lives of thousands of cancer patients, particularly those surviving childhood malignancies.

Stem Cells and Regenerative Medicine

Stem cell-based interventions have been investigated to repair and regenerate radiation-associated injuries outside of the brain as well [18]. Radiation-induced lung injury, such as pneumonitis and fibrosis, is a critical complication of radiotherapy for thoracic cancers [19, 20]; caudal vein injections of mesenchymal stem cells abated early lung damage, oxidative stress, and radiation-associated increases in proinflammatory and profibrotic cytokine plasma concentrations in mice that underwent thoracic irradiation, increasing survival while attenuating lung fibrosis [21, 22]. Salivary gland damage as a result of irradiation to treat head and neck cancer can result in chronic xerostomia [23]. Cells isolated from murine submandibular glands and cultured into salispheres have yielded cells expressing stem cell markers such as c-Kit [24]. Transplantation of these stem cell preparations into irradiated salivary glands of mice has been shown to recapitulate the morphology of unirradiated glands and dramatically increase saliva production

[23-26]. External radiotherapy frequently results in cutaneous radiation reactions (with up to 95% of those treated with irradiation showing some adverse effect) [27]. Human mesenchymal stem cell (MSC) transplantation has been shown to moderate the severity of radiation dermatitis and hasten the healing process in an immunodeficient NOD/SCID mouse model [28], and injection of adipose tissue-derived stromal cells facilitated wound healing, re-epithelization, and angiogenesis in murine models following irradiation [29, 30]. Injections of CD34+ hematopoietic stem cells (HSC) decreased liver degeneration and necrosis and improved liver function following abdominal irradiation in immunodeficient mice, with the transplanted stem cells migrating to the liver and differentiating into hepatocytes [31]. Finally, bone marrow-derived stromal and MSC transplantations have demonstrated beneficial effects in alleviating the negative response of gastrointestinal tissue to irradiation, promoting structural recovery, decreasing radiation-induced apoptosis, and increasing survival in murine models [32–37]. Further, cognitive dysfunction associated with other cancer therapies, such as chemotherapy, is ameliorated with stem cell transplantation, as shown in studies of cyclophosphamide- and adriamycin-induced chemobrain [38, 39]. Additionally, stem cell-based approaches have been used successfully in animal models to ameliorate neurodegenerative conditions such as Alzheimer's disease [40, 41], epilepsy [42-44], and traumatic brain injury [45]. Encouraging results in the utilization of stem cell-based therapies to address radiation injury in other organ systems and the application of stem cells to restore cognition after treatment with chemotherapeutic agents portends the therapeutic potential of stem cells for mitigating radiation-induced cognitive dysfunction.

Stem Cells in the Irradiated Central Nervous System

Acharya *et al*. were the first to demonstrate the potential therapeutic value of transplanting stem cells into the irradiated brain in 2009 [46]. Intrahippocampal transplantation of human embryonic stem cells (hESCs) into cranially irradiated athymic nude rats improved cognitive function on a

hippocampal-dependent task. In that work, transplanted cells were found to migrate throughout the hippocampus, differentiating into neurons (concentrated in the dentate subgranular zone) and astrocytes [46]. A later study by the same group showed that human neural stem cell (hNSC) grafting into the hippocampus also ameliorated radiation-induced cognitive dysfunction as evidenced by performance on the same task at both one month and four months post-surgery [47]. These cells were also shown to migrate throughout the hippocampus, with 23% and 12% of the transplanted cells surviving one and four months after grafting, respectively, while differentiating into neuronal (chiefly in the dentate subgranular zone and CA1) and astroglial lineages (most evident in the corpus callosum) lineages. Intriguingly, upon exploration of novelty, a fraction (11%) of the transplanted cells were also found to co-express the mature neuronal marker NeuN and the activity-regulated cytoskeleton-associated protein (Arc), a behaviorally-induced immediate early gene, one month following irradiation [47]. Since expression of Arc has been used to map the activity of neuronal circuits [48, 49], these data suggested that transplanted cells were functionally integrated into host hippocampal circuitry [47]. Follow-up studies comparing the outcomes of transplanted hESCs to hNSCs in cranially irradiated animals confirmed that engrafting of both cells types rescued cognitive function at one month and four months post-surgery [50]. While survival of the hESCs was higher (35% at one month post-transplantation, 17% at four months) relative to the hNSCs, hNSCs showed preferential neuronal differentiation compared to the hESCs [50]. Moreover, at eight months post-transplantation, hNSCs conferred improvement in cognition while hESCs failed to do so [51]. At eight months following the transplantation of hNSCs, only 4.5% of the engrafted cells survived, but the number of activated microglia were reduced significantly in the transplanted animals relative to animals that had been irradiated and received sham surgery [52]. Interestingly, and again following the recent exploration of novelty, behaviorally-induced Arc expression was rescued in host neurons located in the CA1 and dentate gyrus of the hippocampus [52]. As opposed to the earlier

expression of Arc in transplanted cells, these latter findings pointed to a trophic support mechanism whereby engrafted cells enhanced the functional plasticity of host neuronal circuits [52]. Furthermore, intrahippocampal transplantation of FDA-approved human fetal-derived neural stem cells into irradiated rats also improved behavioral performance on hippocampal-dependent tasks of spatial memory and contextual fear conditioning, with migration of grafted cells throughout the CA1 and CA3 subfields and preferential differentiation to neuronal fates [53].

In addition, the Limoli laboratory has examined the optimal window for stem cell transplantation into the hippocampus following irradiation [54]. As opposed to prior work targeting a 2-day post-irradiation transplantation time, this study found that stem cell grafting four weeks after irradiation yielded more improvement in cognitive function than earlier transplantation times [54]. Protracting the transplantation time also revealed that stem cells were distributed along the septotemporal axis of the hippocampus, with favored differentiation into neuronal fates, and significantly decreased microglial activation throughout all hippocampal subfields, indicating that radiation-induced neuroinflammation was reduced [54]. The clinical utility of stem cell transplantation strategies to offset normal tissue damage caused by irradiation may be limited by the downstream potential for teratoma formation and immune rejection. To circumvent such caveats, work by Baulch et al. demonstrated the promise of using transplanted human neural stem cell-derived extracellular vesicles, in place of stem cells [55]. Intrahippocampal grafting of extracellular vesicles ameliorated the cognitive decrements associated with cranial radiation exposure, decreased neuroinflammation, and preserved dendritic morphology in rats. The transplanted extracellular vesicles were found to migrate throughout the hippocampus and fuse with host brain cells, as determined by tracking a fluorescent marker protein expressed on the surface of the grafted extracellular vesicles [55]. The foregoing data provided some provocative

insight into the mechanisms of cognitive improvement following irradiation, and suggested that the bioactive cargo within extracellular vesicles conferred neurotrophic support to the host brain. Past work has shown similar strategies to be effective in promoting recovery of the CNS after stroke and traumatic brain injury as well [56-59], likely mechanistically due to delivery of critical neuromodulatory extracellular vesicle cargo to the injured regions of the brain [60].

Other studies have also employed the approach of implementing stem cell transplantation for the amelioration of radiation-induced cognitive dysfunction. Early experiments showed that oligodendrocyte progenitor CD4+ cells transplanted into the spinal cord by laminectomy following irradiation migrated throughout the spinal cord without differentiating, contributing to the remyelination of demyelinated areas [61, 62]. Irradiation was found to enhance the subsequent survival of transplanted oligodendrocyte progenitor cells, likely due to radiation-induced depletion of the endogenous oligodendrocyte progenitor population, providing the transplanted cells the opportunity to enter a previously-occupied "niche" [61, 62]. In fact, survival of transplanted CD4 cells was limited in the non-irradiated spinal cord. Evidence for the enhanced survival of stem cells transplanted into the CNS following radiation was bolstered by studies from Niranjan et al. [63] and Marshall et al. [64], which noted the increased survived of neural stem cells transplanted into the brain and multipotent astrocytic stem cells transplanted into the lateral ventricle, respectively. Intramedullary transplantation of neural stem cells three months after local irradiation of the spinal cord were found to significantly ameliorate indications of myelopathy in a rat model [65]. However, it was thought that transplantation of oligodendrocyte progenitor cells had limited clinical utility because the radiation dose needed to deplete endogenous oligodendrocyte progenitor cells to the requisite level to allow for significant survival of the transplanted cells was high enough to approach the ED50 (~20 Gy) for radiation necrosis [66].

More recently, Piao et al. demonstrated that the transplantation of human embryonic stem cell-derived oligodendrocyte progenitors into the corpus callosum of irradiated animals improved performance on behavior tasks that interrogated learning and memory capabilities [67]. The transplanted animals exhibited restoration of the glial cell population and remyelination of axons [67]. Likewise, transplantation of oligodendrocyte progenitors into the cerebellum improved motor balance and coordination, and induced remyelination within the cerebellum [67]. Work by Joo et al. showed that mouse fetal neural stem cells administered through the caudal vein in an irradiated mouse model migrated to the brain, exhibited multipotent differentiation, and improved short-term spatial memory as measured by the Morris water maze [68]. The stem cell injections also protected structural aspects of the brain from radiation damage, maintaining the depth of the granular layer of the dendate gyrus of the hippocampus and the cerebral cortex [68]. This study also found that nerve growth factor was elevated in the brains of mice receiving stem cell injections, indicating a protective neurotrophic effect, while the fate of other transplanted cells were found to trans-differentiate into endothelial cells, exhibiting a reparative effect on cerebral blood flow [68]. In work by Belkind-Gerson et al., enteric neuronal stem and progenitor cells administered systemically through the caudal vein were also shown to home to the irradiated brain and differentiate into neurons, particularly in germinal zones such as the subependymal layer of the ventricular zone and the dentate gyrus, and in white matter tracts [69]. However, Osman et al., indicated that intrahippocampal transplantation of autologous enteric neural stem/progenitor cells in young irradiated mice actually had a deleterious effect on learning [70]. Grafted mice exhibited increased neuroinflammation and deterioration of the granular cell layer of the dentate gyrus, while grafted cells showed limited survival and differentiation [70]. Similarly, neural stem and progenitor cells derived from mouse brains and grafted into the hippocampus of irradiated mice also caused deterioration of the granular cell

layer and astrogliosis [71], revealing further potential limitations of the utility of stem cell-based therapy for resolving the adverse effects of radiation on the brain.

Conclusions

The promise of regenerative medicine continues to move forward, bolstered by a wealth of data pointing to the capability of such interventional strategies to hasten the recovery of injured tissues throughout the body [18]. For survivors of cancer, radio- and chemotherapy treatments have long been associated with adverse neurocognitive complications, unwanted side effects that diminish quality of life with relatively little clinical recourse. Cranial and/or systemic transplantation of neural and related stem and progenitor cells has now been shown to provide a host of neurological benefits that include improved learning and memory and motor control, reduced inflammation, preservation of host neuronal morphometry, increased myelination, protection of the microvascular bed, and increased cerebral blood flow. At early times post-transplantation (≤3–4 months) many of the beneficial effects may be due in part to functional integration of grafted cells into host neuronal circuitry. At latter times (>4 months) the majority of these benefits are most certainly derived from a variety of trophic support mechanisms that act to protect and restore CNS functionality. Despite these exciting developments, stem cell therapies will not be suitable for everyone afflicted with a declining cognitive reserve. Patients will need to be stratified and assessed on an individual basis for various risk factors that will depend greatly on disease status and prognosis, and other social and career variables that inform proper medical decision-making. Immunorejection and teratoma formation remain genuine risks to most transplantation procedures, and while technology has minimized many (but not all) of these potential problems, graft survival seldomly approaches the projected life span of many cancer survivors. Nonetheless, for those suffering from debilitating cognitive impairment, unable to maintain routine duties or unable to conduct prior job duties to acceptable levels, stem cell therapy may one day provide much

sought-after relief. For the here and now however, stem cell research must continue to elucidate further the mechanism of action, the duration of action, and the optimal routes of administration and cellular dosing to provide bona-fide therapeutic efficacy and to deliver useful targeted approaches to personalized medicine.

CHAPTER 2: FUNCTIONAL EQUIVALENCE OF STEM CELL AND STEM CELL-DERIVED EXTRACELLULAR VESICLE TRANSPLANTATION TO REPAIR THE IRRADIATED BRAIN

Adapted From: Smith SM, Giedzinski E, Angulo MC, Lui T, Lu C, Park AL, Tang S, Martirosian V, Ru N, Chmielewski NN, Liang Y, Baulch JE, Acharya MM, Limoli CL. Functional equivalence of stem cell and stem cell-derived extracellular vesicle transplantation to repair the irradiated brain. Stem Cells Translational Medicine. 2020 Jan;9(1):93-105. doi: 10.1002/sctm.18-0227. Epub 2019 Sep 30. PMID: 31568685; PMCID: PMC6954724.

Abstract

Cranial radiotherapy, although beneficial for the treatment of brain tumors, inevitably leads to normal tissue damage that can induce unintended neurocognitive complications that are progressive and debilitating. Ionizing radiation exposure has also been shown to compromise the structural integrity of mature neurons throughout the brain, an effect believed to be at least in part responsible for the deterioration of cognitive health. Past work has shown that cranially transplanted human neural stem cells (hNSCs) or their extracellular vesicles (EVs) afforded long-term beneficial effects on many of these cognitive decrements. To provide additional insight into the potential neuroprotective mechanisms of cell-based regenerative strategies, we have analyzed hippocampal neurons for changes in structural integrity and synaptic remodeling after unilateral and bilateral transplantation of hNSCs or EVs derived from those same cells. Interestingly, hNSCs and EVs similarly afforded protection to host neurons, ameliorating the impact of irradiation on dendritic complexity and spine density for neurons present in both the ipsilateral and contralateral hippocampi 1 month following irradiation and transplantation. These morphometric improvements were accompanied by increased levels of glial cell-derived growth factor and significant attenuation of radiation-induced increases in postsynaptic density protein 95 and activated microglia were found ipsi- and contra-lateral to the transplantation sites of the

irradiated hippocampus treated with hNSCs or hNSC-derived EVs. These findings document potent far-reaching neuroprotective effects mediated by grafted stem cells or EVs adjacent and distal to the site of transplantation and support their potential as therapeutic agents to counteract the adverse effects of cranial irradiation.

Significance Statement

Cranial radiation therapy for the treatment of brain cancers often leads to adverse impacts on cognitive function. This is particularly problematic for childhood cancer survivors who live long post-therapy lives. The past regenerative medicine approaches using human neural stem cells (hNSCs) have shown beneficial neurocognitive effects in the irradiated brain. The present study evaluated the neuroprotective impact of hNSCs and hNSC-derived extracellular vesicles in the irradiated brain, as demonstrated by preservation of host neuronal morphology, reductions in inflammation, and restoration of neurotrophic factors.

Introduction

Radiotherapy represents a beneficial frontline treatment for primary and metastatic brain tumors, resulting in improved local regional control and increased survival of afflicted patients [2, 3]. Unfortunately, these cancer treatments cause a wide spectrum of debilitating and progressive cognitive impairments that adversely impact working memory, learning, executive function, and attention that manifest months to years following the cessation of treatment [4-8, 10]. The mechanisms underlying these multifaceted effects are complex, persistent, and dynamic over time, and can be linked to cycles of secondary reactive processes involving oxidative stress and inflammation that serve to perpetuate the signature of radiation injury in the brain [13-15]. These damaging processes can result in decreased hippocampal neurogenesis, demyelination, microvascular injury, and alterations in neuronal structure that disrupt dendritic morphology, spine

density, and synaptic proteins, factors that have been proposed to be contributory to if not causal of radiation-induced cognitive impairment [2, 9-12, 72].

In the absence of systematic clinical studies, there remains a conspicuous lack of satisfactory solutions for the clinical management of this unmet medical need that greatly diminishes quality of life for cancer patients. These considerations prompted earlier investigations from our laboratory using rodent models to explore the utility of stem cell transplantation for resolving the unintended side effects of cranial radiotherapy [46, 47]. These and related studies have documented the long-term benefits of cranially transplanted human stem cells of multiple types, where evidence of functional integration within and neurotrophic support to the host brain has highlighted the potential clinical promise of such cell-based therapies [50-52, 54]. Interestingly, more recent work has found that replacing human neural stem cells (hNSCs) with stem-cell derived extracellular vesicles (EVs) during transplantation surgery affords similar neurocognitive benefits [55], circumventing some of the more traditional concerns relating to teratoma formation and immunorejection that have hindered the translational advancement of stem cells to the clinic.

Given the prominent role that the restoration of cognitive health plays in the quality of life for survivors of brain tumors [17], particularly for children, we have embarked on a more detailed examination of the impact of hNSC and EV transplantation on the structural integrity and plasticity of mature hippocampal neurons. Although previous studies analyzed how transplanted stem cells ameliorate structural alterations to neurons after chemotherapy alone [38], or how transplanted EV impact similar parameters in the irradiated brain [55], a systematic and detailed analysis of how transplanted stem cells and EV impact neuronal structure has yet to be undertaken. Furthermore, the extent and range of the beneficial effects of cell-based therapies as a function of distance from the transplant site has yet to be investigated, factors that have important therapeutic implications for dosing and administration. Therefore, to shed light on some

of these critical issues, we report on the impact of bilateral and unilateral hemisphere transplantations of hNSCs and hNSC-derived EVs on the structural integrity of hippocampal neurons in the irradiated rodent brain.

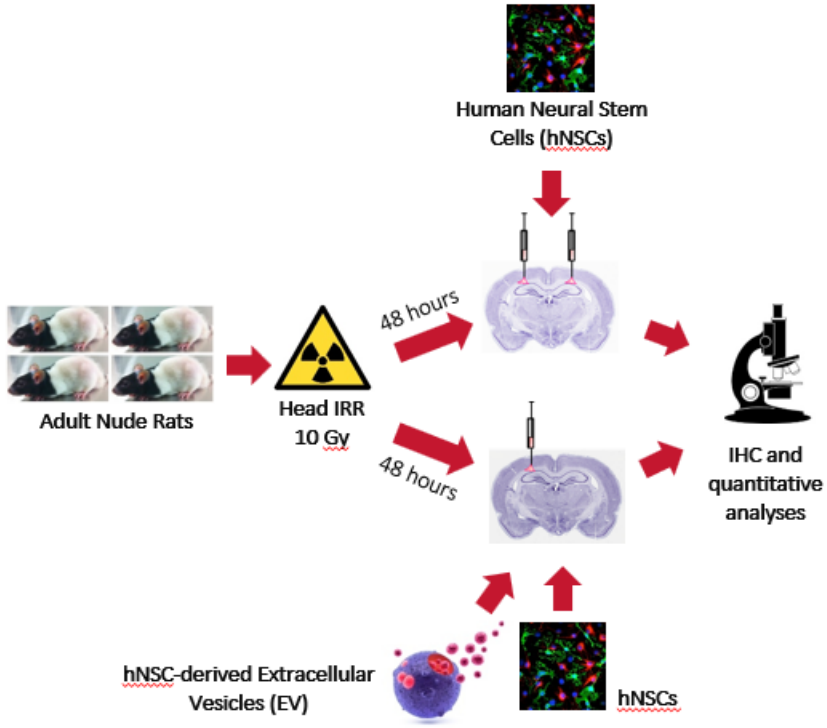

Figure 2.1: Experimental design/ graphical abstract

Materials and Methods

Animals and irradiation

All animal procedures are in accordance with NIH and approved by the University of California Institutional Animal Care and Use Committee. Four-month-old male immunodeficient athymic nude (ATN) rats (Cr:NIHFoxn1rnu, strain 316; Charles River, San Diego) were maintained in sterile housing conditions (20°C ± 1°C; 70% ± 10% humidity; 12 hours:12 hours light and dark cycle) and had free access to sterilized diet and water. The ATN rats were divided into five experimental groups (N = 8-12 per group): 0 Gy receiving sham surgery (Con), 10 Gy head-only irradiation receiving sham surgery (IRR), 10 Gy head-only irradiation receiving bilateral hNSC grafting (IRR + hNSC), 10 Gy head-only irradiation receiving unilateral hNSC grafting (IRR + hNSC Contra), and 10 Gy head-only irradiation receiving unilateral EV grafting (IRR + EV Contra). For cranial irradiation, animals were anesthetized (2.5% isoflurane), placed ventrally and unrestrained on the treatment table (XRAD 320 irradiator, Precision X-ray, North Branford, CT), and positioned under a collimated (1.0 cm^2 diameter) beam for head-only irradiation delivered at a dose rate of 1.0 Gy/minute.

Stem cell growth and EV isolation

The use of hNSCs was approved by the Institutional Human Stem Cell Research Oversight Committee. The validation, expansion, and characterization of hNSCs (ENStem-A; EMD Millipore) have been previously described [47, 73]. EVs were isolated and purified from conditioned hNSC culture medium by ultracentrifugation [74] and characterized using a ZetaView PMX 110 particle analyzer (ParticleMetrix GmbH;Meerbusch, Germany).

Cranial transplantation

Two days following head-only irradiation, rats received bilateral or unilateral, intrahippocampal transplantation of hNSCs or EVs suspended in vehicle (hibernation buffer) using a 33-gauge microsyringe at an injection rate of 0.25 mL/minute. For bilateral transplants, each hippocampus received four distinct injections of live hNSCs (1×10^5 in 2 µL) per hemisphere using precise stereotaxic coordinates, as described previously [46]. For unilateral transplants, each hippocampus received four distinct injections of hNSCs (1×10^5 in 2 µL) or EVs ($\sim 1.0 \times 10^8$ in 2 µL) into a single hemisphere using the same stereotaxic coordinates. Sham surgery controls received an equal volume of sterile hibernation buffer at the same stereotaxic injection coordinates. All cohorts were anesthetized using isoflurane/oxygen (5% (vol/vol) induction, 2.5% (vol/vol) maintenance; VetEquip).

Morphometric analyses of neurons

Animals were euthanized and perfused with 4% paraformaldehyde (Acros Organics, Geel, Belgium), and brain tissues were processed for coronal sectioning using a cryostat (Leica Microsystems, Wetzlar, Germany). For morphometric analyses brain sections (150 µm) from each cohort (N = 4-5 per group) were subjected to Golgi-Cox impregnation and staining of neurons according to the manufacturer's instructions (SuperGolgi kit, Bioenno Tech., Santa Ana, California) and counterstained by nuclear fast red to visualize hippocampal subregions. Details regarding the inclusion criteria for selecting mature neurons for morphometric analysis in the hippocampal DG have been described previously [38]. Briefly, apical and basal dendrites of neurons were traced using NeuroLucida (MicroBrightField) within the DG and CA1 subfields of the hippocampus. All analyses were conducted blind from coded slides. Dendritic complexity was determined by the following equation (Σ branch tip orders + number of branch tips) × (total dendritic length/total number of primary dendrites).

The Stereoinvestigator program (v11, MicroBrightField) was used for the quantification of dendritic spines from the same set of tissues used for morphometric analyses. Briefly, serial sections (every third) through the entire hippocampus were chosen to analyze potential differences in spine density between each of the experimental cohorts (N = 3 per group). Further details regarding these procedures have been published previously [38].

Extraction and ELISA for measurement of neurotrophins

Rats receiving unilateral intrahippocampal transplantation of hNSC-derived EVs or sham surgery were euthanized at 4 weeks after surgery using isoflurane anesthesia. Brains were immediately extracted from the skull (N = 6-8 per group) and the hippocampus was dissected from each cerebral hemisphere. Each hippocampus was weighed and transferred into 300 µL ice-cold lysis buffer (N-PER Neuronal Protein Extraction Reagent, Thermo Scientific Product number 23225) containing sodium orthovanadate (0.5 mM), pheyl-methylsulfonyl fluoride (PMSF, 1 mM), aprotinin (10 µg/mL), and leupeptin (1 µg/mL; Santa Cruz Biotechnology, Santa Cruz, California, http://www.scbt.com). Tissues were sonicated individually, centrifuged at 4°C and the supernatants were collected and diluted 1:5 with Dulbecco's phosphate-buffered saline. The supernatants were acidified to pH 2.6 then neutralized to pH 7.6, and the BDNF and GDNF levels were assayed using Emax ImmunoAssay Systems from Promega (BDNF catalog number G7611, GDNF catalog number G7621) and uncoated ELISA plates (Biolegend Nunc MaxiSorp, catalog number 423501). All measurements were performed at a wavelength of 450 µm on a microplate reader (BioTek SynergyMx).

Immunostaining of PSD-95 and activated microglia

Brains from experimental cohorts not subjected to Golgi-Cox impregnation were prepared for immunohistochemical analyses (N = 4-6 per group) on serial sections (30 µm, 2-4 sections per

animal), and the open blade and enclosed blade of the CA1 of the hippocampus for each section were imaged through the stratum radiatum. Analysis of PSD-95 was performed using the spot tool (Imaris software suite (v7.6, Bitplane, Inc., Zürich, Switzerland). To quantify the density of PSD-95, the number of PSD-95 puncta was converted to spots, derived from confocal Z-stacks taken in 0.5 µm steps at ×60 magnification. The "spot quality threshold" and "minimum spot diameter" parameters were manually adjusted to optimize puncta detection and kept constant thereafter for all subsequent analyses. Additional details regarding the quantification of synaptic puncta have been described previously [11].

Immunostaining for activated microglia (ED-1+ cells) was carried out on serial sections (30 µm coronal) as described previously [38]. Sections were mounted on gelatin-coated slides, air-dried, dehydrated, and counterstained with nuclear fast red (Vector Labs, Burlingame, California). The number of activated microglia (ED1+) within the DH, GCL, and CA3/CA1 regions of hippocampus were analyzed by stereology.

Extracellular vesicle labeling

For in vivo tracking, EVs were labeled with PKH26 (Sigma-Aldrich, St. Louis, Missouri, http://www.sigmaaldrich.com, PKH26GL) the day before transplantation. The EVs were then resuspended in Diluent C, then incubated with Dye Solution for 2 minutes with intermittent mixing as per the manufacturer's protocol. The dye was quenched with 1% bovine serum albumin in water, and EVs were isolated through ultracentrifugation [75] and washed.

Labeled extracellular vesicle tracking and quantification

Animals were euthanized and perfused with 4% paraformaldehyde (Acros Organics), and brain tissues were processed for coronal sectioning using a cryostat (Leica Microsystems). Four serial sections (30 µm, every 10th section) were stained with DAPI and imaged using a confocal

microscope at ×40 magnification. Five images were collected for both the ipsilateral and contralateral hippocampi from each section to image the CA1 pyramidal cell layer. Analysis was performed using the spot tool (Imaris software suite (v7.6, Bitplane, Inc.). To quantify the density of EVs, the number of EVs was converted into spots, derived from confocal Z-stacks taken in 1 μm steps at ×40 magnification.

Statistics

All statistical analyses were conducted using PASW Statistics 18 (SPSS, IBM Corporation) and GraphPad Prism (v6). Significance between the groups was assessed using one-way analysis of variance (ANOVA), and when overall group effects were found, individual groups were then subjected to Bonferroni's multiple comparisons test. All analyses considered a value of $P \leq .05$ to be statistically significant.

Results

Radiation-induced cognitive dysfunction following intrahippocampal stem cell transplantation: The impact on irradiated versus control cohorts

Past work from our laboratory has clearly demonstrated the neurocognitive benefits of hNSCs cranially transplanted in the irradiated brain [46, 47, 50-52, 54]. We have also shown that the benefits of such approaches have been limited to ameliorating deficits caused by irradiation, where unirradiated controls were not found to exhibit improved behavioral performance (Figure 2.2, adapted from [47]). For this reason, and the fact that stem cell grafting of "normal" controls is clinically irrelevant, we chose to omit this group from subsequent analyses.

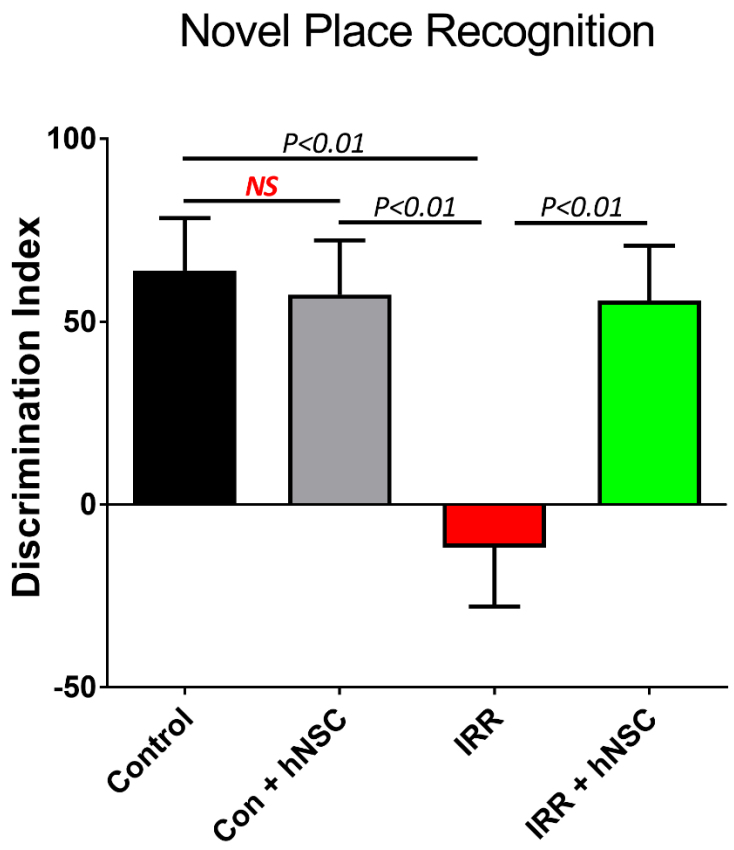

Figure 2.2: Bilateral transplantation with human neural stem cells (hNSCs) improves cranial irradiation (IRR)-induced behavioral impairments. Unirradiated (0 Gy, Control) and cranially irradiated (10 Gy, IRR) animals received bilateral transplantation of hNSCs 48h post-IRR. Animals were administered a hippocampus-dependent novel place recognition (NPR) task one month later. The discrimination index (DI) is calculated as [(novel location exploration time/total exploration time) – (familiar location exploration time/total exploration time)] × 100. The control (0 Gy) animals receiving either sham surgery or hNSC transplantation showed a comparable DI on the NPR task. Cranial IRR led to a significant decline in performance on the NPR task whereas irradiated animals receiving hNSC transplantation showed a significant improvement ($P<0.01$) in the DI at 1-month post-surgery. Data are shown as mean ± S.E.M. (N=8 animals per group). P values are derived from two-way ANOVA. Adapted from Reference 47.

Tracking EVs following unilateral intrahippocampal transplantation

To determine whether EVs migrate to the contralateral hemisphere following unilateral engraftment, PKH26-labeled red fluorescent EVs were transplanted into one hemisphere (hippocampus), and the animals were euthanized 48 hours following surgery (Figure 2.3). Numerous EVs were found migrating to the pyramidal region of the ipsilateral hippocampus relative to the transplantation sites (5.99 μm^3 per 10 mm^3). More importantly, EVs were also present in the contralateral CA1 region near the pyramidal cell layer (3.50 μm^3 per 10 mm^3). Quantification of EVs in the CA1 pyramidal cell layer of four serial sections throughout the hippocampus demonstrated a similar number of EVs on the ipsilateral and contralateral sides ($P = .0618$), although there is a trend toward fewer EVs that had migrated across the brain to the contralateral hippocampus relative to the ipsilateral hippocampus. These data demonstrate that unilaterally transplanted EVs can migrate throughout the irradiated brain, with the potential to deliver widespread neurotrophic support.

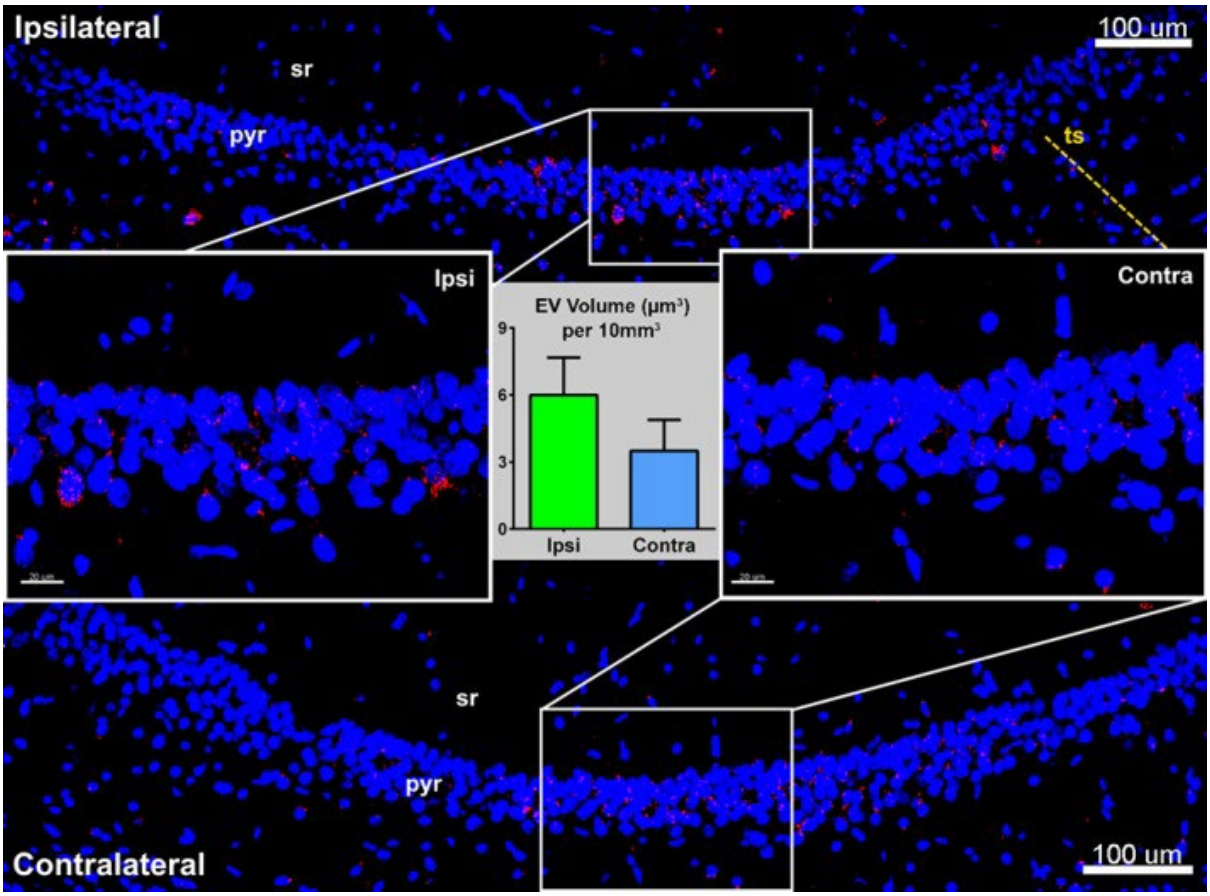

Figure 2.3: In vivo tracking of cranially grafted extracellular vesicles (EVs). Dye-loaded EVs were grafted unilaterally 2 days following irradiation, and coronal brain sections were imaged to detect the presence of EV on each side of the brain 2 days afterward. EV loaded with dye exhibited a strong signal (red) in the ipsilateral CA1 of the hippocampus with migration to the pyramidal cell layer 48 hours later. Analysis of the contralateral side revealed a detectable presence of fluorescently labeled EV near the CA1 pyramidal cell layer at this same time post-surgery. Quantification of EV throughout the CA1 pyramidal cell layer of the hippocampus (4 serial sections, every 10th section) showed similar volume of EV on the ipsilateral and contralateral sides relative to transplantation site. Confocal z stacks were collected at ×40 magnification. Scale bars, 20 and 100 µm, respectively. EV, extracellular vesicles; pyr, pyramidal cell layer; sr, stratum radiatum; ts, transplant site

Structural plasticity of neurons following irradiation and stem cell-based transplantation

Past work has shown that stem cell transplantation preserved the host-neuronal morphology in the chemotherapy-treated brain [38]. Furthermore, EVs transplanted in the irradiated brain were found to be equally protective in preserving the structure of hippocampal neurons [55]. Despite these recent findings, we have not directly tested the impact of stem cell transplantation on the structural integrity of irradiated neurons, nor have we evaluated the distal effects from the site of transplantation. Therefore, the dendritic structure of Golgi-Cox impregnated granule cell neurons in the dentate gyrus of the hippocampus was analyzed after irradiation and following bilateral and unilateral hNSCs and hNSC-derived EV transplantation paradigms (1 month after transplantation). Compared with controls, at 1 month, the neuronal complexity and spine density are severely compromised in the irradiated hippocampus that is reversed in the brain receiving bilateral hNSC transplantation (Figure 2.4). Significant differences between groups were found (one-way ANOVA, $F(4,14) = 12.34$, $P = .0002$), and compared with controls (Figure 2.5), irradiated granule cell neurons exhibited significant reductions (>50%, $P = .0075$) in the dendritic complexity. Bilateral transplantation of hNSCs preserved host neuronal structure 1 month following irradiation, with a statistically significant increase in dendritic complexity compared with the irradiated group ($F(4,14) = 12.34$, $P = .0005$), whereas granule cell neurons from controls and from irradiated animals receiving bilateral hNSC transplantation were morphologically and statistically indistinguishable ($F(4,14) = 12.34$, $P = .9721$) (Figure 2.5). Additional studies comparing control, irradiated, and cohorts bilaterally transplanted with hNSCs demonstrated that the neuroprotective effects of grafted hNSCs in the dentate gyrus extend to 4 months, as dendritic complexity is significantly elevated in the transplanted brain compared with irradiated cohorts ($F(2,10) = 26.25$, $P = .0001$), and statistically indistinguishable from controls ($F(2,10) = 26.25$, $P = .7078$) (Figure 2.6).

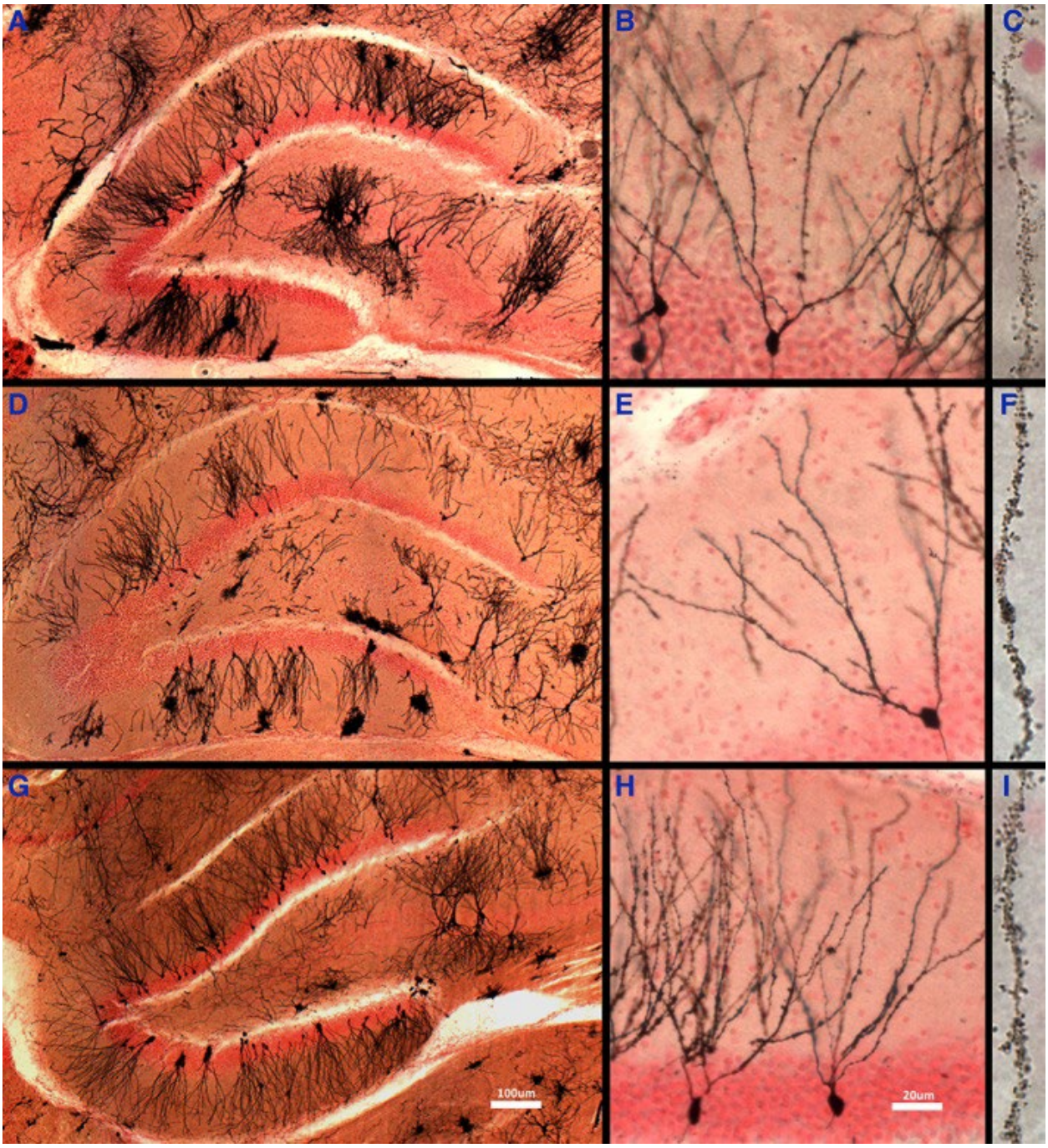

Figure 2.4: Bilateral transplantation of human neural stem cells (hNSCs) preserves host neuronal morphology in the dentate gyrus following irradiation. Four-month-old athymic nude rats received 10 Gy head-only x-ray irradiation, followed by sham surgery or bilateral hNSC transplantation. Golgi-Cox staining was performed 1 month after irradiation and transplantation. A, D, and G,

Panoramic images of the hippocampus of control, irradiated, and irradiated + bilateral hNSC transplanted animals, respectively. B, E, and H, Images of granular cell layer neurons in the dentate gyrus of control, irradiated, and irradiated + bilateral hNSC transplanted animals, respectively. C, F, and I, Images of dendritic spines of granular cell layer neurons of control, irradiated, and irradiated + bilateral hNSC transplanted animals, respectively. Images from irradiated + bilateral hNSC transplanted animals are also representative of sections from animals who received unilateral transplantation of hNSCs or extracellular vesicles (EVs). The bright-field images were collected at ×4 (A, D, G), ×40 (B, E, H), and ×100 (C, F, I) magnifications. Scale bar, 100 μm (A, D, G) and 20 μm (B, E, H)

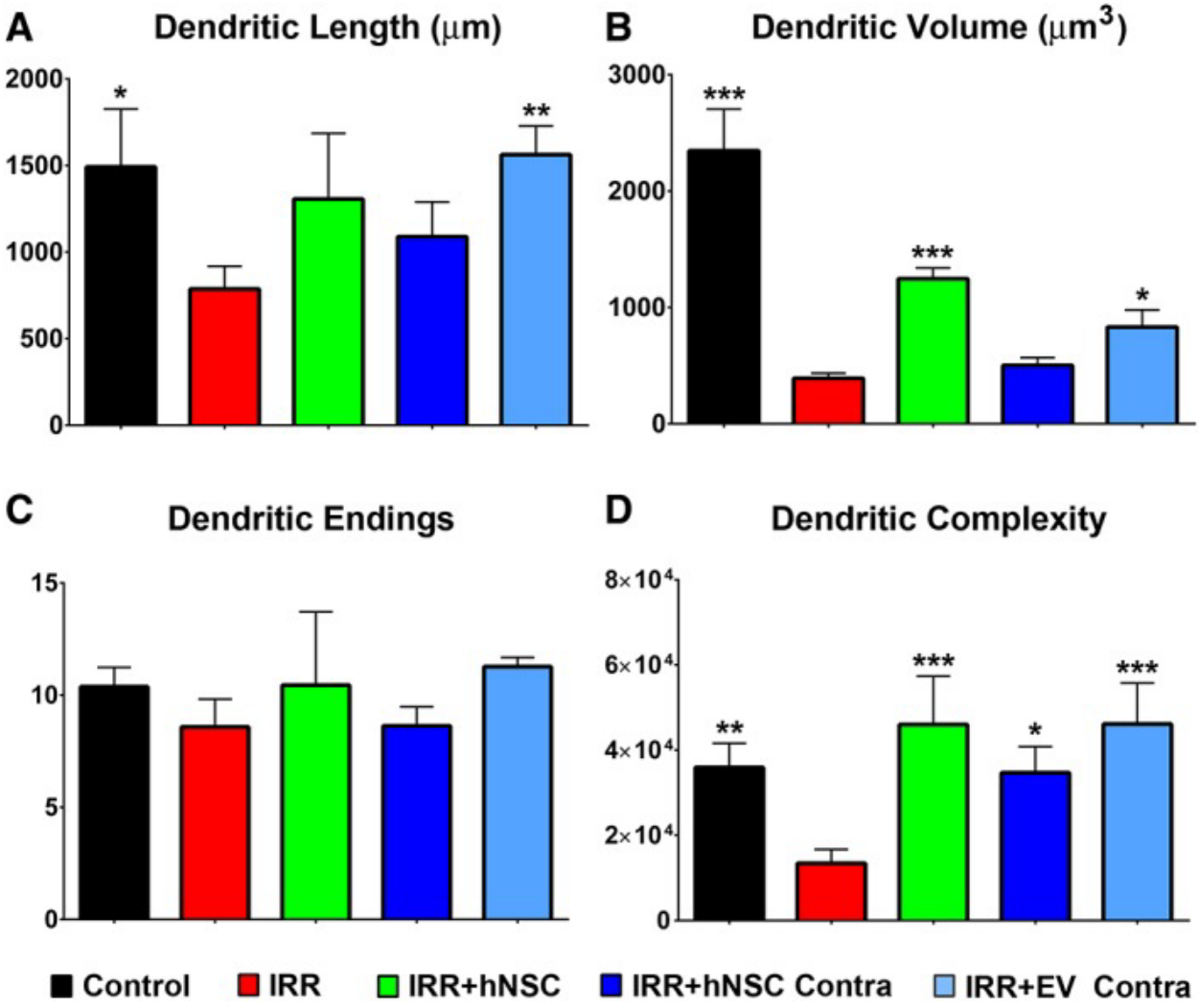

Figure 2.5: Unilateral transplantation of human neural stem cells (hNSCs) or hNSC-derived extracellular vesicles (EVs) protects dendritic complexity in the contralateral dentate gyrus following irradiation. Four-month-old athymic nude rats received 10 Gy head-only x-ray irradiation or sham irradiation/surgery (Control), bilateral or unilateral hNSC transplantation, or unilateral transplantation of hNSC-derived EV. Golgi-Cox staining was performed 1 month after irradiation and morphometric analysis of dendritic complexity of granular cell layer neurons was calculated using Neurolucida. A, Dendritic length of granular cell layer neurons in the dentate gyrus. B, Dendritic volume of granular cell layer neurons. C, Quantification of dendritic endings of traced granular cell neurons. D, Computed dendritic complexity for traced granular cell neurons.

Irradiation (IRR) resulted in a significant decrease in dendritic complexity relative to control animals, and bilateral (IRR + hNSC) and unilateral (IRR + hNSC Contra) transplantation of hNSCs and unilateral transplantation of EVs (IRR + EV Contra) rescued complexity. Data are presented as the mean ± SEM (N = 4 animals/group, 4 neurons traced per animal). *P*-values are derived from analysis of variance and Bonferroni's multiple comparisons test. *, $P < .05$; **, $P < .01$; ***, $P < .001$ all compared against the irradiated group

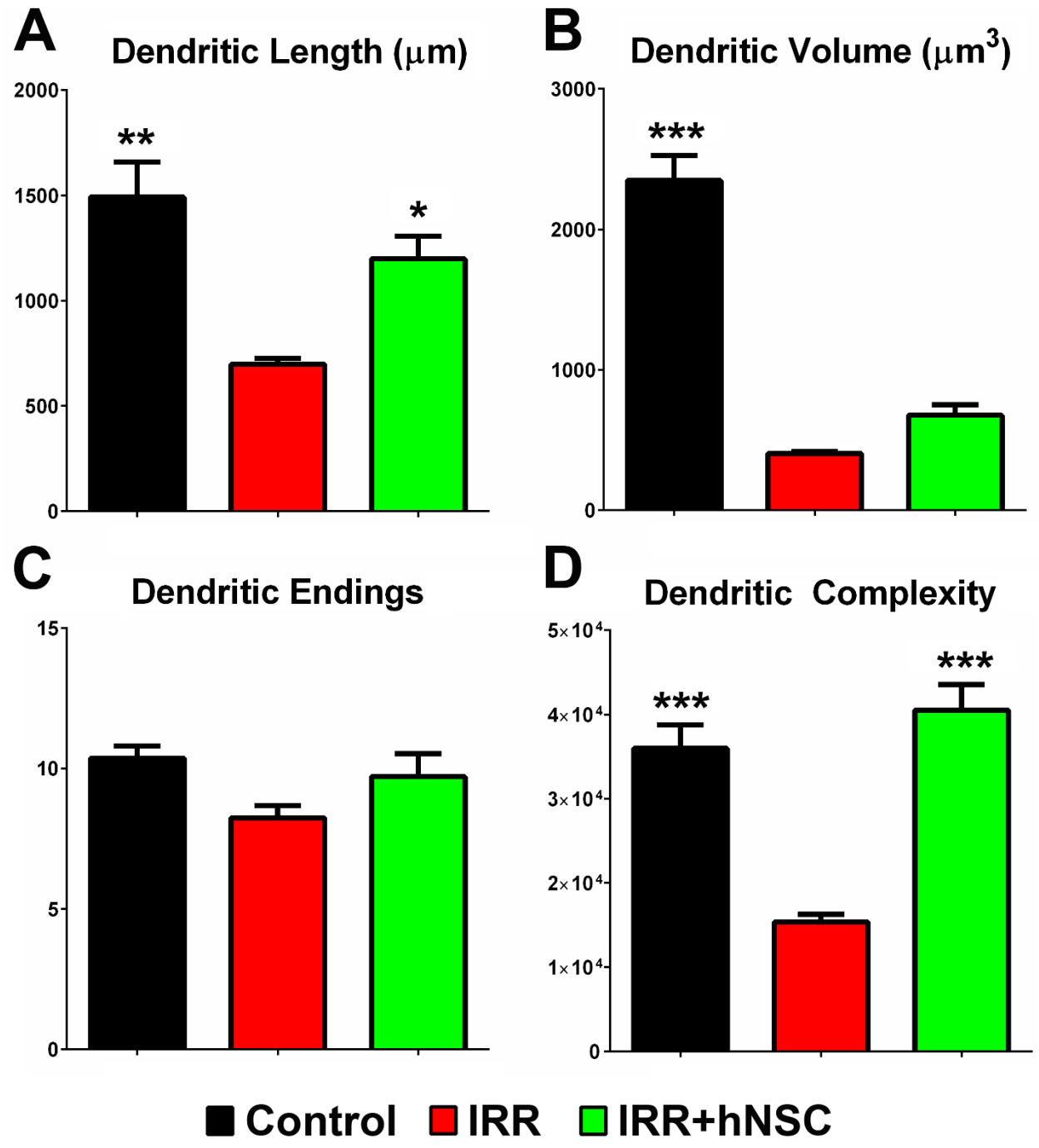

Figure 2.6: Beneficial effects of bilateral transplantation of human neural stem cells (hNSC) on dendritic morphology in the dentate gyrus persist at four months following irradiation. Four-month-old athymic nude rats received 10 Gy head-only x-ray irradiation (IRR) or sham irradiation/surgery (Control), or bilateral hNSC transplantation (IRR+hNSC). Golgi-Cox staining

was performed four months post-irradiation and morphometric analysis of dendritic structure of granule cell layer neurons was characterized using Neurolucida. Exposure to radiation caused a significant decrease in dendritic length, volume, and complexity at four months following exposure. Bilateral hNSC transplantation in irradiated animals preserved dendritic length and complexity in the dentate gyrus relative to irradiated animals that received sham surgery. Data are presented as the mean ± SEM (N = 4 animals/group, 4 neurons traced per animal). P values are derived from ANOVA and Bonferroni's multiple comparisons test. *P < 0.05; **P<0.01; ***P<0.001 all compared against the irradiated group.

Our past studies [55] have shown that hippocampal transplantation of hNSC-derived EVs alleviated radiation-induced microglial activation distal to the transplantation sites (amygdala). To assess the spatial reach of beneficial effects to host brain neuronal structure, unilateral transplantations of hNSCs or EVs were performed. Analysis of neuronal morphology in the contralateral hippocampus revealed that both hNSC and EV transplantations exerted far-reaching neuroprotective effects (Figure 2.5). Significant overall group effects were found ($F(4,14) = 12.34$, $P = .0002$) as the impact of unilateral transplantation using either hNSCs ($F(4,14) = 12.34$, $P = .012$) or EVs ($F(4,14) = 12.34$, $P = .0002$) preserved dendritic complexity in the irradiated brain compared with the sham surgery irradiated cohort (Figure 2.5D). The morphology of the contralateral granule cell neurons resembled that of controls and was statistically indistinguishable for unilateral transplantation of both hNSCs ($F(4,14) = 12.34$, $P > .9999$) and EVs ($F(4,14) = 12.34$, $P = .7315$), demonstrating that hNSC or EV grafting could protect host neurons against radiation-induced degradation at sites distal to the region of transplantation. There were no statistically significant differences in dendritic complexity between bilateral and unilateral transplantation of hNSCs ($F(4,14) = 12.34$, $P = .3938$], between unilateral transplantation of hNSCs and unilateral transplantation of EVs ($F(4,14) = 12.34$, $P > .9999$], or between bilateral transplantation of hNSCs and unilateral transplantation of EVs ($F(4,14) = 12.34$, $P = .3943$].

To complement the dendritic complexity measurements, analysis of higher resolution images (e.g., Figure 2.4C, F, I) was undertaken to assess the impact of the transplantation paradigms on dendritic spine density. Significant overall group effects were found ($F(4,10) = 5.844$, $P = .0109$), and consistent with past results [38], irradiation significantly reduced overall dendritic spine density compared with unirradiated controls ($F(4,10) = 5.844$, $P = .0286$) 1 month following exposure (Figure 2.7). Importantly, significant group differences were found between

irradiated and transplanted cohorts, where bilateral transplantation of hNSCs was found to restore dendritic spine density against radiation-induced depletion ($F(4,10) = 5.844$, $P = .0251$). Dendritic spine density levels in animals receiving bilateral hNSC transplantation were similar to that of control animals ($F(4,10) = 5.844$, $P > .9999$). Assessment of spine densities in the contralateral hippocampus following unilateral transplantation of hNSCs or EVs showed an increase in spine density along granule cell dendrites compared with irradiated cohorts, but these positive trends did not reach statistical significance (Figure 2.7).

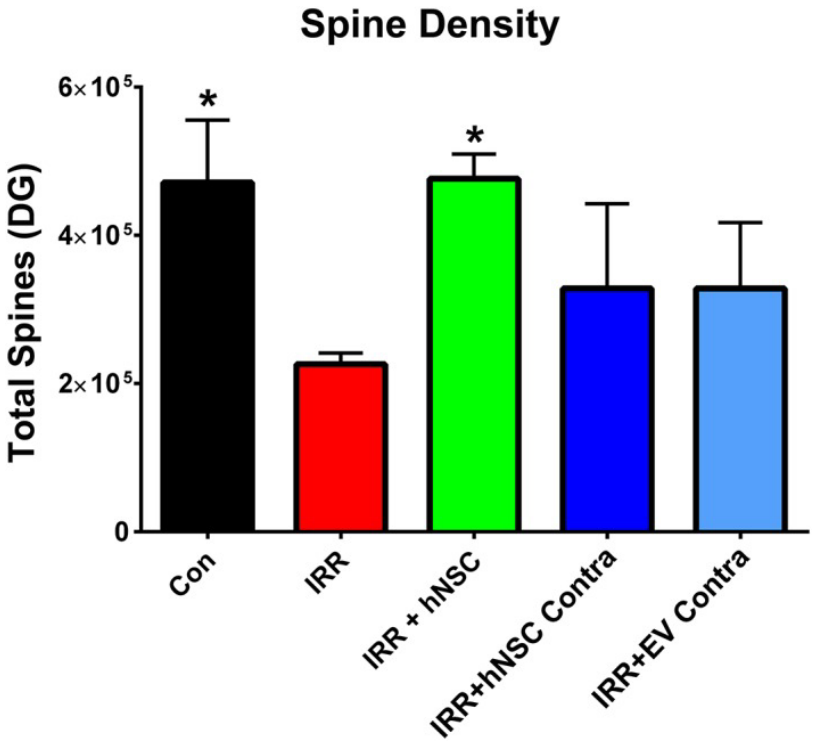

Figure 2.7: Bilateral transplantation of human neural stem cells (hNSCs) rescues the radiation-induced reduction in dendritic spine density in the dentate gyrus (DG). Four-month-old athymic nude rats received 10 Gy head-only x-ray irradiation or sham irradiation/surgery (Con), bilateral or unilateral hNSC transplantation, or unilateral transplantation of hNSC-derived extracellular vesicles (EVs). Quantification of dendritic spines along Golgi-Cox impregnated granule cell neurons 1 month after irradiation revealed that bilateral hNSC transplantation (IRR + hNSC) rescued spine density in the dentate gyrus from the reduction seen in irradiated animals (IRR). Unilateral transplantation of hNSC (IRR + hNSC Contra) and hNSC-derived EV (IRR + EV Contra) showed a trend toward increasing dendritic spine density in the contralateral DG relative to the irradiated brain, but failed to reach statistical significance. Data are presented as the mean ± SEM (N = 4 animals/group, three sections per animal). P-values are derived from analysis of variance and Bonferroni's multiple comparisons test. *, $P < .05$ compared against the irradiated group

Neurotrophin levels in the hippocampus following irradiation and unilateral stem cell-derived EV transplantation

In the next experiment, we sought to interrogate potential mechanisms by which unilateral transplantation of EVs conferred benefits to the CNS. Brain-derived neurotrophic factor (BDNF) and glial cell line-derived neurotrophic factor (GDNF) levels were assayed in both the ipsilateral and contralateral hemispheres of the hippocampus following irradiation and surgery. The levels of BDNF were unchanged 4 weeks following irradiation with and without unilateral EV transplantation ($F(3,16) = -0.4619$, $P = .7128$) (Figure 2.8A). However, GDNF levels were reduced in the irradiated brain ($F(3,18) = 8.989$, $P = .0015$), and restored following unilateral EV transplantation on the ipsilateral site relative to GDNF levels of irradiated animals ($F(3,18) = 8.989$, $P = .0035$) (Figure 2.8B). The GDNF levels in the ipsilateral hippocampus of animals receiving unilateral EV transplantation were statistically similar to those of control animals ($F(3,18) = 8.989$, $P > .999$). The GDNF levels in the contralateral hippocampus of transplanted animals were increased compared with the irradiated hippocampus, but this elevation was not statistically significant ($F(3,18) = 8.989$, $P = .4958$). These data suggest that the beneficial effects of grafted EVs in the irradiated brain may in part be due to a restoration of neurotrophic factors.

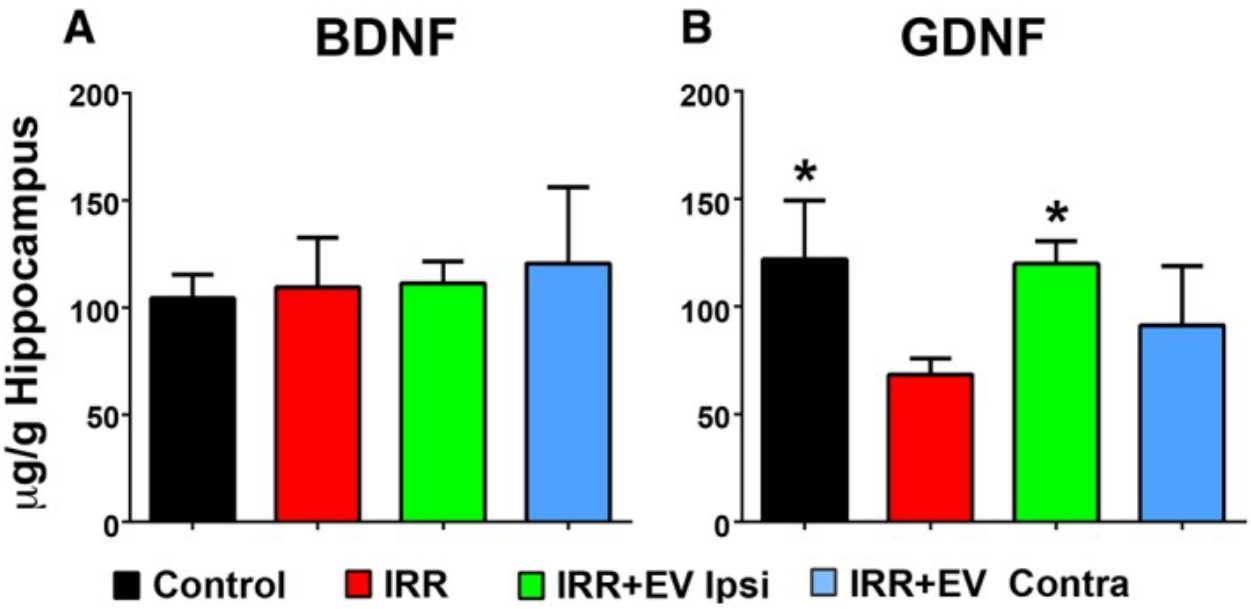

Figure 2.8: Unilateral transplantation of human neural stem cell-derived extracellular vesicles (EVs) modulate glial cell line-derived neurotrophic factor (GDNF) in the irradiated hippocampus. Two-month-old athymic nude rats received 10 Gy head-only x-ray irradiation (IRR) or sham irradiation/ surgery (Control) or unilateral transplantation of hNSC-derived EV. Animals were euthanized at 4 weeks after surgery and neurotrophic growth factor levels were assessed (N = 6-8 per group). A, Brain-derived neurotrophic factor (BDNF) levels in the control, irradiated, ipsilateral transplanted (IRR + EV Ipsi), and contralateral (IRR + EV Contra) hippocampus remained relatively unaffected by EV grafting. B, In contrast, GDNF levels that were reduced by irradiation were recovered on the ipsilateral side after EV grafting. On the contralatral side, EV grafting only showed trends toward improvement. P-values are derived from analysis of variance and Bonferroni's multiple comparisons test. *, $P < .05$ each compared against the irradiated group

Synaptic signaling protein levels after irradiation and stem cell-based transplantation

The ability of irradiation to compromise neuronal morphology is also linked with the disruption of synaptic protein expression. Our past data have shown that radiation exposure elicits a marked rise in the level of PSD-95 in the hippocampal dentate gyrus [11]. Present results corroborate those past findings, as significant overall group effects were found ($F(4,174) = 7.393$, $P < .0001$), and demonstrate that following cranial irradiation, levels of PSD-95 are significantly elevated compared with unirradiated controls ($F(4,174) = 7.393$, $P < .0001$; Figure 2.9). Interestingly, both transplantation paradigms were found to reduce the radiation-induced increase in PSD-95 levels. Bilateral ($F(4,174) = 7.393$, $P = .0003$) and unilateral transplantation paradigms using either hNSCs ($F(4,174) = 7.393$, $P = .002$) or EVs ($F(4,174) = 7.393$, $P = .0005$) were all effective at attenuating the rise in PSD-95 observed in the irradiated brain (Figure 2.9D). There were no significant differences in PSD-95 levels of the dentate gyrus between bilateral versus unilateral hNSC transplantation ($F(4,174) = 7.393$, $P > .9999$), between unilateral transplantation of hNSCs versus EVs ($F(4,174) = 7.393$, $P > .9999$), and between bilateral transplantation of hNSCs versus unilateral transplantation of EVs ($F(4,174) = 7.393$, $P > .9999$); the control levels of PSD-95 were also statistically indistinguishable from that of the bilateral hNSC transplantation group ($F(4,174) = 7.393$, $P > .9999$), the unilateral hNSC transplantation group ($F(4,174) = 7.393$, $P = .093$), and the unilateral EV transplantation group ($F(4,174) = 7.393$, $P = .1791$). These data provide the first evidence that increased levels of PSD-95 found after radiation exposure can be restored back to the control level by engraftment of hNSCs or hNSC-derived EVs, and provide further support for the neuromodulatory role of this therapeutic strategy in the irradiated brain.

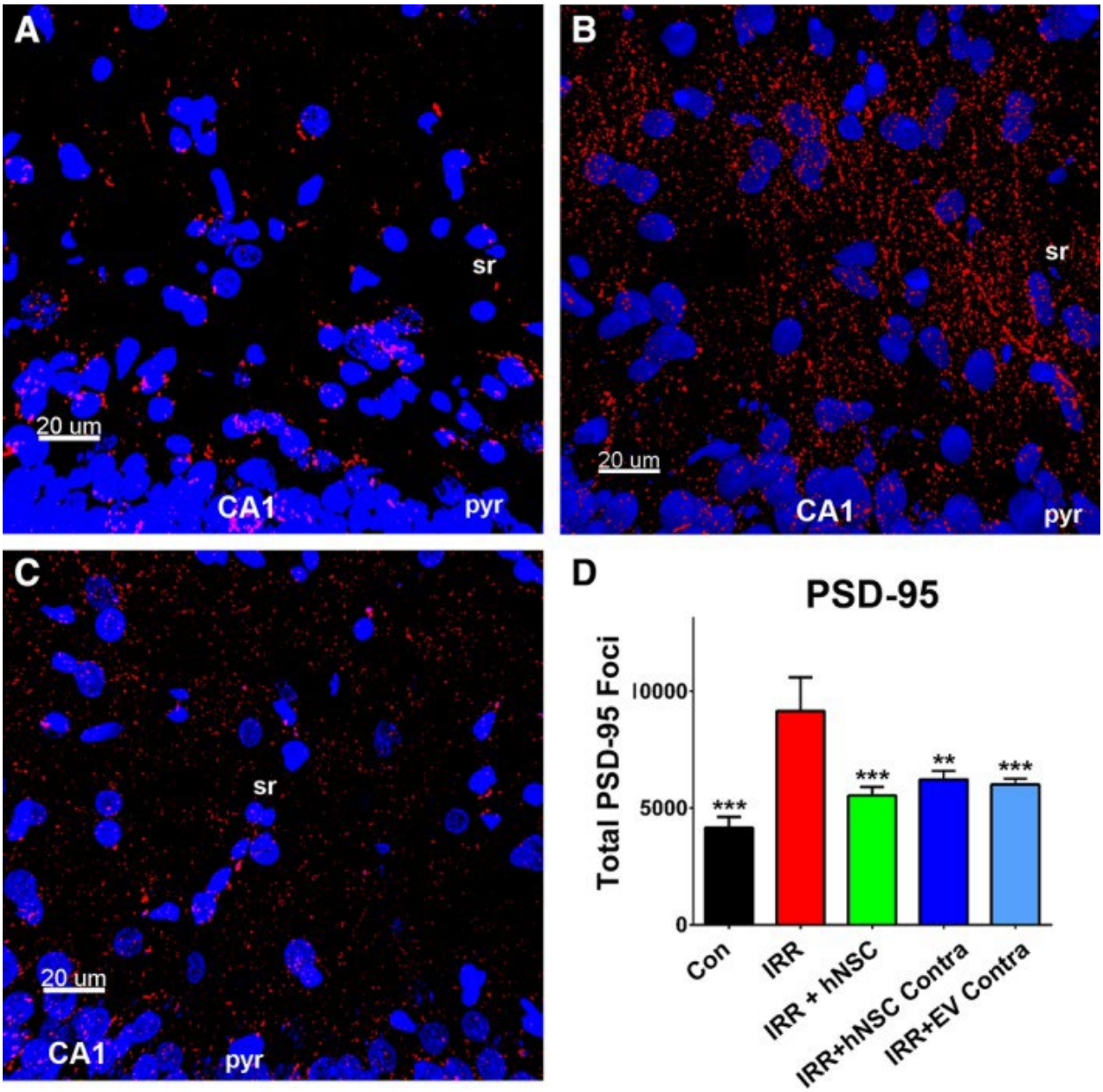

Figure 2.9: The numbers of PSD-95 puncta are increased after irradiation and were attenuated by unilateral transplantation of human neural stem cells (hNSCs) or unilateral transplantation of hNSC-derived extracellular vesicles (EVs) in the contralateral hemisphere. Bilateral transplantation of hNSCs also attenuates radiation-induced increases in PSD-95 puncta. Four-month-old athymic nude rats received 10 Gy head-only x-ray irradiation or sham irradiation/ surgery (control), bilateral or unilateral hNSC transplantation, or unilateral transplantation of hNSC-derived EV. A-

C, Representative immunofluorescence images showing PSD-95 foci (red) in the (A) control, (B) irradiated, and (C) bilateral hNSC-grafted hippocampal CA1. PSD-95 puncta are dramatically elevated in the sr following irradiation (IRR) as compared with the control group (Con). Transplantation of hNSCs, either bilaterally (IRR + hNSC) or unilaterally (IRR + hNSC Contra), and hNSC-derived EV unilaterally (IRR + EV Contra) ameliorate elevated PSD-95 in the CA1 both ipsi- and contra-lateral to the sites of transplantation. D, Quantification of total PSD-95 synaptic puncta in the CA1 of control, irradiated, and transplanted animals, analyzed using the spot tool of the Imaris software suite. Data are presented as the mean ± SEM (N = 4 animals/group, two sections stained and analyzed per animal). *P*-values are derived from analysis of variance and Bonferroni's multiple comparisons test. **, $P < .01$; ***, $P < .001$ each compared against the irradiated group. Confocal *z* stacks were collected at ×40 magnification. Scale bar, 20 μm (A-C). pyr, pyramidal cell layer; sr, striatum radiatum

The impact of stem cell-based transplantation on radiation-induced neuroinflammation

Significant work from our group has demonstrated the ability of ionizing radiation exposure to elevate inflammation in the brain [54, 55]. Microglial activation represents a reliable marker of neuroinflammation that has been shown to increase significantly in the context of various cranial irradiation paradigms [14, 75, 76]. Present results support past findings and indicate that cranial irradiation induces increased numbers of activated microglia throughout distinct subfields of the hippocampus (Figure 2.10; $F(5,14) = 16.92$, $P < .0001$). Bilateral transplantation of hNSCs was found to reduce the microglial activation throughout the hippocampus ($F(5,14) = 16.92$, $P = .0004$), with the most significant effect in the dentate gyrus ($F(5,14) = 14.40$, $P = .0003$; Figure 2.10D). Interestingly, data adapted from a prior publication22 for comparative purposes indicate a similar if not more pronounced benefit of bilaterally grafted EVs at reducing numbers of activated microglia in the irradiated brain to control levels ($F(5,14) = 16.92$, $P < .0001$). Unilateral transplantation of hNSCs ($F(5,14) = 16.92$, $P = .0008$) or EVs ($F(5,14) = 16.92$, $P < .0001$) was also found to confer significant benefits, demonstrating effective reductions in the numbers of activated microglia throughout various regions of the contralateral hippocampus (Figure 2.10D,E). Similar numbers of activated microglia were found in the hippocampus of bilateral and unilateral hNSC-transplanted animals ($F(5,14) = 16.92$, $P > .9999$), bilateral and unilateral EV-transplanted animals ($F(5,14) = 16.92$, $P = .4516$), animals receiving bilateral transplantation of hNSCs versus EVs ($F(5,14) = 16.92$, $P = .9675$), and animals receiving unilateral transplantation of hNSCs versus EVs ($F(5,14) = 16.92$, $P > .9999$). There were no statistically significant differences between the activated microglia quantification in the control group versus any of the transplanted groups, either ($F(5,14) = 16.92$, $P > .9999$ for control vs. bilateral hNSC transplantation; $P > .9999$ for control vs. bilateral EV transplantation; $P = .7414$ for control vs. unilateral hNSC transplantation; $P = .9999$ for control vs. unilateral EV

transplantation). The ability of hNSC and EV transplantation to minimize the numbers of radiation-induced activated microglia suggests that such strategies can play a significant role in facilitating the neurocognitive recovery of the irradiated brain.

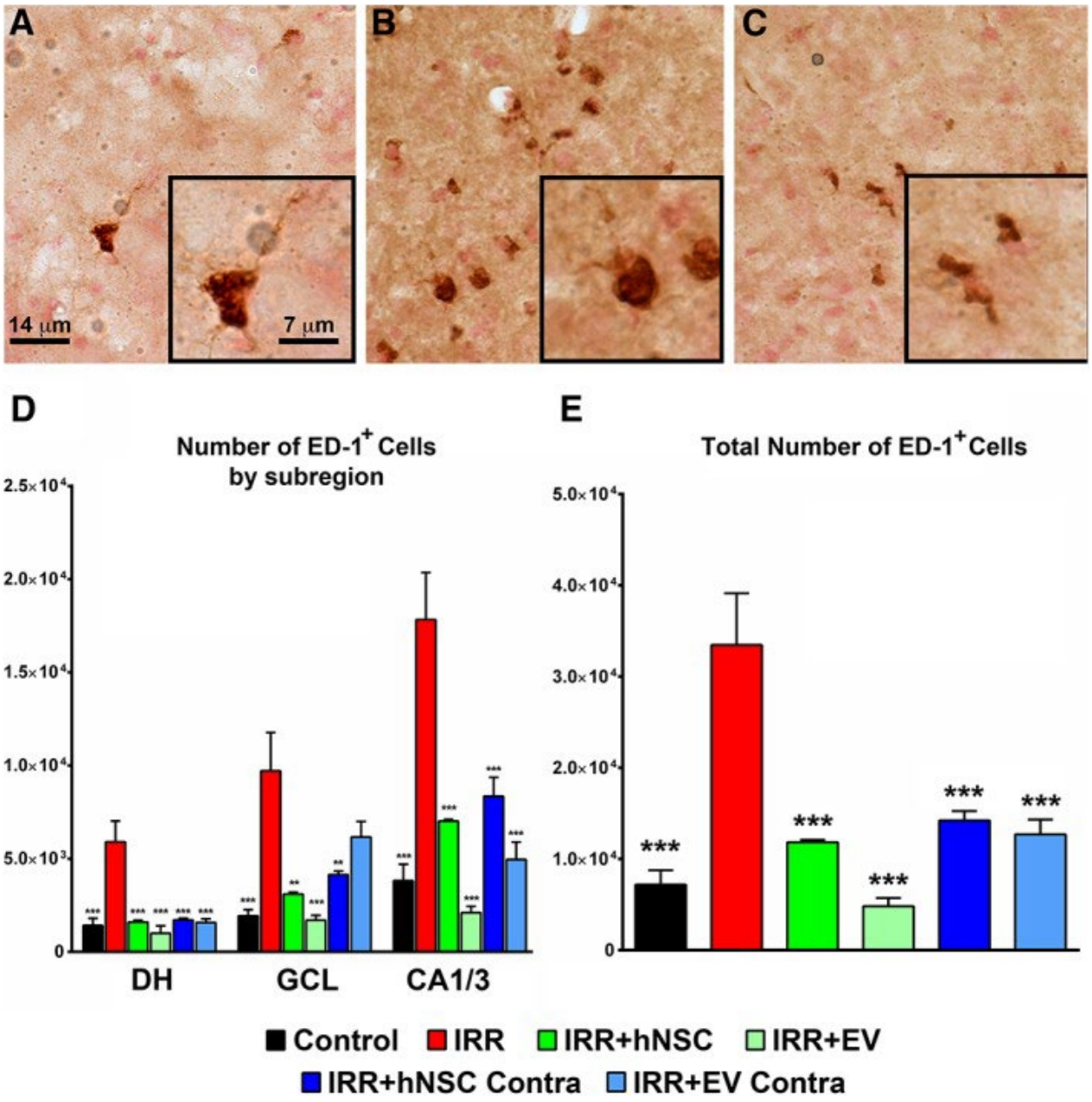

Figure 2.10: Either bilateral or unilateral transplantation of human neural stem cells (hNSCs), or bilateral or unilateral transplantation of hNSC-derived extracellular vesicles (EVs) ameliorates the increase in activated microglia following irradiation, as examined in the contralateral hippocampus for unilateral transplantations. Four-month-old athymic nude rats received 10 Gy head-only x-ray irradiation, sham irradiation/surgery (control) or bilateral or unilateral hNSC transplantation, or bilateral or unilateral transplantation of hNSC-derived EV. Unbiased

stereology was conducted using Neurolucida. A-C, Representative bright-field images depict ED-1+ microglia (dark brown) in the (A) control, (B) irradiated, and (C) bilateral hNSC-grafted hippocampus (dentate hilus, DH). D, Bilateral (IRR + hNSC) and unilateral (IRR + hNSC Contra) transplantation of hNSCs diminishes the number of activated microglia in hippocampal subfields (DH, granular cell layer [GCL], and CA3 and CA1), compared with the elevated activated microglia in irradiated animals (IRR) and similar to control levels, (E) and in the total hippocampus; this effect is also seen following bilateral (IRR + EV) and unilateral (IRR + EV Contra) transplantation of hNSC-derived EV. Data are presented as the mean ± SEM (N = 4 animals/group, three sections stained and analyzed per animal). *P*-values are derived from analysis of variance and Bonferroni's multiple comparisons test. **, $P < .01$; ***, $P < .001$ each compared against the irradiated group. Bright-field images were collected at ×40 (A-C) and ×100 (inserts) magnification. Scale bar, 14 μm (A-C), and 7 μm (inserts)

Discussion

Radiation-induced cognitive dysfunction is a severe and unintended side effect of radiotherapy used to forestall the progression of primary and secondary CNS malignancies. Despite the many benefits of these regimens, curative treatments are limited by normal tissue tolerances that dictate dose limits to minimize unacceptable normal tissue complications. In this light, mitigation of the progressive and debilitating neurocognitive decline following treatment remains an unmet medical need that hampers the recovery and impacts quality of life of pediatric and adult cancer survivors alike [72]. Much of our past work has focused on this pressing problem and demonstrated the neuroprotective benefits of cranially transplanted human stem cells [50, 51] and EVs [55] in the irradiated brain. Importantly, many of these past studies have subjected rodents to extensive behavioral testing, where we demonstrated significant improvements in neurocognitive outcomes at protracted times following irradiation and transplantation [51, 52]. Here, we present data from a systematic study of transplanted hNSCs and EVs that implicate several of the potential routes by which stem cell-based transplantation strategies bestow therapeutic benefits.

Precisely how irradiation impacts the brain to disrupt neurotransmission and cognitive processing has been a subject of intense investigation over the years, and many excellent reviews have described various features believed to be critical to the radioresponse of the CNS [10, 12, 72, 77]. More recent evidence, however, has provided some important clues regarding the structural sensitivity of mature neurons to ionizing radiation exposure, changes that are posited to have significant functional consequences within the irradiated brain [11, 78]. Since the original descriptions of the morphometric alterations observed in irradiated hippocampal neurons [11, 79], subsequent studies from multiple groups have corroborated these findings in other brain regions after exposure to a variety of radiation types [75, 76, 80, 81]. Importantly, many if not

all of these changes were found to persist over time, suggesting that alterations to irradiated neurons were either permanent or exhibited time constants of recovery that far exceeded the length of reported experimentation.

In fact it was the temporal coincidence of radiation-induced cognitive impairment and dendritic degradation that suggested cause and effect, although this remained largely corollary until a series of follow-up studies linked poor individual behavioral performance to reductions in dendritic spine density [*75*, *76*]. Although these heavy ion studies strengthened the structure function relationship between impaired cognition and altered neuronal morphometry, it was not until improvements in cognition found after stem cell-based interventions were linked to the preservation of host neuronal structure that this idea became increasingly difficult to dismiss [38, *55*]. Thus, a major focus of the present work was to support this idea further, by critically determining the nature and extent of stem cell- and EV-based neurotrophic support in the irradiated brain.

Findings presented here provide the first evidence that cranially transplanted stem cells preserve host neuronal morphometry after irradiation. Bilateral and unilateral transplantation of hNSCs preserved the dendritic morphology in both hemispheres of the brain, demonstrating that locally transplanted stem cells can impact neurons residing 6-8 mm distal from the site of grafting. Similar findings were found with transplanted EVs, indicating that a likely mechanism of neurotrophic support from grafted stem cells involves the secretion of such vesicles that can mediate local and distal effects through yet-to-be-defined paracrine signaling mechanisms.

Quantification of fluorescent EVs between the hemispheres was, however, not found to differ, pointing to the widespread regenerative capabilities of transplanted EVs. Dendritic spine density was also protected after the grafting procedures, although only to a significant extent after bilateral hNSC transplantation. Although the benefits of unilateral transplantation showed trends

toward increased spine density, neither hNSCs nor EVs were able to increase spine densities significantly over irradiated cohorts. Noteworthy too is that past results implementing bilateral EV transplantation in the irradiated brain were also unable to demonstrate a protective effect on spine densities, despite improvements in cognition, pointing to the complexities of structure-function relationships in the irradiated brain [55]. Despite certain caveats regarding the functional importance of dendritic spines to cognition, present findings suggest that transplanted EVs might be devoid of certain bioactive cargo required for robust protection of dendritic spines, contrary to the situation with grafted hNSCs.

One of the many possible avenues that grafted EVs might impact the irradiated brain can be by modulation of endogenous neurotrophic support [82, 83]. Past work from our group has shown that a significant fraction of cranially grafted human stem cells ultimately differentiate along glial lineages [38, 46, 47, 54]. Neurotrophic support from grafted and/or host glial cells could augment host neuronal function by the secretion of exosomes able to provide a variety of neuroprotective benefits. Analyses of hippocampi derived from either side of the grafted brain revealed significantly elevated levels of GDNF on the ipsilateral side with trends on the contralateral side. in vitro models have demonstrated the capability of GDNF to promote axonal sprouting [84] and protect neurons from transient ischemia induced damage [85]. Other work in different stem cell-based systems has noted various beneficial effects of secreted exosome-derived GDNF [86, 87]. Although such changes were not found for BDNF, data provide evidence that EV grafting is neuromodulatory, able to stimulate neurotrophic growth factors long after irradiation and surgery.

As a critical postsynaptic scaffolding protein, PSD-95 immunostaining has proven to be a remarkably robust marker of ionizing radiation exposure in the brain, increasing after nearly every irradiation dose, type, and post-exposure time analyzed [11, 75, 76, 78]. Although the

role of PSD-95 in organizing and stabilizing postsynaptic glutamate receptors and in synapse maturation has been well studied [88], the significance of elevated PSD-95 levels post-irradiation remains uncertain. Importantly, radiation-induced decrements in cognition correlate strongly with elevated PSD-95 levels, suggesting that the renormalization of PSD-95 found after each transplantation paradigm may have functional significance in regulating neurotransmission after the global stress of irradiation. It is tempting to speculate that changes in PSD-95 expression alter the function of excitatory synapses, and past findings in proton irradiated mice have shown changes in the ratio of phosphorylated GluR1/R2 AMPA receptor subunits [15], although PSD-95 levels were not measured in that work.

For decades, neuroinflammation has been implicated as one of the primary driving forces behind numerous chronic and degenerative conditions of the CNS [12, 89-91]. As alluded to above, irradiation initiates a cascade of secondary reactive processes that may never completely resolve [77, 92-94], manifesting as a persistent pro-inflammatory state associated with chronically activated microglia. The persistence of the inflammatory footprint has the potential to impact nearly all neurocognitive processes, and it comes as no surprise that radiation-induced cognitive dysfunction is routinely associated with elevated levels of activated microglia. Findings reported here corroborate significant past data [14, 54, 55], and reveal that cranial irradiation elicits a robust increase in the number of activated microglia throughout all hippocampal subfields analyzed. Importantly, current findings indicate that bilateral hNSC transplantation significantly reduces the number of activated microglia throughout the hippocampus, supporting earlier results obtained with a different source of hNSCs [54]. Furthermore, data derived from the unilateral transplantations indicate that both hNSCs and EVs exert anti-inflammatory effects on the contralateral side of the brain. Substantial reductions in activated microglia distal to the site of

transplantation provide further support for the extended range of neurotrophic support imparted by grafted hNSCs and EVs.

Conclusion

Regenerative medicine holds promise for restoring tissue functionality in a variety of diseased, damaged, and aged tissues, aiming to ameliorate adverse changes while minimizing treatment complications [18]. For survivors of cancer, adverse neurocognitive outcomes have become an unfortunate burden, with little promise of long-term relief. Cranial transplantation of various human stem cell types and stem cell-derived EVs has now been shown to impart significant neuroprotective effects within the irradiated microenvironment of the brain. Improved learning and memory may reflect any combination of the factors related to reduced neuroinflammation and preserved host neuronal morphology and synaptic machinery. Furthermore, the beneficial effects of these transplantation paradigms are likely to be enhanced through the use of EVs, as they are clearly non-teratogenic, less immunogenic, and capable of migrating extensively throughout the irradiated brain. Although precise mechanistic links between stem cell and EV engraftment and enhanced cognition following irradiation require further elucidation, current data add to the evidence that stem cell-based transplantation strategies may one day provide a certain fraction of cancer survivors with much sought after relief from their persisting declines in cognitive health.

CHAPTER 3: INITIAL RESULTS — EFFECTS OF A CLINICALLY-RELEVANT COMBINED CHEMOTHERAPY/ RADIATION PROTOCOL USING TEMOZOLOMIDE

Introduction

Studies undertaken in the Limoli laboratory and by others have indicated that both irradiation and chronic chemotherapy treatment, including cyclophosphamide and doxorubicin, adversely impact cognitive function one to four months following exposure; further, though there are no satisfactory treatments for reducing the progressive adverse effects of radiation- and chemotherapy-induced brain injury, intracranial stem cell transplantation has shown promise in improving the cognitive decrements associated with both radiation and chemotherapy. My work has demonstrated the broader capability of human neural stem cells and human neural stem cell-derived extracellular vesicles to attenuate irradiation-induced neuroinflammation and increases in PSD-95, preserve host neuronal morphology, and modulate reduced levels of glial cell line-derived neurotrophic factor and dendritic spine density in the distal irradiated hippocampus, in part, mediated by their ability to migrate throughout the brain. As a logical follow-up, I then turned to examining whether these same therapies could have utility in ameliorating the negative neurocognitive behavioral effects associated with a systemic insult to the brain, intraperitoneal injections of the chemotherapeutic agent temozolomide (TMZ), in the context of a clinically-relevant treatment protocol also including fractionated radiation. Temozolomide is an alkylating agent that crosses the blood-brain barrier and is used primarily to treat glioblastoma [95]. After some unexpected results in the initial model system used for the combined chemotherapy/ irradiation paradigm, I shifted to a new model system to ameliorate some of the challenges faced, and first investigated the effects of temozolomide and irradiation, separately, on the cognition of Fischer 344 rats. The long-term deleterious effects of numerous chemotherapeutic

agents on the brain and cognitive function, known as “chemo-brain”, have been well-characterized [96]; however, the impact of temozolomide on the brain is not well understood.

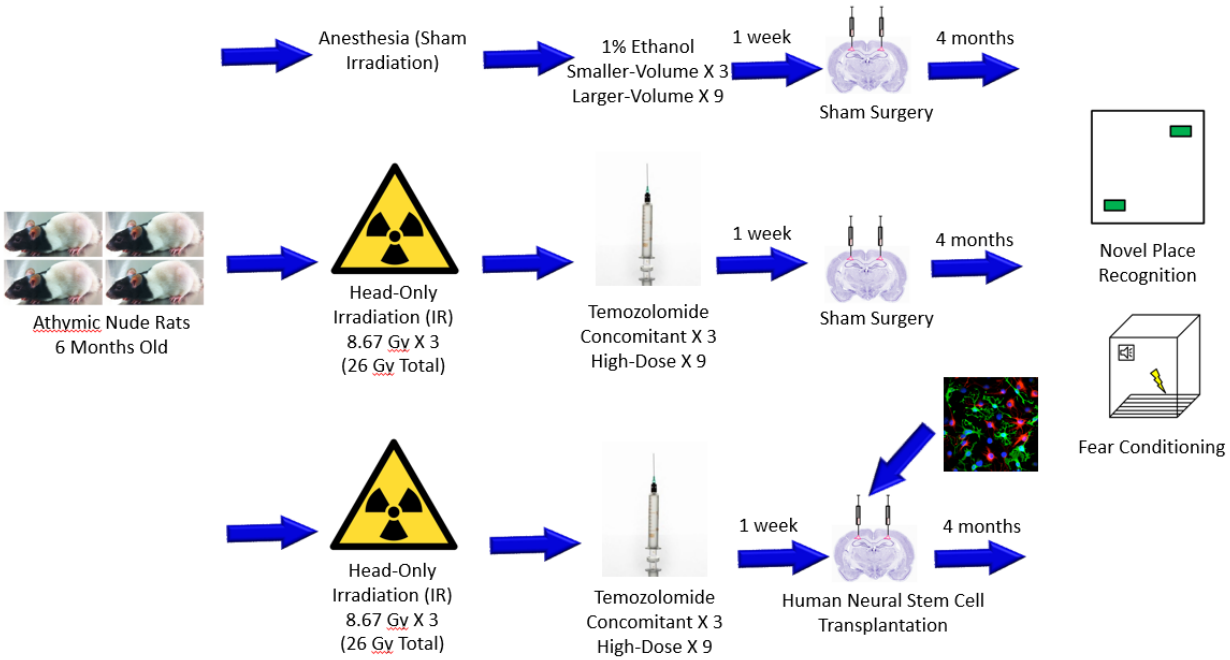

Figure 3.1: Experimental design (athymic nude rats)

Materials and Methods – Athymic Nude Rats

Animals and irradiation/ chemotherapy treatment

All animal procedures are in accordance with NIH and approved by the University of California Institutional Animal Care and Use Committee. Six-month-old male immunodeficient athymic nude (ATN) rats (Cr:NIHFoxn1rnu, strain 316; Charles River, San Diego) were maintained in sterile housing conditions (20°C ± 1°C; 70% ± 10% humidity; 12 hours:12 hours light and dark cycle) and had free access to sterilized diet and water. The ATN rats were divided into four experimental groups: 0 Gy receiving sham surgery (Con), 26 Gy head-only fractionated irradiation and temozolomide injection receiving sham surgery (IRR+TMZ), 26 Gy head-only fractionated irradiation and temozolomide injection receiving bilateral human neural stem cell (hNSC) grafting (hNSCs – IRR+TMZ), and 26 Gy head-only fractionated irradiation and temozolomide injection receiving bilateral hNSC-derived extracellular vesicle (EV) grafting (EVs – IRR+TMZ). For cranial irradiation, animals were anesthetized (2.5% isoflurane), placed ventrally and unrestrained on the treatment table (XRAD 320 irradiator, Precision X-ray, North Branford, CT), and positioned under a collimated (1.0 cm^2 diameter) beam for head-only irradiation delivered at a dose rate of 1.0 Gy/minute. Whole-brain irradiation for the TMZ+IRR group was delivered in 3 fractionated doses of 8.67 Gy for a total dose of 26 Gy. The 3 fractionated radiation treatments were be delivered to each rat over the course of 5 days (i.e. days 1, 3 and 5). This group also received TMZ delivered concurrently and post-irradiation, with the first concomitant injection of TMZ (3-Methyl-4-oxo-8-imidazolo[5,1-d][1,2,3,5]tetrazinecarboxa-mide or Temodar®, Sigma, St. Louis, MO, USA) delivered intraperitoneally on the day following each fractionated dose of irradiation (i.e., days 2, 4, and 6) at a dose of 12.5 mg/kg. One week following IRR and then again during the following two weeks, the TMZ+IRR animals received three TMZ injections delivered over the course of five days at a dose of 33.3 mg/kg, delivered

intraperitoneally and diluted in 1% ethanol. Thus, animals received 12 total TMZ injections over the course of 1 month, 3 during week 1 at 12.5 mg/kg and 9 during the subsequent 3 weeks at 33.3 mg/kg. Untreated control animals were anesthetized and handled identically to those undergoing irradiation, and received injections of 1% ethanol at the same volumes as TMZ injections.

Cranial transplantation

For the hNSC and hNSC-derived EV transplantations, the proprietary stem cell line HK532.UbC-IGF1 was used (Neuralstem Inc.), and the transplanted groups received bilateral intrahippocampal injections 1.5 weeks after the final TMZ injection. The TMZ+IRR and control cohorts underwent sham surgeries. Rats received bilateral intrahippocampal transplantation of hNSCs or EVs suspended in vehicle (hibernation buffer) using a 33-gauge microsyringe at an injection rate of 0.25 mL/minute. Each hippocampus received four distinct injections of live hNSCs (1×10^5 in 2 µL) per hemisphere using precise stereotaxic coordinates, as described previously [46]. Sham surgery controls received an equal volume of sterile hibernation buffer at the same stereotaxic injection coordinates. All cohorts were anesthetized using isoflurane/oxygen (5% (vol/vol) induction, 2.5% (vol/vol) maintenance; VetEquip).

	TMZ+IRR, hNSC Transplantation						
	Mon	Tues	Wed	Thurs	Fri	Sat	Sun
Week 1	IRR	TMZ	IRR	TMZ	IRR	TMZ	
Week 2	TMZ		TMZ		TMZ		
Week 3	TMZ		TMZ		TMZ		
Week 4	TMZ		TMZ		TMZ		
Week 5							
Week 6	hNSC						

Table 3.1: Timing of treatments for athymic nude rats

Behavioral cognitive testing

The rats were subjected to a battery of behavioral tasks four months after surgery. The animals were tested on spontaneous exploration tasks, namely Novel Place Recognition, which is sensitive to spatial cognitive impairments caused by hippocampal damage; Novel Object Recognition, which assesses episodic memory retention dependent on the frontal and pre-frontal cortex; Object in Place, which evaluates spatial memory retention facilitated by both the hippocampus and the pre-frontal cortex; Temporal Order, which interrogates recency memory dependent on the medial prefrontal cortex and perirhinal cortex; Elevated Plus Maze, which assesses anxiety-like behavior; and Light-Dark Box, which also serves as an assay for anxiety-like behavior. For the Novel Place Recognition, Novel Object Recognition, Object in Place and Temporal Order tasks, the trials were scored for exploration time of the novel and familiar objects for each animal and the discrimination index was calculated from the equation: [(Novel Object/Total Exploration Time) – (Familiar/Total Exploration Time)] × 100. A cognitively-intact animal is expected to exhibit a preference for novelty in each of these tasks. The Elevated Plus Maze was comprised of an acrylic surface with four elevated arms (75 cm above the floor, 110 cm long and 10 cm arm width) with two opposing closed arms enclosed with 42-cm high walls. Rats were initially placed in the central zone of the EPM, with their head facing towards an open arm, and allowed to freely explore the maze for five minutes. The frequency of entries in the open arms were recorded, with entry into an open arm defined as all four paws of the rat crossing into the open arm. For the Light-Dark Box testing, the rats were initially positioned in the center of the light compartment facing away from the opening to the dark compartment and allowed to explore freely for 10 minutes. The number of transitions between the light and dark chambers was assessed. Statistical analysis was performed using a repeated measure ANOVA with Bonferroni

correction in GraphPad Prism 6.0 Software (GraphPad Software Inc.), and data was plotted as mean ± SEM with significance set at $\alpha = 0.05$.

Results and Conclusions

There were no statistically significant differences between groups on any of the tasks, though some showed a trend towards a cognitive decrement in the IRR+TMZ group. This was due in part to significant variation within groups, as well as a decreased N for the IRR+TMZ, hNSCs – IRR+TMZ, and EVs – IRR+TMZ groups secondary to significant mortality among rats who had received the IRR+TMZ paradigm. In each cohort, numerous rats developed large abdominal masses that impeded their movement and ability to eat, and thus had to be sacrificed; several other rats developed vestibular deficits leading to head tilts; and additional rats also developed malocclusions which needed to be trimmed intermittently and disrupted normal feeding. Because of these problems with the aged ATN rats tolerating the IRR+TMZ protocol, I made the decision to move to using 2-month-old Fischer 344 (immunocompetent) rats for the remainder of my studies.

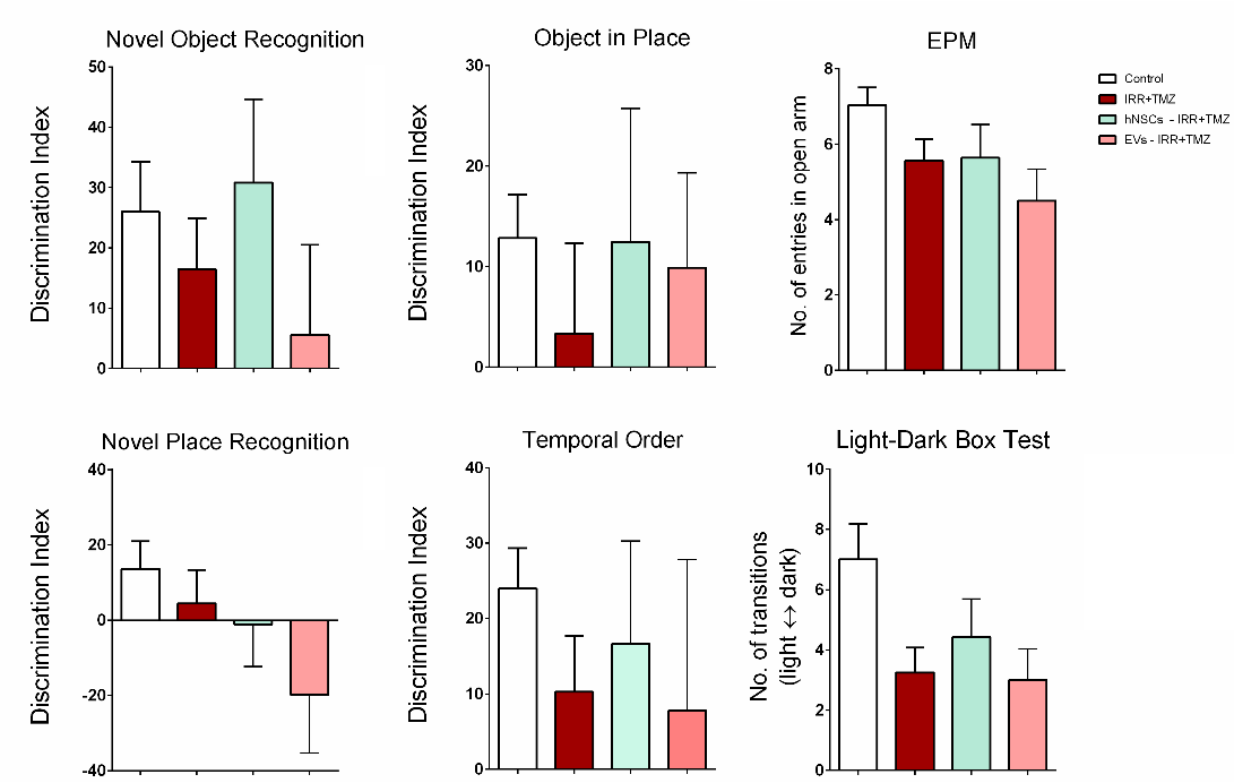

Figure 3.2: Spontaneous exploration data for athymic nude rats receiving a combined irradiation (IRR) and temozolomide (TMZ) treatment paradigm, including several hippocampal- and pre-frontal cortex-dependent learning and memory tasks– Novel Object Recognition (NOR), Novel Place Recognition (NPR), Object in Place (OiP), and Temporal Order (TO); and two assays intended to assess anxiety– Elevated Plus Maze (EPM) and Light-Dark Box (LDB). There were no statistically-significant differences between groups (P values derived from ANOVA and Bonferroni's multiple comparisons test), and significant variability within groups, although some tasks suggest a potential cognitive deficit in the IRR+TMZ group.

Introduction – The Effects of Fractionated Irradiation and Temozolomide Treatment on Cognitive Function in Fischer 344 Rats

We next compared the effects of temozolomide and the effects of fractionated irradiation as separate treatment groups on cognition in 2-month-old Fischer 344 animals. The athymic nude rats that were first administered the combined TMZ+IRR protocol experienced significant peripheral toxicity unrelated to cognitive function (abdominal masses, vestibular issues, malocclusions), which made it difficult to maintain a sufficient sample size to observe potential cognitive decrements; it is also possible that the exclusion of animals from these behavioral studies based on other toxicities selected for the rats that were least affected by the TMZ+IRR exposure overall, and thus had the best neurological function in the cohort, while excluding the animals that were most impacted and may have had the most profound cognitive impairments. To try to circumvent these unforeseen challenges, we elected to move from six-month-old athymic nude rats to two-month-old Fischer 344 rats as our model system. We hypothesized that the younger age of the animals would inculcate more resilience to the cancer therapies being employed in our studies. We also favored using immunocompetent (Fischer 344) rats over immunocompromised (athymic nude) rats due to their improved vitality. Athymic nude rats had been used in my previous studies to evade the threat of immunorejection of the transplanted human neural stem cells proffered as therapeutic interventions for irradiation-induced cognitive dysfunction. However, our findings published in *Stem Cells Translational Medicine* (see: Chapter 2) as well as other concurrent studies in the Limoli lab [97] offered increasingly-strong evidence that stem cell-derived extracellular vesicles hold significant promise for ameliorating radiation-induced brain injury while mitigating the risk of host immunorejection associated with transplanted cells, suggesting that future studies investigating the potential of extracellular vesicles as a clinically-relevant therapy could be viable in immunocompetent models.

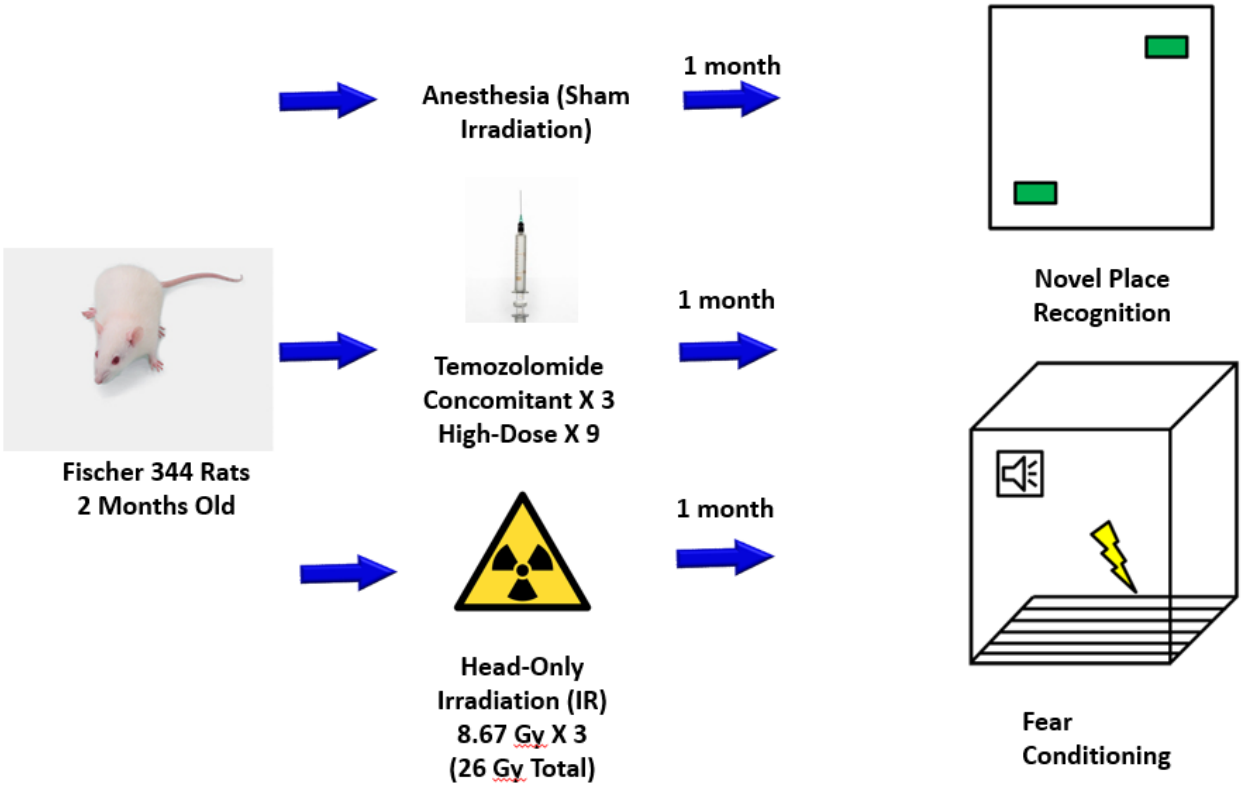

Figure 3.3: Experimental design (Fischer 344 rats)

Materials and Methods – Fischer 344 Rats

Animals and irradiation/ chemotherapy treatment

All animal procedures are in accordance with NIH and approved by the University of California Institutional Animal Care and Use Committee. Two-month old male Fischer 344 rats (Crl:CD(Fischer 344), strain 002, Charles River Laboratories, Wilmington, MA) were maintained in standard housing conditions (20°C ± 1°C; 70% ± 10% humidity; 12 h:12 h light and dark cycle) and provided *ad libitum* access to food and water. The rats were divided into three experimental groups: animals that received sham irradiation/ anesthesia and intraperitoneal injections of 1% ethanol solvent (Control), animals that received 26 Gy fractionated irradiation (IRR), and animals that received intraperitoneal injections of temozolomide (TMZ). The TMZ cohort received three injections of TMZ (3-Methyl-4-oxo-8-imidazolo[5,1-d][1,2,3,5]tetrazinecarboxa-mide or Temodar®, Sigma, St. Louis, MO, USA) delivered intraperitoneally and diluted in 1% ethanol, over five days at a concommitant dose of 12.5 mg/kg during the first week of treatment, followed by 3 weeks of three TMZ injections delivered over five days at a dose of 33.3 mg/kg, delivered intraperitoneally and diluted in 1% ethanol. Thus, animals received 12 total TMZ injections over the course of 1 month, 3 during week 1 at 12.5 mg/kg and 9 during the subsequent 3 weeks at 33.3 mg/kg. During the last week of injections for the TMZ cohort, the IRR group received a total of 26 Gy in three fractionated doses over the course of five days. Whole-brain irradiation for the IRR group was delivered in 3 fractionated doses of 8.67 Gy for a total dose of 26 Gy. For cranial irradiation, animals were anesthetized (2.5% isoflurane), placed ventrally and unrestrained on the treatment table (XRAD 320 irradiator, Precision X-ray, North Branford, CT), and positioned under a collimated (1.0 cm^2 diameter) beam for head-only irradiation delivered at a dose rate of 1.0 Gy/minute. Untreated control animals were

anesthetized and handled identically to those undergoing irradiation, and received injections of 1% ethanol at the same volumes as TMZ injections.

	TMZ Cohort						
	Day 1	Day 2	Day 3	Day 4	Day 5	Day 6	Day 7
Week 1	TMZ (low dose)		TMZ (low dose)		TMZ (low dose)		
Week 2	TMZ (high dose)		TMZ (high dose)		TMZ (high dose)		
Week 3	TMZ (high dose)		TMZ (high dose)		TMZ (high dose)		
Week 4	TMZ (high dose)		TMZ (high dose)		TMZ (high dose)		
Week 5							
Week 6							
Week 7							
Week 8							
Week 9	Behavioral Testing						

	IRR Cohort						
	Day 1	Day 2	Day 3	Day 4	Day 5	Day 6	Day 7
Week 1							
Week 2							
Week 3							
Week 4	8.67 Gy IRR		8.67 Gy IRR		8.67 Gy IRR		
Week 5							
Week 6							
Week 7							
Week 8							
Week 9	Behavioral Testing						

Table 3.2: Timing of treatments for TMZ and IRR cohorts of Fischer 344 rats

Behavioral cognitive testing

These animals likewise underwent a series of behavioral tests at one month following the last set of TMZ injections and dose of fractionated IRR. The animals were tested on spontaneous exploration tasks, namely Novel Place Recognition, which is sensitive to spatial cognitive impairments caused by hippocampal damage; Novel Object Recognition, which assesses episodic memory retention dependent on the frontal and pre-frontal cortex; Object in Place, which evaluates spatial memory retention facilitated by both the hippocampus and the pre-frontal cortex; Light-Dark Box, which serves as an assay for anxiety-like behavior; and Fear Conditioning, which determines whether rats can learn conditioned fear responses. For the Novel Place Recognition, Novel Object Recognition, and Object in Place tasks, the trials were scored for exploration time of the novel and familiar objects for each animal and the discrimination index was calculated from the equation: [(Novel Object/Total Exploration Time) – (Familiar/Total Exploration Time)] × 100. A cognitively-intact animal is expected to exhibit a preference for novelty in each of these tasks. For the Light-Dark Box testing, the rats were initially positioned in the center of the light compartment facing away from the opening to the dark compartment and allowed to explore freely for 10 minutes. The number of transitions between the light and dark chambers was assessed. Statistical analysis was performed using a repeated measure ANOVA with Bonferroni correction in GraphPad Prism 6.0 Software (GraphPad Software Inc.), and data was plotted as mean ± SEM with significance set at $\alpha = 0.05$.

Results

The cohort of animals treated with temozolomide and the cohort of animals treated with irradiation both failed to discriminate between the novel toys and the familiar toys during the learning and memory tests (Figure 3.4), including Novel Object Recognition, Novel Place Recognition, and Object in Place; however, the performance of these animals was not statistically

significantly different from control animals, though they did show a trend towards a cognitive decrement. There were no statistically significant differences in performance among the cohorts on the Light Dark Box task. Most interestingly, there was a statistically significant difference between the time both the TMZ and the IRR cohorts spent freezing during the context test of Fear Conditioning relative to the controls (Figure 3.5), suggesting an inability among animals exposed to these cancer therapies to associate the environment with the aversive stimulus. These data offer the first evidence in the Limoli laboratory of cognitive decrements related to temozolomide administration in immunocompetent rats.

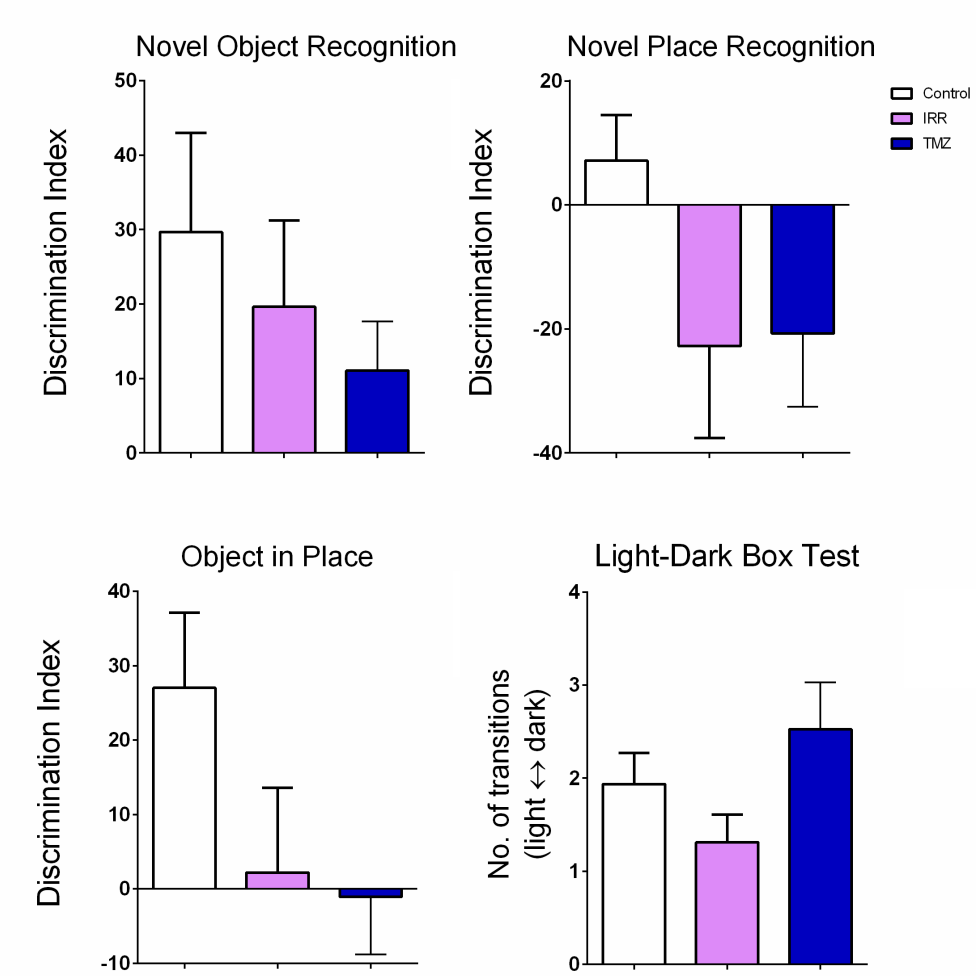

Figure 3.4: Performance on spontaneous exploration tasks by Fischer rats after administration of 26 Gy fractionated irradiation (IRR), a four-week sequence of intraperitoneal injections of temozolomide (TMZ), or sham irradiation/ solvent injection (Control). The TMZ and IRR cohorts exhibit a failure to discriminate between novel and familiarity on the learning and memory tasks (Novel Object Recognition, Novel Place Recognition, and Object in Place); however, the differences in discrimination index between these animals and the control animals was not statistically significant. The Control, IRR, and TMZ cohorts demonstrated statistically comparable performance on the Light Dark Box task. Data are presented as the mean ± SEM (N = 16 animals/group). *P*-values are derived from analysis of variance and Bonferroni's multiple comparisons test.

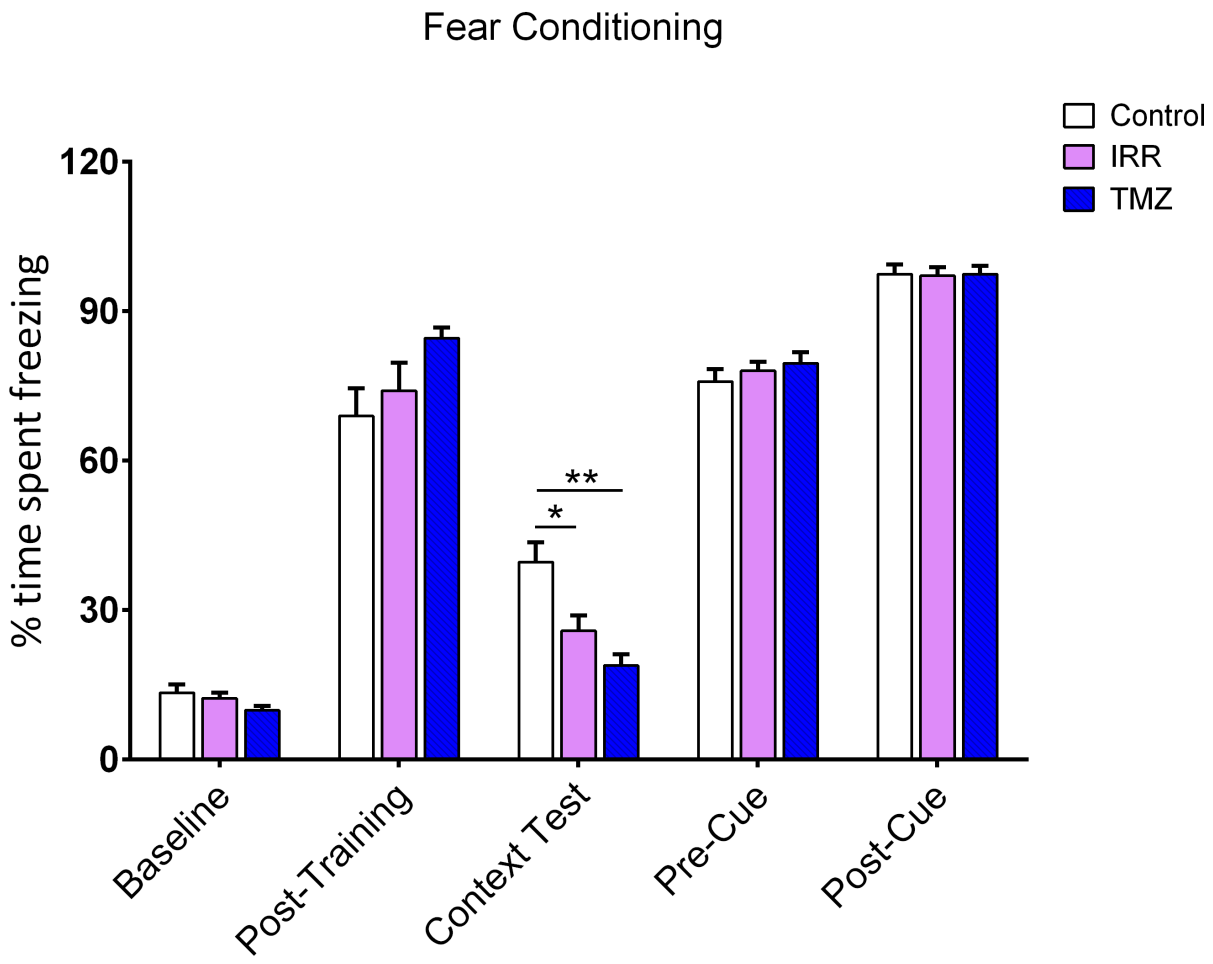

Figure 3.5: Percentage of time spent freezing by Fischer 344 rats receiving fractionated irradiation (IRR), intraperitoneal temozolomide (TMZ), or sham irradiation/ intraperitoneal 1% ethanol in a fear conditioning paradigm. The three cohorts had statistically indistinguishable percentages of time freezing at baseline, post-training, pre-cue, and post-cue; however, both the IRR animals and the TMZ animals showed a significant reduction in time spent freezing during the context test, implying an inability of these animals to remember the association of the testing environment with the foot-shocks. Data are presented as the mean ± SEM (N = 16 animals/group). *P*-values are derived from analysis of variance and Bonferroni's multiple comparisons test. *, $P < .05$; **, $P < .01$; all compared against the control group

CHAPTER 4: GABAERGIC EXTRACELLULAR VESICLES IMPROVE COGNITION FOLLOWING IRRADIATION, WHILE GLUTAMATERGIC EXTRACELLULAR VESICLES FAIL TO DO SO — THE NEUROBIOCHEMICAL MECHANISTIC BASIS

Introduction

Our studies further explored whether retro-orbital injection of extracellular vesicles (EVs) derived from GABAergic neurons can ameliorate the adverse effects of irradiation exposure on cognition by assessing performance on hippocampus-, prefrontal cortex- and amygdala-dependent tasks. cognitive function and determining whether retro-orbital injection of extracellular vesicles derived from GABAergic neurons can alleviate treatment-associated deficits in cognition at one month following treatment. GABAergic neuron-derived EVs are proposed to improve cognition after IRR treatment through providing an inhibitory impetus to compensate for irradiation- and chemotherapy-induced hippocampal hyperexcitation, as is apparent in preliminary electrophysiology studies in irradiated animals on long-term potentiation (Figure 4.1). We sought to characterize the impact of irradiation and GABAergic neuron-derived EVs on neuroinflammation, host neuronal morphology, and neurotrophin levels. Further, we examined whether EVs derived from glutamatergic neurons proffer the same advantageous impact on cognition after IRR treatment as we observed from EVs derived from GABAergic neurons. We hypothesized that EVs produced by excitatory glutamatergic neurons would not convey the same beneficial effects following fractionated irradiation and evaluated this theory by comparing cognitive behavior in animals receiving injections of EVs from each source.

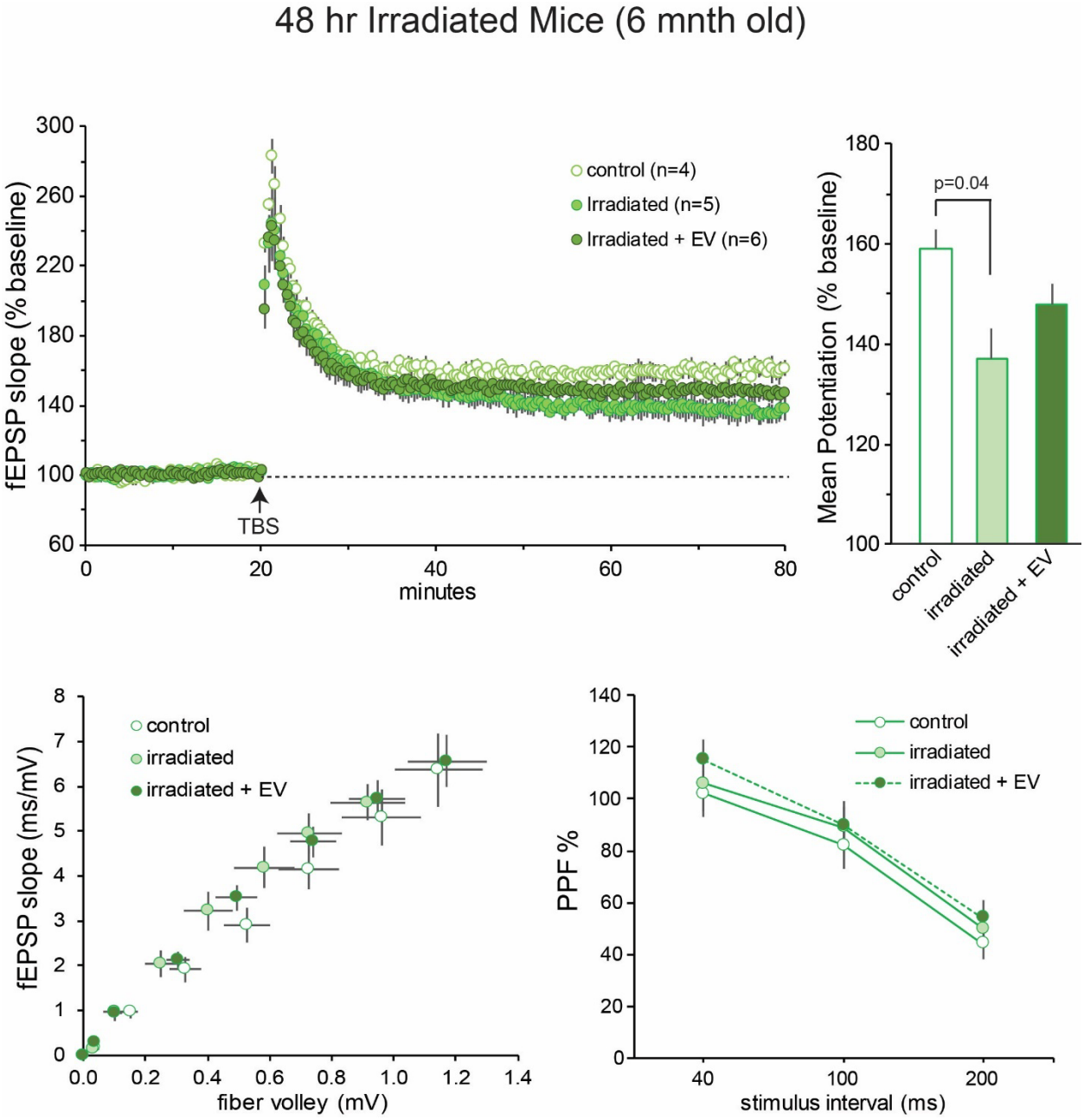

Figure 4.1: Preliminary electrophysiology data in irradiated mice following the retro-orbital application of extracellular vesicles. A reduction in mean potentiation was observed in the irradiated rat, which was attenuated by the retro-orbital injection of extracellular vesicles.

Materials and Methods

Animals and irradiation

All animal procedures are in accordance with NIH and approved by the University of California Institutional Animal Care and Use Committee. Eight-week-old male Fischer 344 rats (Crl:CD(Fischer 344), strain 002, Charles River Laboratories, Wilmington, MA) were maintained in standard housing conditions (20°C ± 1°C; 70% ± 10% humidity; 12 h:12 h light and dark cycle) and provided *ad libitum* access to food and water. For both the GABAergic extracellular vesicle cohort and the glutamatergic extracellular vesicle cohort, the Fischer 344 rats were divided into three experimental groups (N = 16 animals per group): a control group that received sham irradiation (exposure to anesthesia) and vehicle (hibernation buffer) retro-orbital injections, a group that received 26 Gy total fractionated irradiation and vehicle injections, and a group that received 26 Gy total fractionated irradiation and injections of GABAergic or glutamatergic neuron-derived extracellular vesicles. Rats were anesthetized using an isoflurane gas system (VWR Mobile RC2; induction=3.5% vol/vol isoflurane/oxygen) for irradiation, which was delivered using a self-shielded 320 kV X-irradiator (X-RAD320 irradiator, Precision X-Ray, North Branford, CT) and lead shielding to facilitate head-only irradiation over a 2 cm^2 area at a dose rate of 1 Gy/min. The study was initiated with the irradiated experimental groups receiving three fractionated doses of whole-brain irradiation of 8.67 Gy x 3 (total 26 Gy) over the course of five days (i.e. on days 1, 3, and 5). Control animals were anesthetized for the same amount of time as the irradiated animals to ensure corresponding isoflurane exposure, and handled identically to those undergoing irradiation.

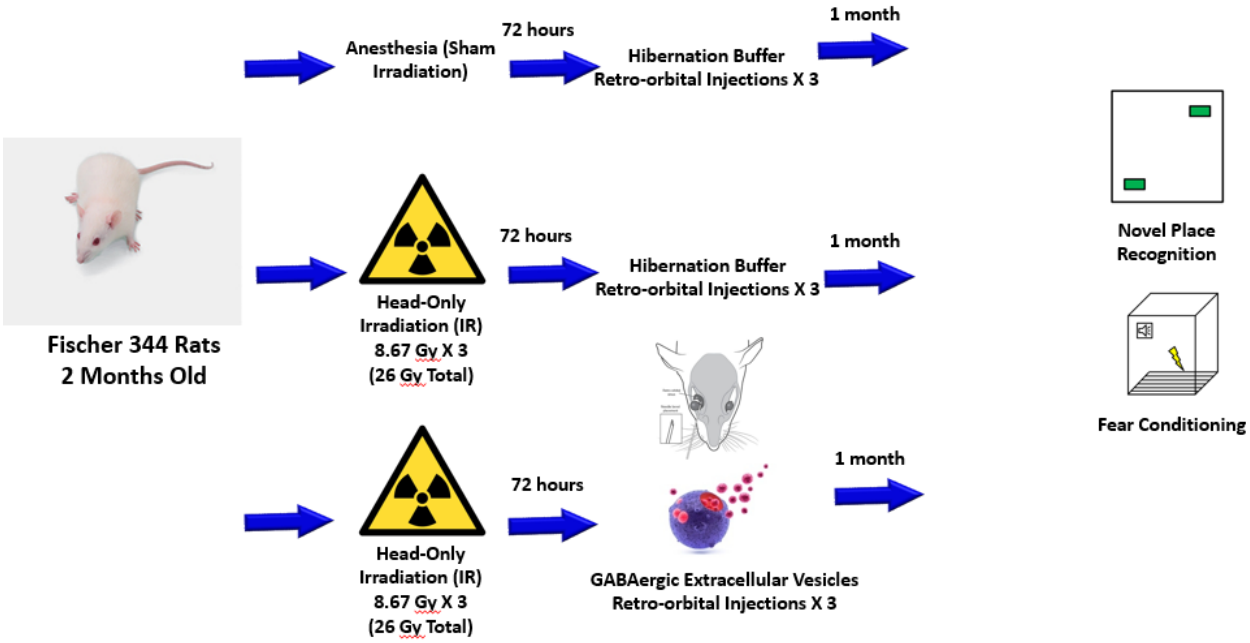

Figure 4.2: Experimental design

Extracellular vesicle isolation

GABAergic neuron-derived extracellular vesicles were collected from conditioned culture media in which induced pluripotent stem (iPS) cell-derived GABAergic neurons (iCell GABANeurons, 01434, FUJIFILM Cellular Dynamics, Inc, Madison, WI) were cultured. The extracellular vesicles were isolated and purified from the conditioned media by ultracentrifugation. The conditioned media was first centrifuged at 300 x g for 10 minutes to remove cells and cellular debris. The media was then centrifuged at 100,000 × g for 90 minutes and the extracellular vesicles were collected in hibernation buffer; the extracellular vesicles were pooled and purified in sterile Dulbecco's phosphate-buffered saline at 100,000 x g for 120 minutes, and collected in hibernation buffer. The extracellular vesicles were characterized using a ZetaView PMX 110 particle analyzer (Particle Metrix GmbH; Meerbusch Germany).

Glutamatergic neuron-derived extracellular vesicles were collected from conditioned culture media in which iPS cell-derived glutamatergic neurons (iCell GlutaNeurons, 01279, FUJIFILM Cellular Dynamics, Inc, Madison, WI) were cultured. The extracellular vesicles were isolated and purified from the conditioned media by the same ultracentrifugation protocol as for the GABAergic extracellular vesicles.

Retro-orbital injections

At 72 hours following the final fractionated dose of irradiation (i.e. on day 8), the rats were anesthetized using an isoflurane gas system (VWR Mobile RC2; maintenance=3.5% vol/vol isoflurane/oxygen), and extracellular vesicles or vehicle (hibernation buffer) were delivered to the rats through circulation via the retro-orbital sinus. A 31-gauge needle with a 0.5 ml syringe attached (BD Veo™ insulin syringes with BD Ultra-Fine™ 6mm x 31G needle) was used to pierce 2 to 3 mm into the rat's orbital venous sinus with the bevel on the needle facing upward at a 45° angle before injecting the extracellular vesicles. The control and irradiated experimental groups

for both the GABAergic and glutamatergic cohorts received retro-orbital injections of 100 microliters hibernation buffer (vehicle). For the GABAergic extracellular vesicle group, 1.5 x 10^9 extracellular vesicles in 100 microliters hibernation buffer were delivered by retro-orbital injection. For the glutamatergic extracellular vesicle group, 1.0 x 10^9 extracellular vesicles in 100 microliters hibernation buffer were delivered by retro-orbital injection.

	Day 1	Day 2	Day 3	Day 4	Day 5	Day 6	Day 7
Week 1	IRR		IRR		IRR		
Week 2	EV RO						
Week 3	EV RO						
Week 4	EV RO						
Week 5							
Week 6	Behavioral Testing						

Table 4.1: Timeline of treatments for irradiation +/- GABAergic or glutamatergic extracellular vesicles

Behavioral cognitive testing

Two weeks following the last retro-orbital injections, the rats underwent a battery of behavioral tasks designed to interrogate cognitive function. The animals were tested on spontaneous exploration tasks, namely Novel Place Recognition, which is sensitive to spatial cognitive impairments caused by hippocampal damage; Novel Object Recognition, which assesses episodic memory retention dependent on the frontal and pre-frontal cortex; Object in Place, which evaluates spatial memory retention facilitated by both the hippocampus and the pre-frontal cortex; and Light-Dark Box, which serves as an assay for anxiety-like behavior. For the Novel Place Recognition, Novel Object Recognition, and Object in Place tasks, the trials were scored for exploration time of the novel and familiar objects for each animal (n=16 per experimental group) and the discrimination index was calculated from the equation: [(Novel Object/Total Exploration Time) – (Familiar/Total Exploration Time)] × 100. A cognitively-intact animal is expected to exhibit a preference for novelty in each of these tasks. For the Light-Dark Box testing, need to measure dimensions of light-dark box. The rats were initially positioned in the center of the light compartment facing away from the opening to the dark compartment and allowed to explore freely for 10 minutes. The number of transitions between the light and dark chambers was assessed. Statistical analysis was performed using a repeated measure ANOVA with Bonferroni correction in GraphPad Prism 6.0 Software (GraphPad Software Inc.), and data was plotted as mean ± SEM with significance set at $\alpha = 0.05$.

Extraction and ELISA for assessment of neurotrophins

Following the behavioral testing at approximately six weeks post-final retro-orbital injections, the rats were euthanized using isoflurane anesthesia. Brains were immediately extracted from the skull (N = 4-5 per group) and the hippocampus was dissected from each cerebral hemisphere. Each hippocampus was weighed and transferred into 300 µL ice-cold lysis buffer (N-PER

Neuronal Protein Extraction Reagent, Thermo Scientific Product number 23225) containing sodium orthovanadate (0.5 mM), pheyl-methylsulfonyl fluoride (PMSF, 1 mM), aprotinin (10 µg/mL), and leupeptin (1 µg/mL; Santa Cruz Biotechnology, Santa Cruz, California). Tissues were sonicated individually, centrifuged at 4°C for 15 minutes at 13,200 rpm, and the supernatants were collected and diluted 1:5 with Dulbecco's phosphate-buffered saline. The supernatants were acidified to pH 2.6 then neutralized to pH 7.6 to liberate the neurotrophic factors, and the BDNF and GDNF levels were assayed using E_{max} ImmunoAssay Systems from Promega (BDNF catalog number G7611, GDNF catalog number G7621) and uncoated ELISA plates (Biolegend Nunc MaxiSorp, catalog number 423501). All measurements were performed at a wavelength of 450 µm on a microplate reader (BioTek Synergy Mx).

Quantification of dendritic spine density

At approximately six weeks post-final retro-orbital injections, the rats were euthanized using isoflurane anesthesia and perfused with saline + heparin. Brains (N = 4 per group) were extracted from the skull and subjected to Golgi-Cox impregnation and staining of neurons according to the manufacturer's instructions (SuperGolgi kit, Bioenno Tech., Santa Ana, California). The brains were sectioned to 100 µm using a vibratome (need details on vibratome) and counterstained by nuclear fast red to visualize hippocampal subregions. The Stereoinvestigator program (v11, MicroBrightField) was used for the quantification of dendritic spines using four serial sections (every second) throughout the hippocampus to analyze potential differences in spine density between each of the experimental cohorts.

Immunostaining of Activated Microglia

Following behavioral testing, rats were euthanized using isoflurane and perfused with 4% paraformaldehyde (Acros Organics, Geel, Belgium), and brain tissues were processed for coronal

sectioning using a cryostat (Leica Microsystems, Wetzlar, Germany) and prepared for immunohistochemistry. Immunostaining for activated microglia (ED-1^+ cells) was carried out on serial sections (30 μm coronal, every tenth section) with six sections per animal (N = 4 per experimental group), via a primary anti-ED-1 antibody (mouse, 1:200; AbD Serotec) followed by a donkey anti-mouse biotinylated secondary antibody (1:200; Invitrogen). Sections were mounted on gelatin-coated slides, air-dried, dehydrated and counterstained with nuclear fast red (Vector Labs, CA, USA). The number of activated microglia (ED1+) within the DH, GCL and CA3/CA1 regions of hippocampus were analyzed by stereology.

Extracellular Vesicle Labeling

To interrogate the distribution of extracellular vesicles administered by retro-orbital injections throughout the hippocampus, GABAergic neuron-derived extracellular vesicles were labeled with PKH26 (Sigma-Aldrich, PKH26GL) the morning before injection. The extracellular vesicles were resuspended in Diluent C, incubated with Dye Solution for 4 minutes with intermittent mixing as per the manufacturer's protocol. The dye was quenched with 1% bovine serum albumin in water, and the extracellular vesicles were isolated through ultracentrifugation at 100,000 × g for 90 minutes and collected in hibernation buffer. For each animal, $1.5x10^{10}$ extracellular vesicles were dyed and prepared for injection.

Labeled Extracellular Vesicle Administration, Tracking, and Quantification

Male Fischer 344 rats (Crl:CD(Fischer 344), strain 002, Charles River Laboratories, Wilmington, MA) were divided into two groups (N =2 animals per group): a control group that received sham irradiation (exposure to anesthesia) and an irradiated group that received 26 Gy total fractionated irradiation (8.67 Gy x 3). At 72 hours post-irradiation, the animals received injections of PKH26-labeled extracellular vesicles in 100 microliters hibernation buffer by retro-

orbital injection as described above. The rats were euthanized at 24 hours following the injections using isoflurane and perfused with 4% paraformaldehyde. The brains were processed for coronal sectioning using a cryostat (Leica Microsystems, Wetzlar, Germany) in the dark to preserve the dye labeling. Four serial sections (30 μm, every 10th section) were stained with DAPI and imaged using a confocal microscope at ×40 magnification. Analysis was performed using the spot tool (Imaris software suite (v7.6, Bitplane, Inc.). To quantify the density of EVs, the number of EVs was converted into spots, derived from confocal Z-stacks taken in 1 μm steps at ×40 magnification.

Results:

Retro-Orbital Application of GABAergic Extracellular Vesicles Improves Cognition and Rescues Performance on Behavioral Tasks Following Irradiation

Two weeks subsequent to the final retro-orbital injections and four weeks subsequent to irradiation, the Fischer 344 rats (N = 16 rats per group) were subjected to a series of spontaneous exploration tasks to evaluate their cognitive capabilities. The animals were habituated to the testing room and arena for three days before performing the Novel Object Recognition test to evaluate hippocampal function, in which they were exposed to two identical objects for five minutes, then removed from the arena for five minutes, then returned to the arena with one of the same ("familiar") objects and a new ("novel") object. Control animals were able to discriminate between the novel and familiar objects and exhibited a preference for the novel objects as expected for cognitively-intact animals (mean discrimination index= 29.45%), while the animals that received fractionated irradiation showed no ability to discriminate between novel and familiar (mean discrimination index=-1.72%). The rats treated with GABAergic extracellular vesicles following irradiation demonstrated improvement in cognitive function on the Novel Object Recognition Task (mean discrimination index= 32.55%). Significant overall group effects were

found (F (2, 47) = 4.738; P=0.0134), and the differences between the performance of the control group and the irradiated group (F (2, 47) = 4.738; P=0.0480) and that of the irradiated group and the extracellular vesicle-treated group (F (2, 47) = 4.738; P=0.0206) were statistically significant (Figure 4.3). In contrast, the mean discrimination index of the control group and the extracellular vesicle group were statistically indistinguishable (F (2, 47) = 4.738; P>0.9999).

The rats were next tested on the Novel Place Recognition test to evaluate the capability of the pre-frontal and frontal cortex. The animals were placed in an arena with two identical objects for five minutes, then returned to their housing for one hour, and finally placed back in the arena with one of the objects in its original position ("familiar") and the other object moved to a different position ("novel"). The Novel Place Recognition test detected an overall group effect (F (2, 45) = 3.829; P=0.0291), and the control (mean discrimination index=24.88%) and extracellular vesicle-treated (mean discrimination index= 26.45%) groups had higher mean discrimination indices than the irradiated group (mean discrimination index= -12.17%); however, neither the difference between the control and the irradiated groups (F (2, 45) = 3.829; P= 0.0705) nor the difference between the irradiated and extracellular vesicle-treated groups (F (2, 45) = 3.829; P= 0.0554) met the threshold for statistical significance (Figure 4.4).

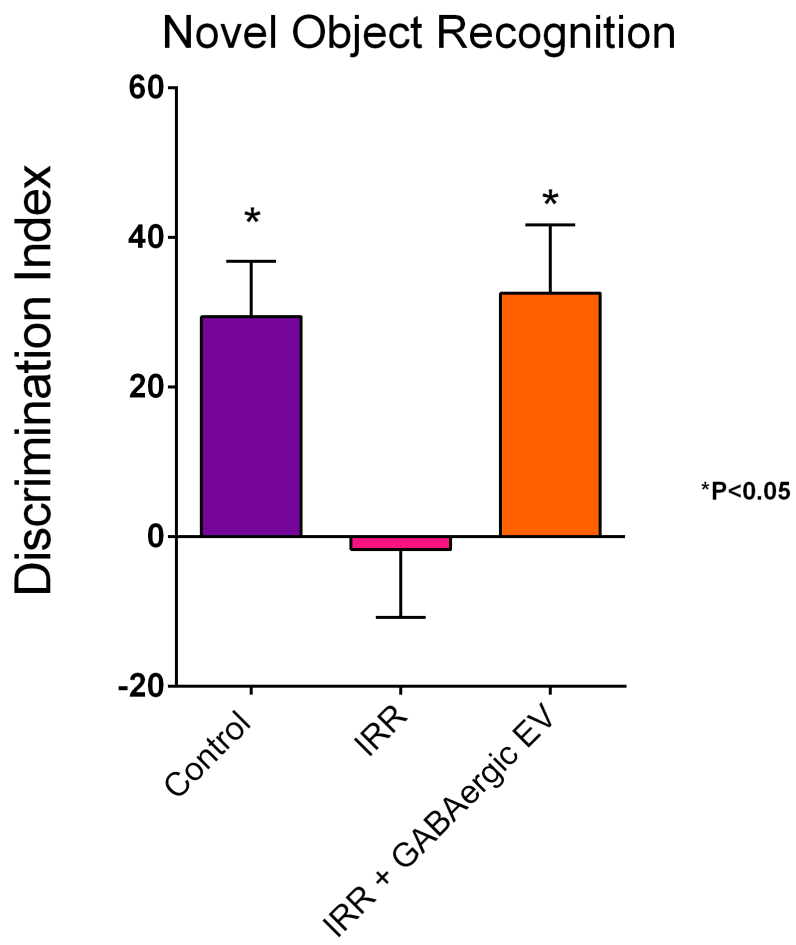

Figure 4.3: Retro-orbital injection of GABAergic extracellular vesicles improves performance on the Novel Object Recognition test following fractionated irradiation. Data are presented as the mean ± SEM (N = 16 animals/group. *P*-values are derived from analysis of variance and Bonferroni's multiple comparisons test. *, $P < .05$; all compared against the irradiated group

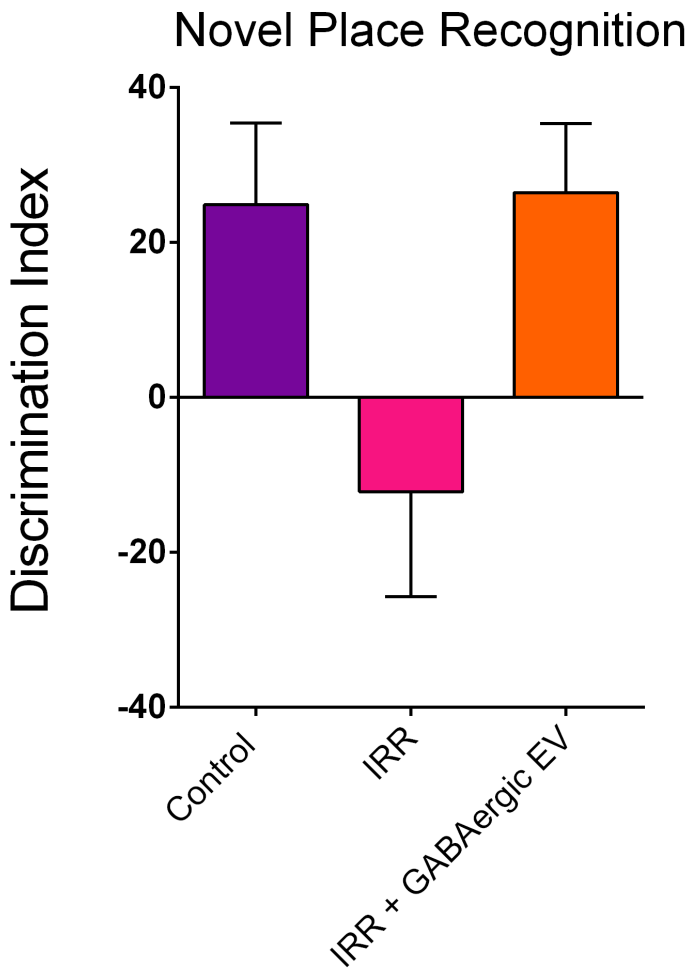

Figure 4.4: Performance on the Novel Place Recognition task following 26 Gy fractionated irradiation +/- retro-orbital injection of GABAergic extracellular vesicles. The irradiated rats failed to discriminate between novel and familiar, and an overall group effect was detected, with the mean discrimination indices of the control and IRR + GABAergic EV cohorts increased over that of the IRR group; however, the difference was not statistically significant. Data are presented as the mean ± SEM (N = 16 animals/group. *P*-values are derived from analysis of variance and Bonferroni's multiple comparisons test. All compared against the irradiated group

Testing on the Object in Place task was then initiated, which seeks to interrogate the proficiency of the hippocampus and pre-frontal cortex. After two additional days of habituation, the rats were exposed to four different objects in the arena for five minutes, then taken out of the box for five minutes. When they were subsequently returned to the arena for five minutes, the positions of two of the objects were reversed ("novel"), while the other two objects remained in place ("familiar"). As with the other spontaneous exploration tasks, rats with normal cognitive function are expected to exhibit a preference for the novel objects. Significant group effects were observed for this test ($F(2, 45) = 9.104$; $P=0.0005$), and there were statistically-significant increases in the mean discrimination index for both the control group ($F(2, 45) = 9.104$; $P= 0.0492$) and the extracellular vesicle-treated group ($F(2, 45) = 9.104$; $P= 0.0003$) as compared to the irradiated group (Figure 4.5), which failed to discriminate between novel and familiar (mean discrimination index= -17.13%). The performance of the control group (mean discrimination index= 14.05%) and the extracellular vesicle-treated group (mean discrimination index= 35.95%) was statistically similar ($F(2, 45) = 9.104$; $P= 0.2599$).

Finally, the Fischer 344 rats underwent a Light-Dark Box testing paradigm to examine anxiety-like behavior, and the number of transitions between the light compartment and the dark compartment were recorded. Significant overall group effects were detected ($F(2, 45) = 6.466$; $P=0.0034$), and the control animals (Figure 4.6) exhibited a significantly higher ($F(2, 45) = 6.466$; $P=0.0027$) number of transitions (mean number of transitions=3.750) compared to the irradiated rats (mean number of transitions=1.188). The extracellular vesicle-treated group likewise had a higher number of transitions (mean number of transitions=2.125) relative to the irradiated group, but this difference was not statistically significant ($F(2, 45) = 6.466$; $P=0.6005$).

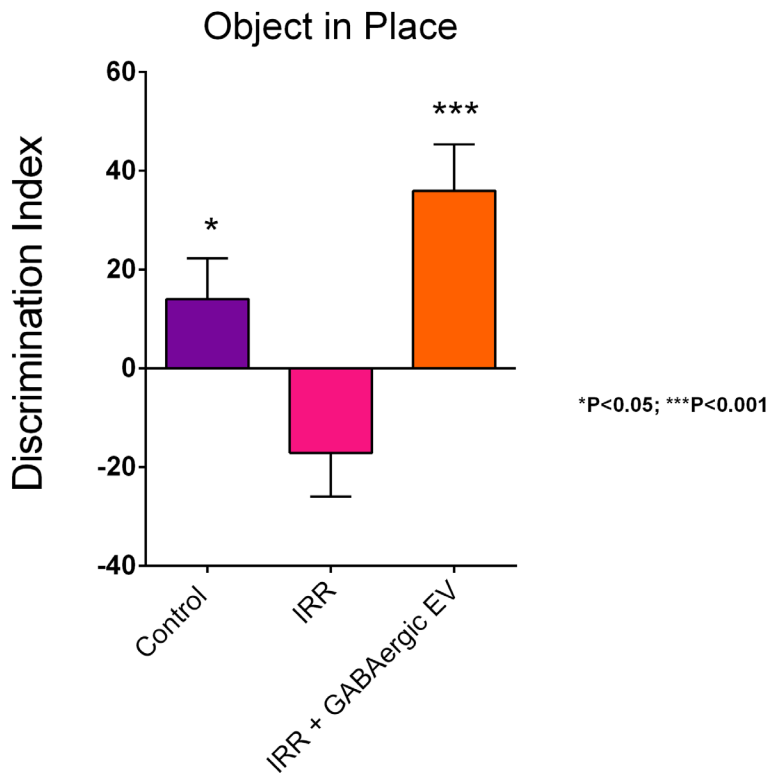

Figure 4.5: Application of GABAergic extracellular vesicles by retro-orbital injection ameliorates irradiation-induced decrements in performance on the Object in Place spontaneous exploration task. Data are presented as the mean ± SEM (N = 16 animals/group). *P*-values are derived from analysis of variance and Bonferroni's multiple comparisons test. *, $P < .05$; ***, $P < .001$ all compared against the irradiated group

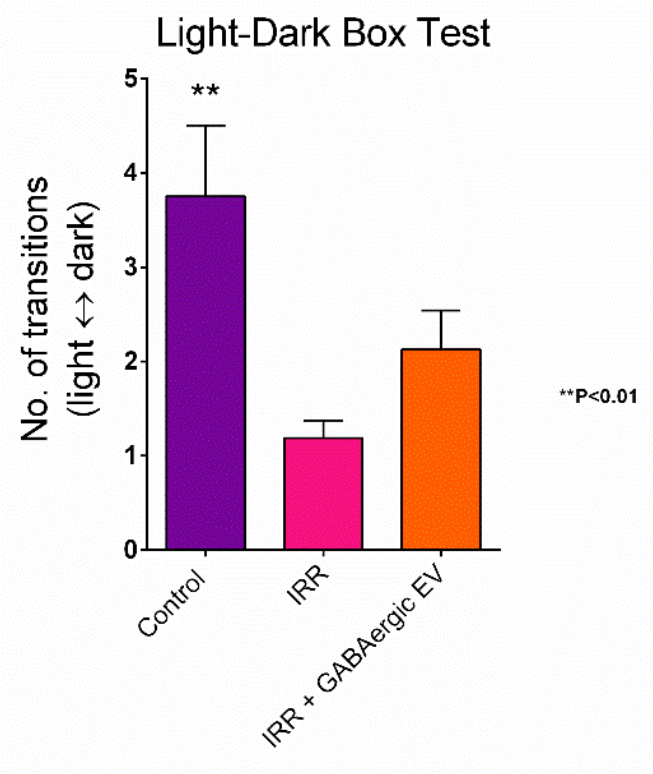

Figure 4.6: Fractionated irradiation (8.67 Gy x 3) reduces the number of transitions between the light and dark areas during the Light-Dark Box Test. The mean number of transitions was higher in the cohort that also received retro-orbital GABAergic extracellular vesicles as compared to the irradiated group, but this increase was not statistically significant. Data are presented as the mean ± SEM (N = 16 animals/group). *P*-values are derived from analysis of variance and Bonferroni's multiple comparisons test. **, $P < .01$ all compared against the irradiated group

Glutamatergic Extracellular Vesicles Administered by Retro-Orbital Injection Are Unable to Attenuate Radiation-Induced Cognitive Impairments

The cohort of rats developed to determine the effects of glutamatergic extracellular vesicles following irradiation were handled identically to the GABAergic cohort, with the same experimental time course, sequence of behavioral tasks, and testing procedures. The Novel Object Recognition test did not reveal significant overall group effects ($F(2, 45) = 2.516$; $P=0.0921$). The mean discrimination index for the control group (mean discrimination index=25.39%) was greater than that of the irradiated group (mean discrimination index=-21.00%), but this difference was not statistically significant ($F(2, 45) = 2.516$; $P= 0.0901$). The extracellular vesicle-treated rats likewise failed to discriminate between novel and familiar (mean discrimination index=0.1461%), and their performance was statistically comparable to that of the irradiated rats ($F(2, 45) = 2.516$; $P= 0.9377$).

Significant overall group effects were demonstrated on the Novel Place Recognition task in the glutamatergic extracellular vesicle cohort ($F(2, 33) = 5.602$; $P=0.0080$). The performance of the control experimental group (mean discrimination index=26.60%) showed a statistically significant enhancement ($F(2, 33) = 5.602$; $P=0.0415$) compared to the irradiated group (mean discrimination index=-8.788%), but there was no statistical difference ($F(2, 33) = 5.602$; $P>0.9999$) in performance between the irradiated group and the extracellular vesicle-treated group (mean discrimination index=-17.73%). Instead, there was a statistically significant increase in mean discrimination index of the control animals over the extracellular vesicle-treated animals ($F(2, 33) = 5.602$; $P= 0.0111$).

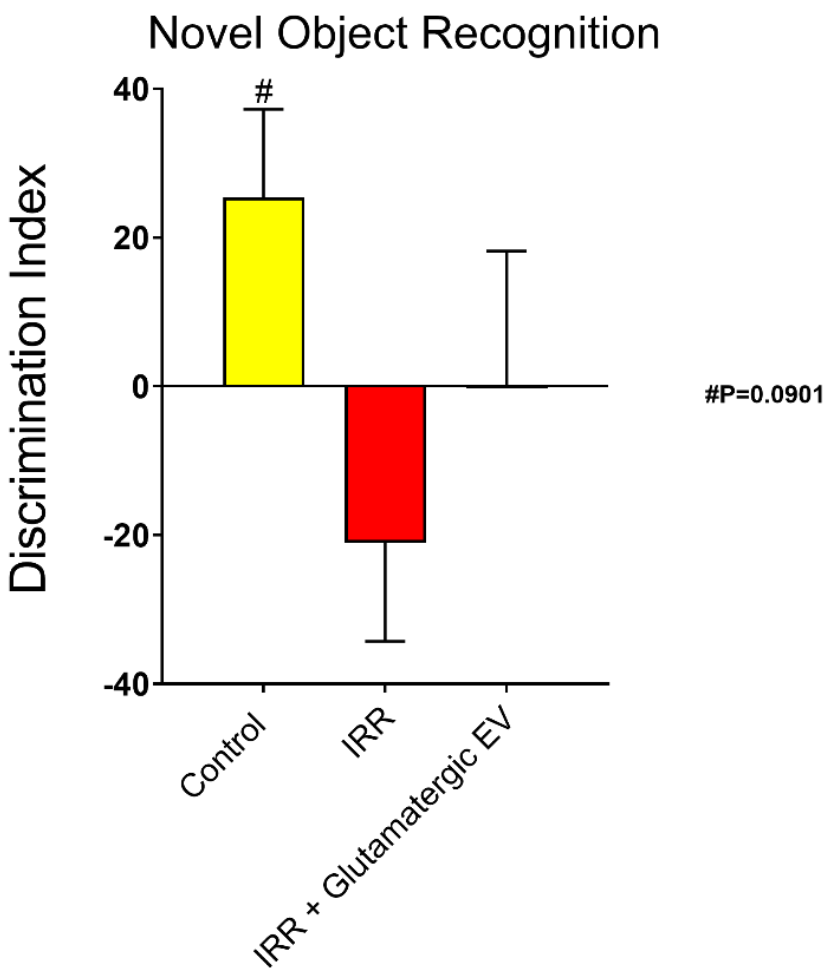

Figure 4.7: Administration of glutamatergic extracellular vesicles fails to improve ability to discriminate between novelty and familiarity in Novel Object Recognition following irradiation. Rats in the irradiated cohort and the cohort receiving both irradiation and glutamatergic extracellular vesicles were unable to discriminate between novel and familiar; control animals had an increased discrimination index, but the difference between the control and irradiated cohorts was not statistically significant. Data are presented as the mean ± SEM (N = 16 animals/group). *P*-values are derived from analysis of variance and Bonferroni's multiple comparisons test. All compared against the irradiated group

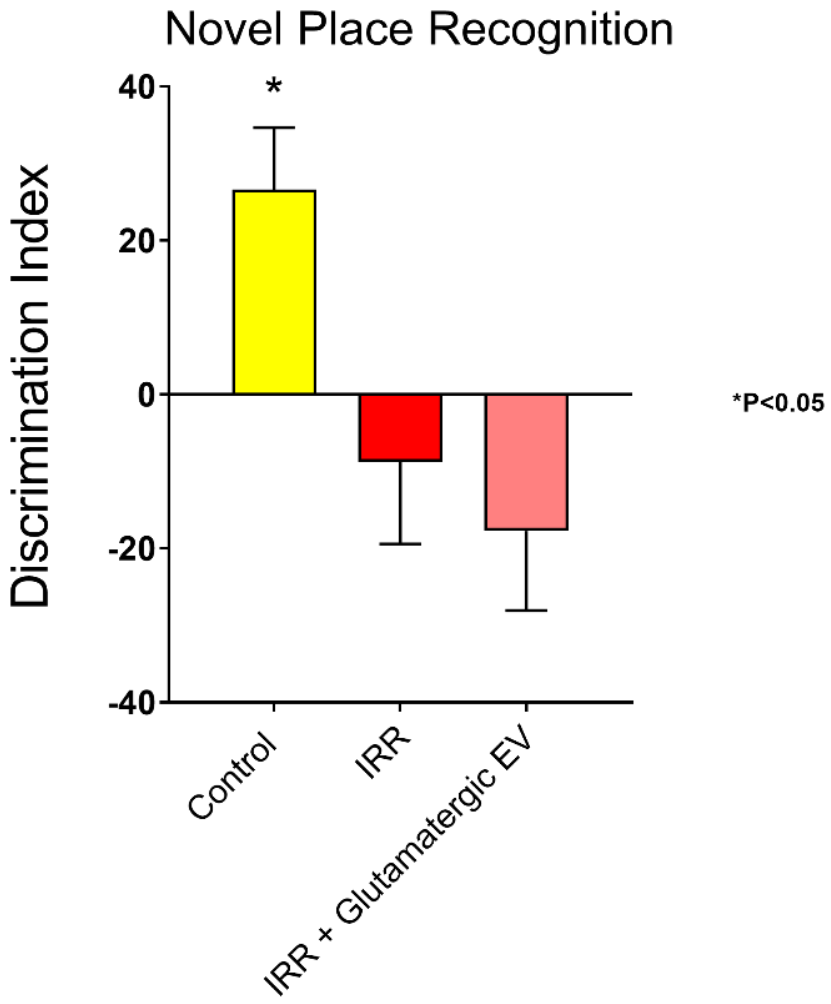

Figure 4.8: Radiation-induced decrements in performance on the Novel Place Recognition task are not mitigated by the injection of glutamatergic extracellular vesicles. As compared to control rats, rats that received fractionated irradiation exhibited statistically poorer performance in discriminating between novel and familiar; the IRR cohort and the IRR + glutamatergic EV cohort are statistically indistinguishable from each other, indicating that the glutamatergic EVs did not facilitate better performance on the behavioral task. Data are presented as the mean ± SEM (N = 16 animals/group). *P*-values are derived from analysis of variance and Bonferroni's multiple comparisons test. *, $P < .05$ all compared against the irradiated group

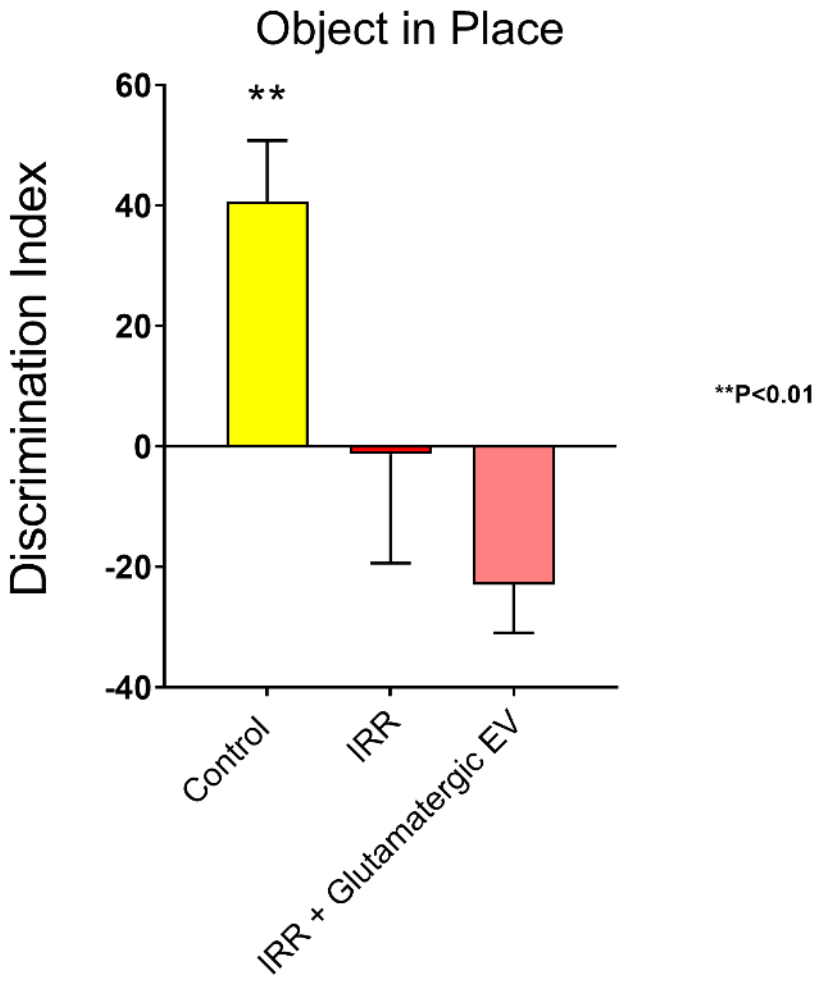

Figure 4.9: Radiation eliminates rats' capacity to identify novelty on the Object in Place task, and this deleterious effect is not alleviated by retro-orbital injection of glutamatergic extracellular vesicles. Control animals demonstrated statistically-significant superior exploration of novel objects over familiar objects relative to irradiated animals; the performance of the irradiated cohort and the cohort that were subjected to irradiation and glutamatergic extracellular vesicles were statistically similar. Data are presented as the mean ± SEM (N = 16 animals/group). *P*-values are derived from analysis of variance and Bonferroni's multiple comparisons test.

**, $P < .01$ all compared against the irradiated group

For the Object in Place task, significant group effects were observed (F (2, 32) = 7.226; P= P=0.0054). The mean discrimination index of the irradiated group (mean discrimination index=-1.263%) was significant reduced (F (2, 32) = 7.226; P=0.0044) compared to the control group (mean discrimination index=40.71%). In contrast, the difference between the mean discrimination index of the irradiated group and the extracellular vesicle-treated group did not reach significance (F (2, 32) = 7.226; P= 0.6433), and the two groups were statistically similar; both groups failed to exhibit a preference for novelty.

Injection of GABAergic Extracellular Vesicles Preserves Neurotrophin Levels Following Irradiation

The effect of GABAergic extracellular vesicles on neurotrophin levels, specifically brain-derived neurotrophic factor and glial cell line-derived neurotrophic factor, in the hippocampus after fractionated irradiation was investigated by ELISA assay. The brain-derived neurotrophic factor (BDNF) analysis showed significant overall group effects (F (2, 57) = 16.17; P<0.0001); there was a significant decrease in hippocampal BDNF following fractionated irradiation (F (2, 57) = 16.17; P <0.0001) as compared to the control animals, but the BDNF levels were preserved in rats that also received GABAergic extracellular vesicles (F (2, 57) = 16.17; P= 0.0001). The BDNF levels in the control group and the group subjected to fractionated irradiation and GABAergic extracellular vesicles were highly similar, with no statistically significant difference between them (F (2, 57) = 16.17; P >0.9999).

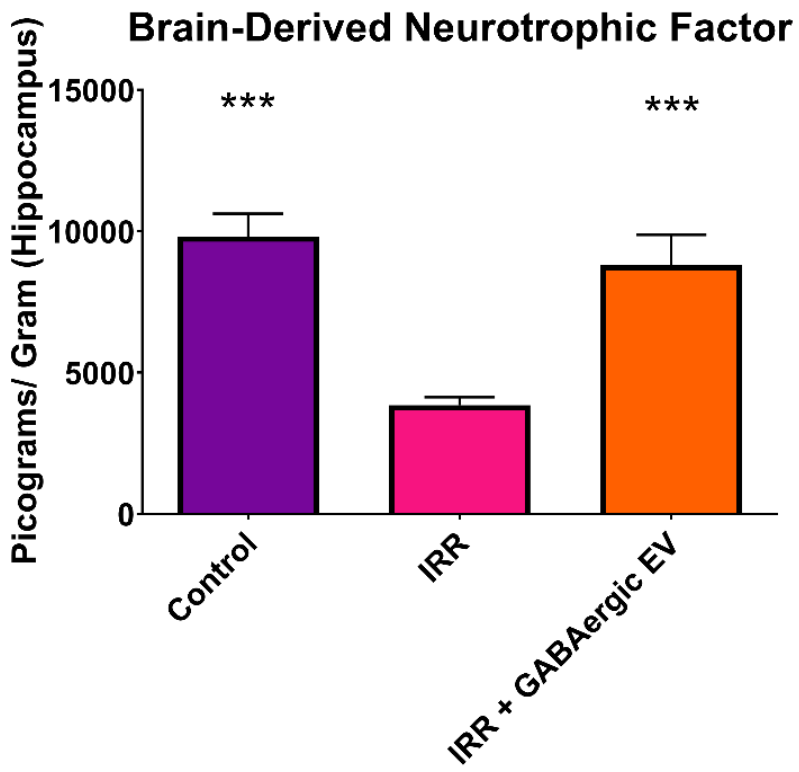

Figure 4.10: Reduction in brain-derived neurotrophic factor (BDNF) due to fractionated irradiation ameliorated with application of GABAergic EVs. At approximately two months post-irradiation, BDNF levels are significantly decreased in the irradiated cohort compared to the controls; however, BDNF levels in the animals that received GABAergic EVs in addition to cranial irradiation showed elevated BDNF relative to the irradiated animals, similar to the levels seen in the control animals. Data are presented as the mean ± SEM (N = 4-5 animals/group). P-values are derived from analysis of variance and Bonferroni's multiple comparisons test. ***, $P < .001$ all compared against the irradiated group

Likewise, significant group effects ($F(2, 57) = 6.186$; $P=0.0037$) were ascertained in the glial cell line-derived neurotrophic factor (GDNF) assay. The irradiated animals experienced a statistically significant reduction in GDNF ($F(2, 57) = 6.186$; $P=0.0038$) relative to the control group; this reduction was blunted by the application of GABAergic extracellular vesicles, which caused a statistically significant increase in GDNF compared to the irradiated animals ($F(2, 57) = 6.186$; $P=0.0459$). Levels of GDNF in the control group and the extracellular vesicle-treated group were statistically equivalent, with no significant difference observed ($F(2, 57) = 6.186$; $P >0.9999$).

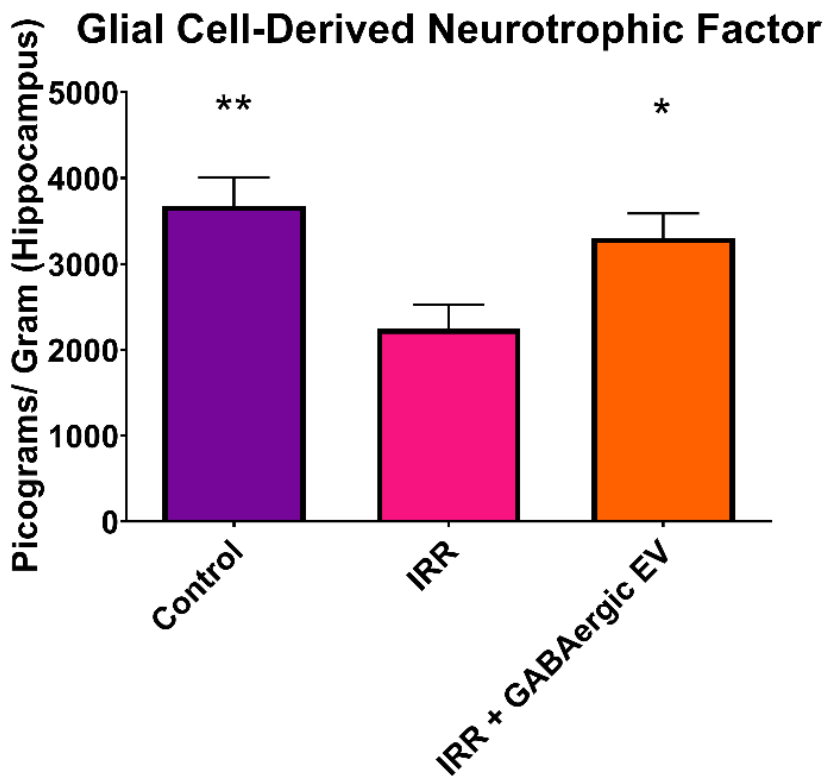

Figure 4.11: Glial cell-derived neurotrophic factor (GDNF) decline due to fractionated irradiation ameliorated with application of GABAergic EVs. At approximately two months post-irradiation, BDNF levels are significantly decreased in the irradiated cohort compared to the controls; however, BDNF levels in the animals that received GABAergic EVs in addition to cranial irradiation showed elevated BDNF relative to the irradiated animals, similar to the levels seen in the control animals. Data are presented as the mean ± SEM (N = 4-5 animals/group). P-values are derived from analysis of variance and Bonferroni's multiple comparisons test. *, $P < .05$; *, $P<.01$ all compared against the irradiated group

Glutamatergic Extracellular Vesicles Likewise Increase BDNF and GDNF Levels Subsequent to Irradiation

To examine whether differences in neurotrophin levels in the hippocampus could be responsible for the differential cognitive performance of rats receiving GABAergic and glutamatergic extracellular vesicles, the levels of BDNF and GDNF were assayed in the glutamatergic extracellular vesicle cohort as well. The BDNF analysis yielded significant overall group effects ($F(2, 45) = 18.30$; $P<0.0001$). This cohort showed an analogous statistically significant decrease in the irradiated group compared to the control group ($F(2, 45) = 18.30$; $P<0.0001$); perhaps counterintuitively, the extracellular vesicle-treated group also exhibited an increase in BDNF levels in the hippocampus over that of the irradiated group (($F(2, 45) = 18.30$; $P<0.0001$), with BDNF levels statistically similar to the control group (($F(2, 45) = 18.30$; $P>0.9999$) detected.

The assay of GDNF levels in the hippocampus the irradiated experimental group also yielded significant overall group effects ($F(2, 45) = 52.57$; $P<0.0001$). As before, there was a statistically significant decrease in hippocampal GDNF in the irradiated animals compared to controls ($F(2, 45) = 52.57$; $P<0.0001$); similarly, the GDNF levels in the extracellular vesicle-treated group exhibited a statistically significant improvement relative to the irradiated group (($F(2, 45) = 52.57$; $P=0.0010$). However, there was also a statistically significant difference in GDNF levels between the control rats and the extracellular vesicle-treated rats ($F(2, 45) = 52.57$; $P<0.0001$), with the controls rats showing significantly greater levels of GDNF in the hippocampus.

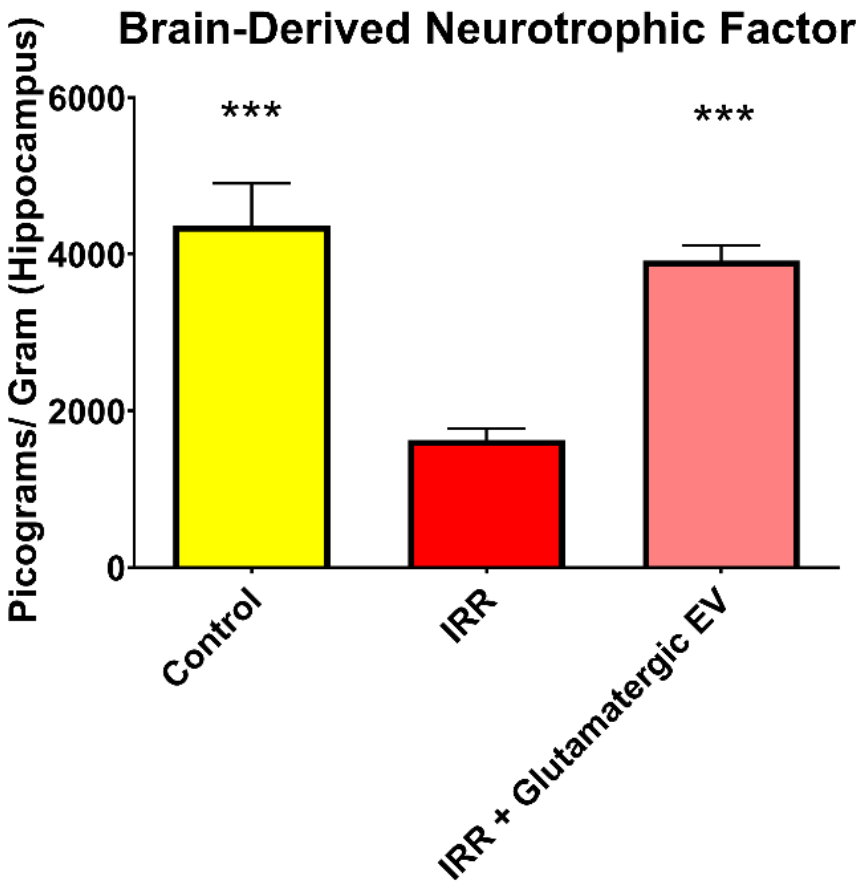

Figure 4.12: Brain-derived neurotrophic factor (BDNF) levels in animals receiving glutamatergic extracellular vesicles after fractionated irradiation are heightened compared to irradiated animals and similar to control levels of BDNF. Irradiation produces a dramatic reduction in BDNF in the hippocampus, but injection of glutamatergic extracellular vesicles substantially recovers BDNF levels to approximate those of control animals. Data are presented as the mean ± SEM (N = 4-5 animals/group). P-values are derived from analysis of variance and Bonferroni's multiple comparisons test. ***, $P < .001$ all compared against the irradiated group

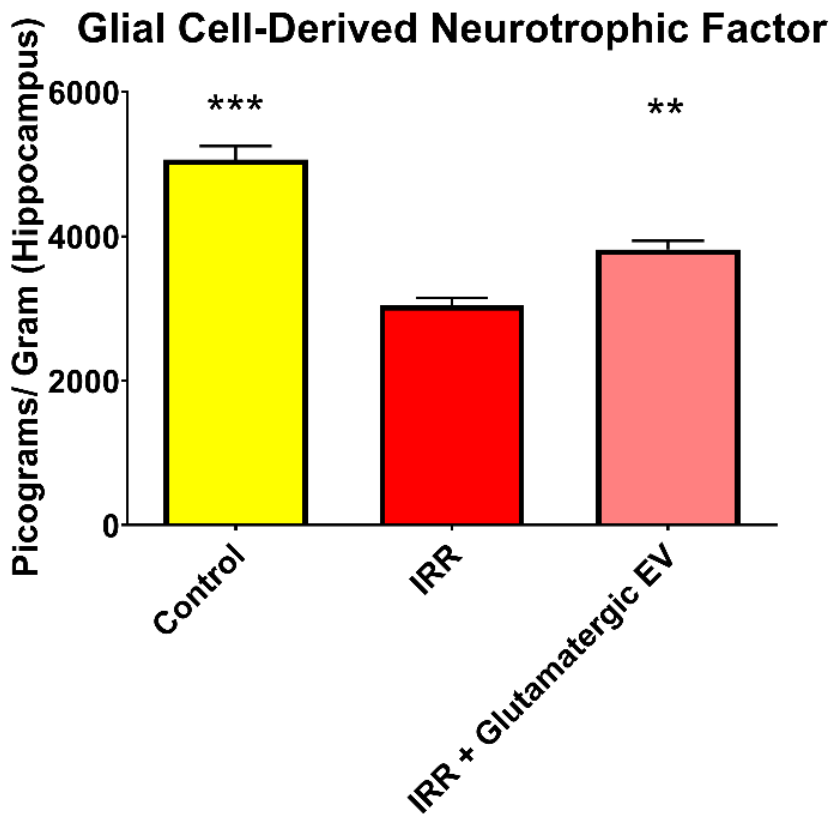

Figure 4.13: Irradiated rats experience a prominent decrease in glial cell-derived neurotrophic factor (GDNF) that is partially attenuated by retro-orbital injection of glutamatergic extracellular vesicles. A statistically significant reduction is observed in the irradiated cohort; the IRR + glutamatergic EV animals exhibit a statistically significant improvement over the irradiated animals. However, there is also a statistical difference between the control group and the IRR + glutamatergic EV group, with the control group possessing greater average GDNF in the hippocampus thus the group receiving glutamatergic EVs after irradiation. Data are presented as the mean ± SEM (N = 4-5 animals/group). P-values are derived from analysis of variance and Bonferroni's multiple comparisons test. **, P<.01; ***, P < .001 all compared against the irradiated group

GABAergic Extracellular Vesicles Mitigate Radiation-Induced Decline in Dendritic Spine Density

To assess the impact of retro-orbital injections of GABAergic extracellular vesicles on dendritic spine density, the brains of rats sacrificed after the progression of behavioral testing (approximately six weeks after the last retro-orbital injection) were prepared using Golgi-Cox impregnation and staining of neurons for morphometric analysis (N = 4 animals per experimental group). The dendritic spine density of the dentate gyrus of the hippocampus was analyzed using the Stereoinvestigator program and serial sections across the rat hippocampus. This analysis demonstrated significant overall group effects ($F(2, 9) = 11.38$; $P=0.0034$), and there was a significant reduction in dendritic spine density in the dentate gyrus following fractionated irradiation as compared to the control group ($F(2, 9) = 11.38$; $P= 0.0040$). However, treatment with GABAergic neuron-derived extracellular vesicles was able to mitigate this decline, with the extracellular vesicle-treated group showing a significant increase in spine density ($F(2, 9) = 11.38$; $P=0.0216$) over that of the irradiated group. The application of GABAergic extracellular vesicles returned dendritic spine density in the dentate gyrus to levels statistically comparable to that of control rats, with no statistically significant difference detected (($F(2, 9) = 11.38$; $P=0.8779$).

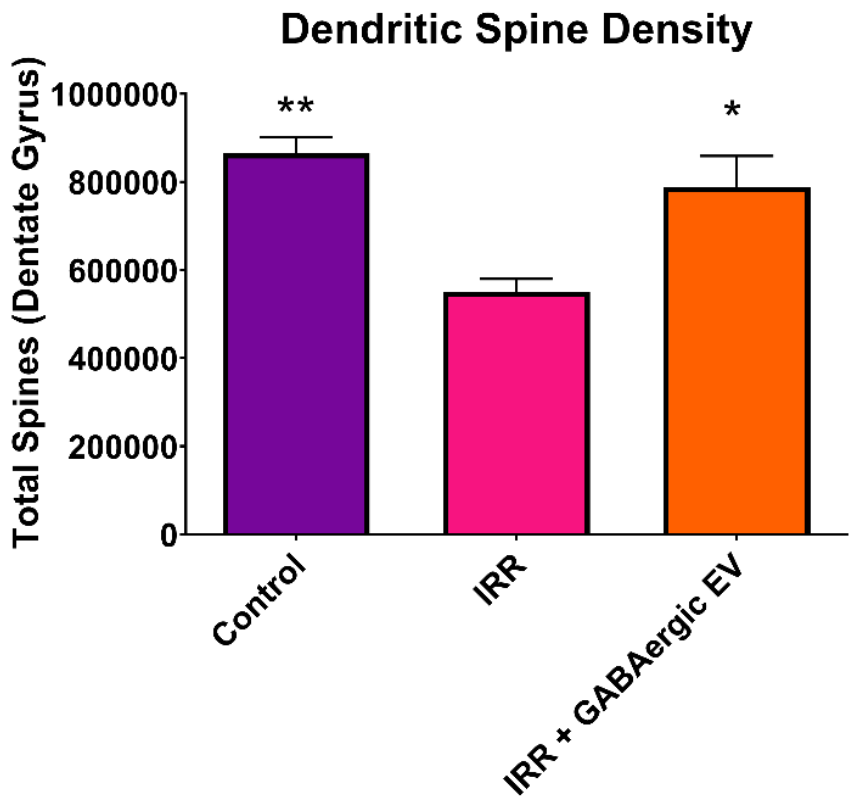

Figure 4.14: Dendritic spine density in the dentate gyrus is diminished after cranial irradiation, but application of GABAergic extracellular vesicles recovers spine density. Both the control and IRR + GABAergic EV groups show statistically-significant improvements over the irradiated cohort in dendritic spine density eight weeks following irradiation. Data are presented as the mean ± SEM (N = 4 animals/ experimental group). P-values are derived from analysis of variance and Bonferroni's multiple comparisons test. *, P<.05; **, P<.01 all compared against the irradiated group

Future Directions/ Studies in Progress

As a comparator to the dendritic spine density data in the GABAergic extracellular vesicle cohort, the dendritic spine density in the hippocampal dentate gyrus of the contingent of experimental groups including the glutamatergic extracellular vesicles is currently under analysis. The impacts of both GABAergic and glutamatergic extracellular vesicles on neuroinflammation in the brain after cranial irradiation is also being assessed, employing staining for activated microglia (ED-1) as a proxy marker. Finally, the extent of spread of GABAergic extracellular vesicles administered by retro-orbital injection into the brains is being explored, both in the intact brain and the irradiated brain, using PKH-26 dye-loading of the extracellular vesicles.

CHAPTER 5: IN A CLINICALLY-RELEVANT COMBINED CRANIAL IRRADIATION/ TEMOZOLOMIDE TREATMENT PARADIGM, GABAERGIC EXTRACELLULAR VESICLES RESTORE NEUROBEHAVIORAL FUNCTION AND NEUROTROPHIN LEVELS

Introduction

Studies undertaken in the Limoli laboratory and by others have indicated that both irradiation and chronic chemotherapy treatment, including cyclophosphamide and doxorubicin, adversely impact cognitive function one to four months following exposure; further, though there are no satisfactory treatments for reducing the progressive adverse effects of radiation- and chemotherapy-induced brain injury, intercranial stem cell transplantation has shown promise in improving the cognitive decrements associated with both radiation and chemotherapy. This study intends to extend these studies to examine a combined fractionated irradiation and chemotherapy (TMZ) paradigm designed to approximate current standard of care for human brain cancer patients. We explored the effects of fractionated TMZ + IRR on hippocampus-, prefrontal cortex- and amygdala-dependent cognitive function and determine whether retro-orbital injection of extracellular vesicles derived from GABAergic neurons, delivered in a manner significantly less invasive than intrahippocampal transplantation, can alleviate treatment-associated deficits in cognition at one month following treatment. Further, upon finding that retro-orbital administration of GABAergic extracellular vesicles did improve behavioral performance in this paradigm, we investigated the neurobiological mechanisms by which the GABAergic neuron-derived EVs improve cognition after TMZ+IRR exposure by assessing the functional consequences of retro-orbital injection and the impact on the host microenvironment.

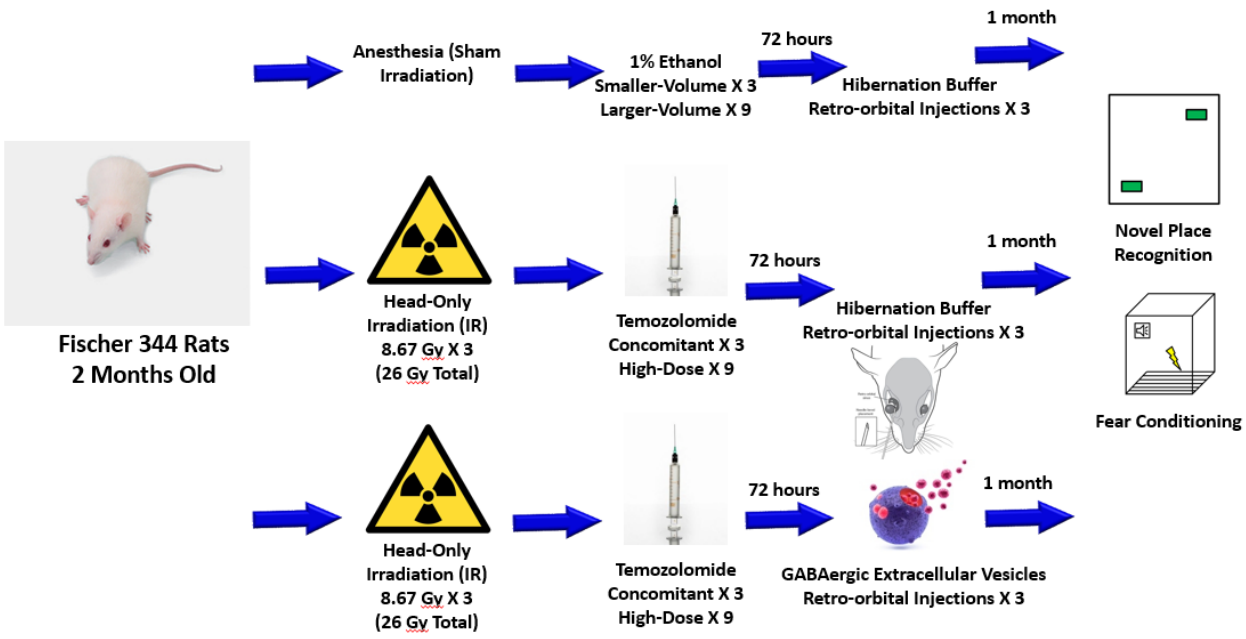

Figure 5.1: Experimental design

Materials and Methods

Animals and irradiation

All animal procedures are in accordance with NIH and approved by the University of California Institutional Animal Care and Use Committee. Eight-week-old male Fischer 344 rats (Crl:CD(Fischer 344), strain 002, Charles River Laboratories, Wilmington, MA) were maintained in standard housing conditions (20°C ± 1°C; 70% ± 10% humidity; 12 h:12 h light and dark cycle) and provided *ad libitum* access to food and water. The rats were divided into three experimental groups (N=16 animals per experimental group). Two cohorts received the combined temozolomide (TMZ) and irradiation therapy paradigm; the third cohort served as a control. One of the TMZ+IRR cohorts received retro-orbital injections of GABAergic neuron-derived extracellular vesicles; the other TMZ+IRR cohort and the control group received concurrent retro-orbital injections of hibernation buffer (solvent). Rats were anesthetized using an isoflurane gas system (VWR Mobile RC2; induction=4%, maintenance=2.5%) for irradiation, which delivered using a self-shielded 320 kV X-irradiator (X-RAD320, Precision X-Ray) and lead shielding to facilitate head-only irradiation over a 2 cm^2 area at a dose rate of 1 Gy/min. The study was initiated with the TMZ+IRR cohorts receiving three fractionated doses of whole-brain irradiation of 8.67 Gy each (total 26 Gy) over the course of five days (i.e. on days 1, 3, and 5). Control animals were anesthetized for the same amount of time as the irradiated animals to ensure corresponding isoflurane exposure, and handled identically to those undergoing irradiation. Interspersed between the radiation doses, the TMZ+IRR cohorts received three concomitant doses (12.5 mg/kg) of TMZ (3-Methyl-4-oxo-8-imidazolo[5,1-d][1,2,3,5]tetrazinecarboxamide or Temodar®, Sigma, St. Louis, MO, USA) dissolved in 1% ethanol with heating, likewise over the course of five days (i.e. on days 2, 4, and 6). The TMZ solution for concomitant doses were prepared at 6.25 mg/ml, and administered by intraperitoneal injection (i.p.), alternating the side

(left versus right) of the peritoneal cavity being injected. Untreated control rats received injections of 1% ethanol at the same volume as would be administered for a TMZ injection. One week after the first irradiation dose, the TMZ+IRR cohorts received adjuvant injections of TMZ dissolved in 1% ethanol at 7 mg/ml (to ensure all injection volumes are less than 3 ml), dosed at 33.3 mg/kg, with three injections each week over the course of five days (i.e. on days 8, 10, and 12 for the first week of high-dose injections). Thus, animals received twelve total TMZ injections over the course of four weeks, three during week 1 at 12.5 mg/kg and nine during the subsequent three weeks at 33.3 mg/kg. The rats were weighed weekly to ensure accurate dosing. The TMZ doses have been calculated using the body surface area normalization method to most closely approximate the clinical doses of TMZ that human patients receive; the fractionated radiation protocol delivers a biological effective dose of 101 Gy, which approaches the standard treatment for glioblastoma patients (60 Gy in 2 Gy fractions).

Extracellular vesicle isolation

GABAergic neuron-derived extracellular vesicles were collected from conditioned culture media in which induced pluripotent stem (iPS) cell-derived GABAergic neurons (iCell GABANeurons, 01434, FUJIFILM Cellular Dynamics, Inc, Madison, WI) were cultured. The extracellular vesicles were isolated and purified from the conditioned media by ultracentrifugation. The conditioned media was first centrifuged at 300 x g for 10 minutes to remove cells and cellular debris. The media was then centrifuged at 100,000 × g for 90 minutes and the extracellular vesicles were collected in hibernation buffer; the extracellular vesicles were pooled and purified in sterile Dulbecco's phosphate-buffered saline at 100,000 x g for 120 minutes, and collected in hibernation buffer. The extracellular vesicles were characterized using a ZetaView PMX 110 particle analyzer (Particle Metrix GmbH; Meerbusch Germany).

	TMZ+IRR, EV RO						
	Day 1	Day 2	Day 3	Day 4	Day 5	Day 6	Day 7
Week 1	IRR	TMZ	IRR	TMZ	IRR	TMZ	
Week 2	TMZ		TMZ		TMZ		
Week 3	TMZ		TMZ		TMZ		
Week 4	TMZ		TMZ		TMZ		
Week 5	EV RO						
Week 6	EV RO						
Week 7	EV RO						

Table 5.1: Timeline of treatments for combined irradiation/ temozolomide paradigm to probe the impact of GABAergic extracellular vesicles

Retro-orbital injections

At 72 hours following the final fractionated dose of temozolomide, the rats were anesthetized using an isoflurane gas system (VWR Mobile RC2; maintenance=3.5% vol/vol isoflurane/oxygen), and extracellular vesicles or vehicle (hibernation buffer) were delivered to the rats through circulation via the retro-orbital sinus. A 31-gauge needle with a 0.5 ml syringe attached (BD Veo™ insulin syringes with BD Ultra-Fine™ 6mm x 31G needle) was used to pierce 2 to 3 mm into the rat's orbital venous sinus with the bevel on the needle facing upward at a 45° angle before injecting the extracellular vesicles. The control and irradiated experimental groups received retro-orbital injections of 100 microliters hibernation buffer (vehicle). For the GABAergic extracellular vesicle group, 1.5 x 10^9 extracellular vesicles in 100 microliters hibernation buffer were delivered by retro-orbital injection.

Behavioral cognitive testing

Two weeks following the last retro-orbital injections, the rats underwent a battery of behavioral tasks designed to interrogate cognitive function. The animals were tested on spontaneous exploration tasks, namely Novel Place Recognition, which is sensitive to spatial cognitive impairments caused by hippocampal damage; Novel Object Recognition, which assesses episodic memory retention dependent on the frontal and pre-frontal cortex; and Elevated Plus Maze, which assesses anxiety-like behavior. For the Novel Place Recognition and Novel Object Recognition, the trials were scored for exploration time of the novel and familiar objects for each animal (n=16 per experimental group) and the discrimination index was calculated from the equation: [(Novel Object/Total Exploration Time) – (Familiar/Total Exploration Time)] × 100. A cognitively-intact animal is expected to exhibit a preference for novelty in each of these tasks. . The Elevated Plus Maze was comprised of an acrylic surface with four elevated arms (75 cm above the floor, 110 cm long and 10 cm arm width) with two opposing closed arms enclosed with

42-cm high walls. Rats were initially placed in the central zone of the EPM, with their head facing towards an open arm, and allowed to freely explore the maze for five minutes. The frequency of entries in the open arms were recorded, with entry into an open arm defined as all four paws of the rat crossing into the open arm. Statistical analysis was performed using a repeated measure ANOVA with Bonferroni correction in GraphPad Prism 6.0 Software (GraphPad Software Inc.), and data was plotted as mean ± SEM with significance set at $\alpha = 0.05$.

Extraction and ELISA for assessment of neurotrophins

Following the behavioral testing at approximately six weeks post-final retro-orbital injections, the rats were euthanized using isoflurane anesthesia. Brains were immediately extracted from the skull (N = 4-5 per group) and the hippocampus was dissected from each cerebral hemisphere. Each hippocampus was weighed and transferred into 300 µL ice-cold lysis buffer (N-PER Neuronal Protein Extraction Reagent, Thermo Scientific Product number 23225) containing sodium orthovanadate (0.5 mM), pheyl-methylsulfonyl fluoride (PMSF, 1 mM), aprotinin (10 µg/mL), and leupeptin (1 µg/mL; Santa Cruz Biotechnology, Santa Cruz, California). Tissues were sonicated individually, centrifuged at 4°C for 15 minutes at 13,200 rpm, and the supernatants were collected and diluted 1:5 with Dulbecco's phosphate-buffered saline. The supernatants were acidified to pH 2.6 then neutralized to pH 7.6 to liberate the neurotrophic factors, and the BDNF and GDNF levels were assayed using E_{max} ImmunoAssay Systems from Promega (BDNF catalog number G7611, GDNF catalog number G7621) and uncoated ELISA plates (Biolegend Nunc MaxiSorp, catalog number 423501). All measurements were performed at a wavelength of 450 µm on a microplate reader (BioTek Synergy Mx).

Quantification of dendritic spine density

At approximately six weeks post-final retro-orbital injections, the rats were euthanized using isoflurane anesthesia and perfused with saline + heparin. Brains (N = 4 per group) were extracted from the skull and subjected to Golgi-Cox impregnation and staining of neurons according to the manufacturer's instructions (SuperGolgi kit, Bioenno Tech., Santa Ana, California). The brains were sectioned to 100 μm using a vibratome (need details on vibratome) and counterstained by nuclear fast red to visualize hippocampal subregions. The Stereoinvestigator program (v11, MicroBrightField) was used for the quantification of dendritic spines using four serial sections (every second) throughout the hippocampus to analyze potential differences in spine density between each of the experimental cohorts.

Immunostaining of activated microglia

Following behavioral testing, rats were euthanized using isoflurane and perfused with 4% paraformaldehyde (Acros Organics, Geel, Belgium), and brain tissues were processed for coronal sectioning using a cryostat (Leica Microsystems, Wetzlar, Germany) and prepared for immunohistochemistry. Immunostaining for activated microglia (ED-1$^+$ cells) was carried out on serial sections (30 μm coronal, every tenth section) with six sections per animal (N = 4 per experimental group), via a primary anti-ED-1 antibody (mouse, 1:200; AbD Serotec) followed by a donkey anti-mouse biotinylated secondary antibody (1:200; Invitrogen). Sections were mounted on gelatin-coated slides, air-dried, dehydrated and counterstained with nuclear fast red (Vector Labs, CA, USA). The number of activated microglia (ED1+) within the DH, GCL and CA3/CA1 regions of hippocampus were analyzed by stereology.

Results

In a Combined Cranial Irradiation/ Temozolomide Treatment Protocol, Administration of GABAergic Extracellular Vesicles Elevate Neurobehavioral Function and Improves Anxiety-Like Behavior

Four weeks after the last TMZ injection and two weeks following the last EV injection, the Fischer 344 rats (N = 16 rats per group) underwent a battery of behavioral tasks designed to interrogate cognitive function. The animals were habituated to the testing room and arena for three days before performing the Novel Object Recognition test to evaluate hippocampal function, in which they were exposed to two identical objects for five minutes, then removed from the arena for five minutes, then returned to the arena with one of the same ("familiar") objects and a new ("novel") object. The control cohort demonstrated the capacity to express a preference for novelty, as would be predicted for animals without cognitive disruption (mean discrimination index= 36.56%), and the rats treated GABAergic extracellular vesicles subsequent to the combined cranial irradiation/ temozolomide protocol likewise exhibited the ability the discriminate between novelty and familiarity on the Novel Object Recognition task (mean discrimination index= 46.55%). While the experimental animals that received fractionated irradiation and temozolomide chemotherapy alone had a decreased mean discrimination index, indicating a trend towards a lesser propensity to discriminate between novelty and familiarity (mean discrimination index=8.11%), no significant overall group effects were found at α=0.05 ($F(2, 31) = 2.550$; P=0.0511), and the differences between the performance of the control group and the irradiated group ($F(2, 31) = 2.550$; P=0.2166) and that of the irradiated group and the extracellular vesicle-treated group ($F(2, 31) = 2.550$; P=0.0587) were not statistically significant (Figure 5.2). Similarly, the mean discrimination index of the control group and the TMZ/IRR + extracellular vesicle group were statistically indistinguishable ($F(2, 31) = 2.550$; P>0.9999).

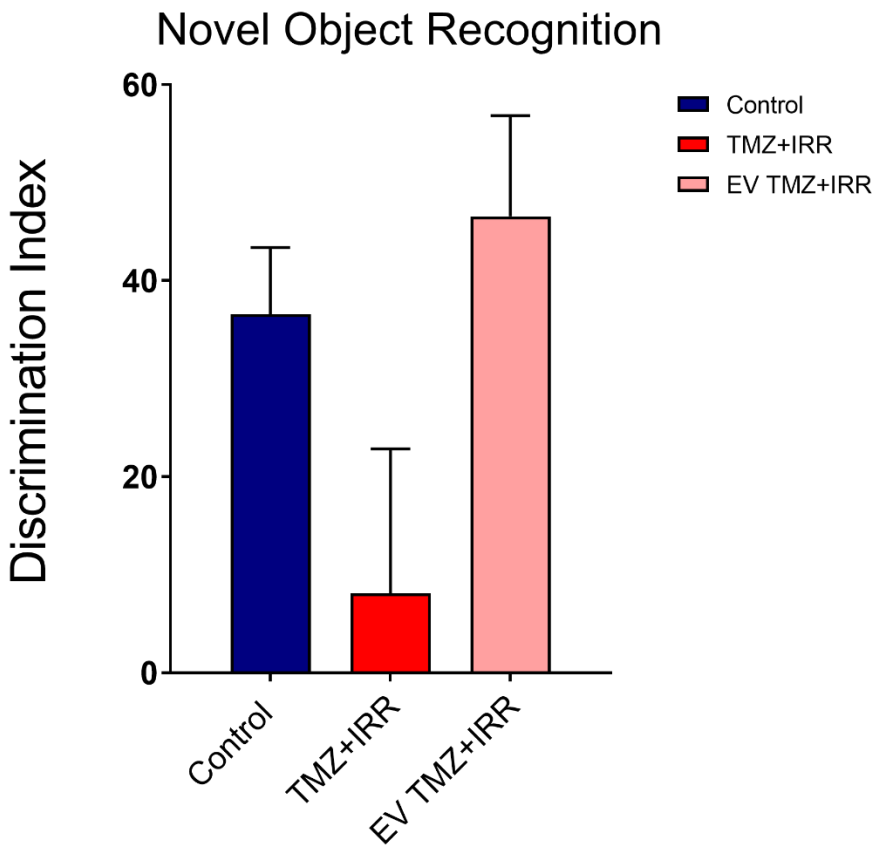

Figure 5.2: Fischer 344 rats display a trend towards a deficit in performance on the Novel Object Recognition task after receiving a combined TMZ+IRR treatment as compared to control animals and animals receiving GABAergic extracellular vesicles along with the TMZ+IRR, but differences are not statistically significant. Data are presented as the mean ± SEM (N = 16 animals/group). *P*-values are derived from analysis of variance and Bonferroni's multiple comparisons test. All compared against the irradiated group

The rats were later subjected to the Novel Place Recognition test to evaluate the integrity of function of the pre-frontal and frontal cortex. The animals were placed in an arena with two identical objects for five minutes, then returned to their housing for one hour, and finally placed back in the arena with one of the objects in its original position ("familiar") and the other object moved to a different position ("novel"). In contrast to the rats' performance on the Novel Object Recognition Test, the Novel Place Recognition test did detect an overall group effect ($F(2, 42) = 5.036$; $P=0.0110$), with the control (mean discrimination index=37.45%) and extracellular vesicle-treated (mean discrimination index= 41.27%) groups evincing higher mean discrimination indices than the irradiation/ temozolomide group (mean discrimination index= -21.99%). Both the differences in performance between the control animals and the irradiation/ temozolomide animals ($F(2, 42) = 5.036$; $P= 0.0444$) and between the irradiation/ temozolomide animals and the animals additionally treated with GABAergic extracellular vesicles ($F(2, 42) = 5.036$; $P= 0.0294$) met the threshold for statistical significance (Figure 5.3). On the contrary, the control group and the GABAergic EV + TMZ/IRR groups were statistically similar ($F(2, 42) = 5.036$; $P>0.9999$).

Lastly, the rats in these experimental groups displayed among the most dramatic results on the Elevated Plus Maze testing of any of our studies. Rats were initially placed in the central zone of the maze, with their head facing towards an open arm, and allowed to freely explore the maze for five minutes as the frequency of entries in the open arms were recorded. An overall group effect was detected for this task ($F(4, 44) = 4.908$; $P=0.0119$), and the control experimental group had a statistically significantly increased mean number of transitions (1.188 mean transitions) as compared to the mean number of transitions (0.1333 mean transitions) for the combined cranial irradiation/ chemotherapy group ($F(4, 44) = 4.908$; $P=0.0024$). A statistically significant difference ($F(4, 44) = 4.908$; $P=0.0081$) was also ascertained between the number

of transitions in the combined irradiation/ temozolomide group (Figure 5.4) and the group receiving both the combined cancer therapies and the GABAergic extracellular vesicles (1.063 mean transitions). No meaningful difference could be found between the control animals and the animals receiving GABAergic extracellular vesicles along with irradiation/ temozolomide ($F(4, 44) = 4.908$; $P>0.9999$).

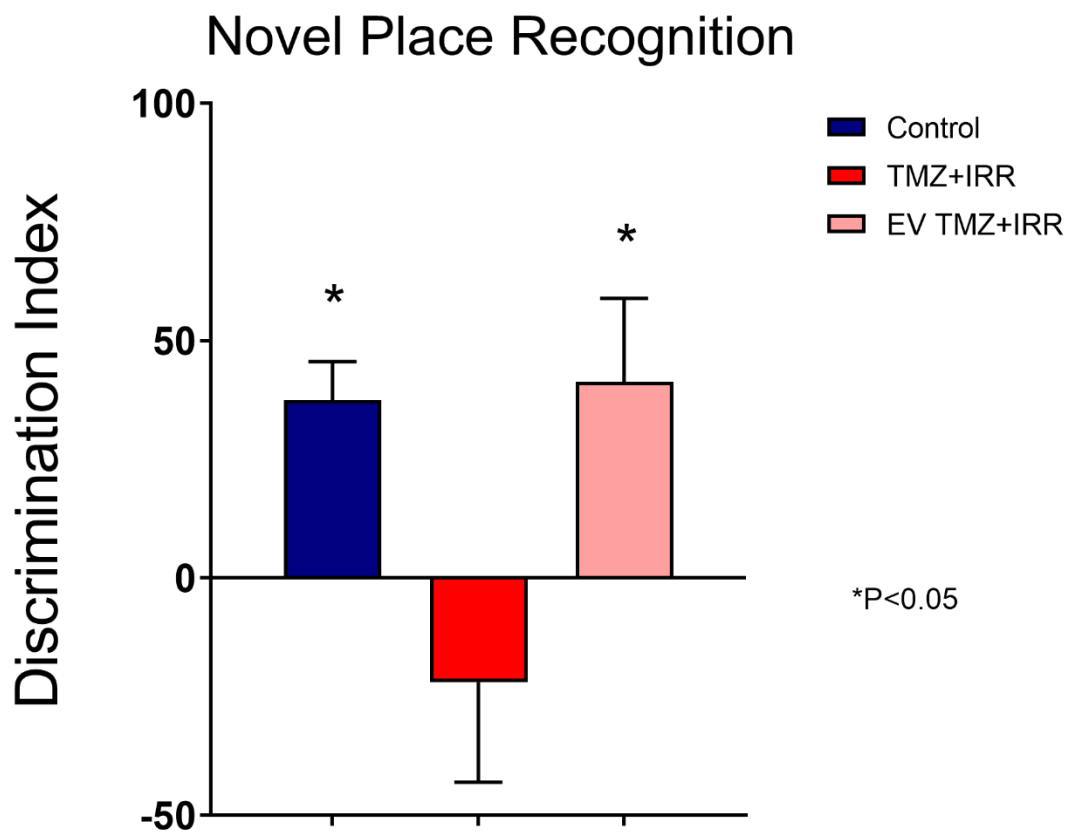

Figure 5.3: Control two-month-old rats demonstrated superior cognitive performance on the Novel Place Recognition task relative to rats received combined temozolomide/ irradiation therapy, but those animals that also received GABAergic extracellular vesicles exhibited rescued ability to discriminate similar to that of the controls. Data are presented as the mean ± SEM (N = 16 animals/group). *P*-values are derived from analysis of variance and Bonferroni's multiple comparisons test. *, $P < .05$ all compared against the irradiated group

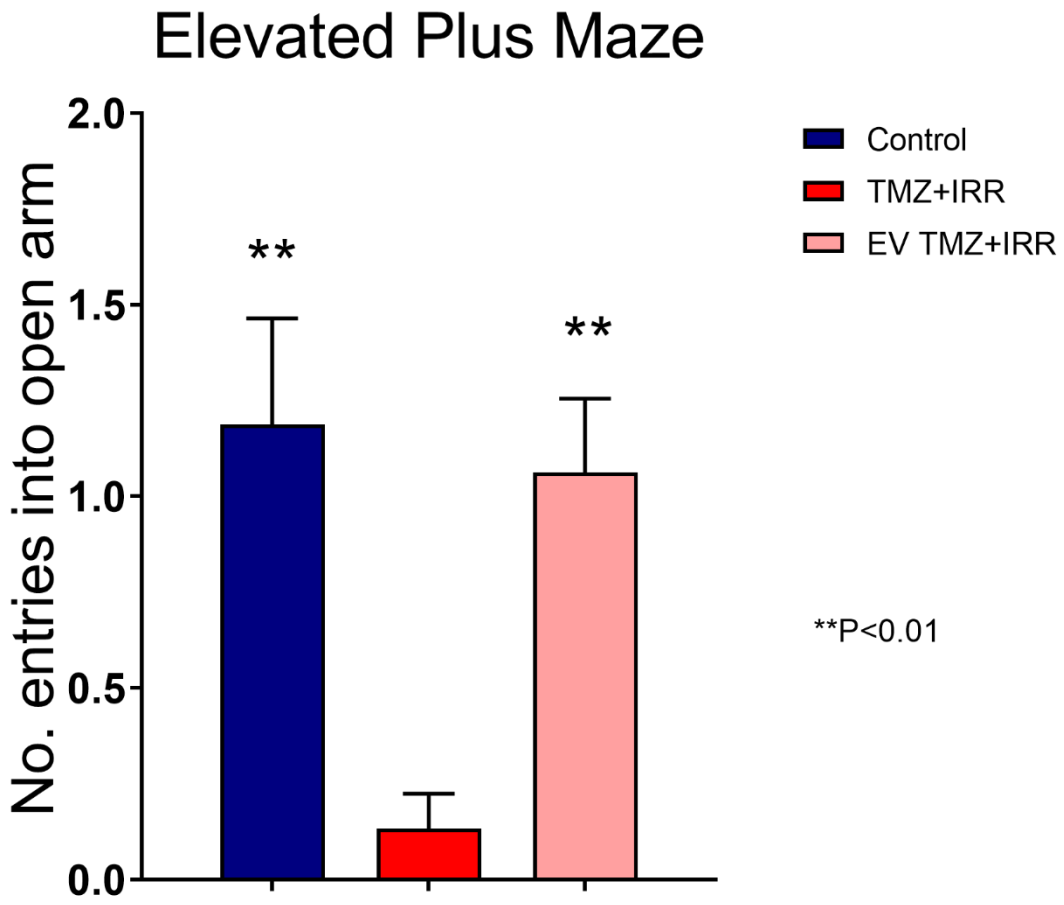

Figure 5.4: Retro-orbital administration of GABAergic extracellular vesicles restored performance on an assay for anxiety-like behavior subsequent to combined temozolomide/ irradiation therapy, approximating the performance of control animals. Data are presented as the mean ± SEM (N = 16 animals/group). *P*-values are derived from analysis of variance and Bonferroni's multiple comparisons test. **, $P < .01$ all compared against the irradiated group

Administration of GABAergic Extracellular Vesicles Sustains Glial Cell-Derived Neurotrophic Factor Quantities in the Hippocampus After Combined Temozolomide/ Irradiation

As part of a mechanistic evaluation to determine the neurobiochemical basis for the cognitive improvement exhibited, an ELISA assay for glial cell line-derived neurotrophic factor (GDNF) in the hippocampus was prepared to investigate the neurotrophin levels among control rats, temozolomide/irradiation rats, and rats receiving both the cancer treatments and GABAergic extracellular vesicles. after fractionated irradiation was investigated by ELISA assay. The glial cell-derived neurotrophic factor analysis showed significant overall group effects ($F(2, 53) = 8.044$; $P=0.0009$); there was a significant decrease in hippocampal GDNF following fractionated irradiation/ temozolomide therapy ($F(2, 53) = 8.044$; $P <0.0001$) as compared to the control animals, but the BDNF levels were improved in rats that also received GABAergic extracellular vesicles ($F(2, 53) = 8.044$; $P= 0.0038$). Interestingly, the GDNF levels in the control group and the group subjected to cranial irradiation/ chemotherapy and GABAergic extracellular vesicles also were significantly different ($F(2, 53) = 8.044$; $P <0.0001$) – the control animals had a higher mean GDNF level (61.85) relative to the GABAergic EV + TMZ/IRR animals (41.99).

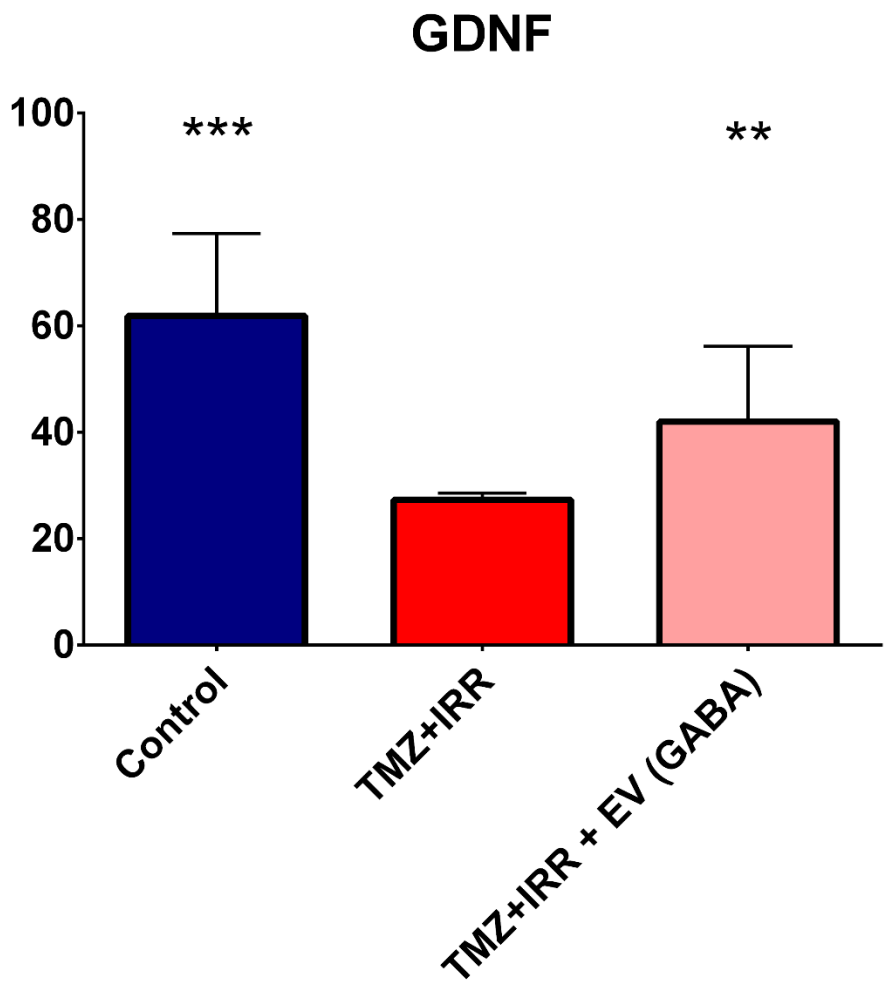

Figure 5.5: Glial cell-derived neurotrophic factor (GDNF) in the hippocampus experiences a striking decline after the administration of a combined temozolomide/ irradiation paradigm; this drastic decrease is attenuated by the retro-orbital injections of GABAergic extracellular vesicles, although GDNF levels still do not return to control levels. Data are presented as the mean ± SEM (N = 4-5 animals/group). P-values are derived from analysis of variance and Bonferroni's multiple comparisons test. **, P<.01; ***, P < .001 all compared against the irradiated group

Future Directions/ Studies in Progress

Similar to previous related studies, brains have been processed by Golgi staining to ascertain information about dendritic spine density and host neuronal morphology in the dentate gyrus of the hippocampus via spine counting and neuron tracing. Likewise, PFA-perfused sections have been stained for the activated microglia marker ED-1, to be used as a proxy for neuroinflammation, and the tissues await quantitative analysis. Further, the expression of 5-HT_{1A} receptors could be explored, to help interrogate the mechanism behind the unambiguous results of the Elevated Plus Maze task. 5-HT_{1A} receptor agonists have demonstrated efficacy in alleviating anxiety and depression, and disruption of the receptor's neurotransmission is known to have negative repercussions resulting in psychiatric disorders [98, 99]. The receptors are known to be expressed on several populations of GABAergic neurons [98]. Finally, we could reprise our previous studies exploring synaptic integrity by quantifying the level of post-synaptic scaffolding protein PSD-95 in the CA1.

CHAPTER 6: PROTECTIVE ADMINISTRATION OF GABAERGIC EXTRACELLULAR VESICLES BEFORE IRRADIATION PRESERVES COGNITIVE PERFORMANCE AND NEUROTROPHIC FACTOR LEVELS AFTER IRRADIATION

Introduction

Previous studies utilizing stem cell-based therapies to improve cognition following irradiation or chemotherapy entailed dosing the animals with stem cells or stem cell-derived EVs two days to four weeks following the final exposure, to avoid abolishing any benefit conferred by stem cell transplantation by subsequent irradiation, which could lead to the rapid deterioration of the transplanted cells. The mechanism of delivery (e.g. cranial transplantation) was also invasive enough to threaten the viability of undertaking such a surgery among the intermittent administration of radio- and chemotherapy. However, both theoretical drawbacks are eliminated by utilizing extracellular vesicles, as the biocargo they bear is less likely to be damaged by subsequent radiation or temozolomide. The retro-orbital route of administration for the EVs also lends itself more suitably to delivery before or during the treatment with cranial-only fractionated irradiation. Thus, we hypothesized that injecting GABAergic neuron-derived EVs three times the week before the first fractionated radiation dose could result in a preemptive protective effect that inhibits the deleterious effects of IRR exposure before they take place, and thus investigated a potentially-superior translational approach to mitigate the adverse neurocognitive complications associated with clinically relevant brain tumor treatments.

This study seeks to extend previous work by evaluating whether pre-treatment with GABAergic neuron-derived EVs can confer a protective effect to prevent the deleterious effects of fractionated irradiation on cognition, recognizing that it would be preferable clinically to prevent the neurocognitive insults associated with irradiation and chemotherapy before they occur rather

than trying to mollify them after they have occurred. Additionally, the logic behind transplanting neural stem cells subsequent to irradiation and chemotherapy exposure (rather than prior to such exposure) is not necessarily applicable to the administration of extracellular vesicles derived from neural stem cells. Specifically, neural stem cells exhibit an exquisite sensitivity to irradiation, such that engrafting them in advance of radiation exposure would only lead to the death of the cells after radiation, which, rather than alleviating subsequent cognitive deficits, would be likely to exacerbate them. However, the bioactive cargo contained within stem cell-derived EVs, which can include proteins, lipids, mRNAs, and micro-RNAs [100], is unlikely to present the same radiosensitivity, and thus may not be negatively impacted by subsequent exposure to radiation. Instead, the benefits conferred by the EVs may be amplified by injecting them before subjecting them to irradiation treatment, by allowing them to evoke a protective reaction in the brain that holds the potential to inhibit the mechanisms by which irradiation and chemotherapy damage the central nervous system and thereby avert neurocognitive decline after the cancer therapies are administered. The other obstacle to pre-emptive administration of stem cell-based therapies in advance of irradiation/ chemotherapy in past studies was the nontrivial recovery time associated with cranial transplantation surgeries, during which time period the animals would be ill-equipped to tolerate the additional neurological injury caused by cancer treatment. However, with the promising results previously described suggesting that retro-orbital delivery of EVs is equally efficacious, this obstacle to antecedent injection has likewise been removed.

However, some potential caveats remain in developing therapies predicated on pre-treatment with extracellular vesicles for oncologic utilization. Chiefly, these include the possibility that pretreatment with extracellular vesicles may alter the course of cancer treatments themselves, either by directly modulating tumor growth and progression or by changes to the tumor microenvironment that are more permissive to tumorigenesis. Though there is some safety risk

associated with stem cell-based extracellular vesicles regardless of treatment timeline relative to irradiation and/or chemotherapy treatments, the threat would be more likely to be exacerbated if the administration of extracellular vesicles transpires before rather than after cancer treatments. The Limoli lab has published a study [101] undertaking an assessment of retroorbital injections of human embryonic stem cell-derived extracellular vesicles, finding that the administration of these extracellular vesicles did not cause an increase the growth of flank tumors in mice harboring TC1 tumor xenografts as a model system for cancer. However, if or how these findings translate to other clinically relevant contexts remains to be studied.

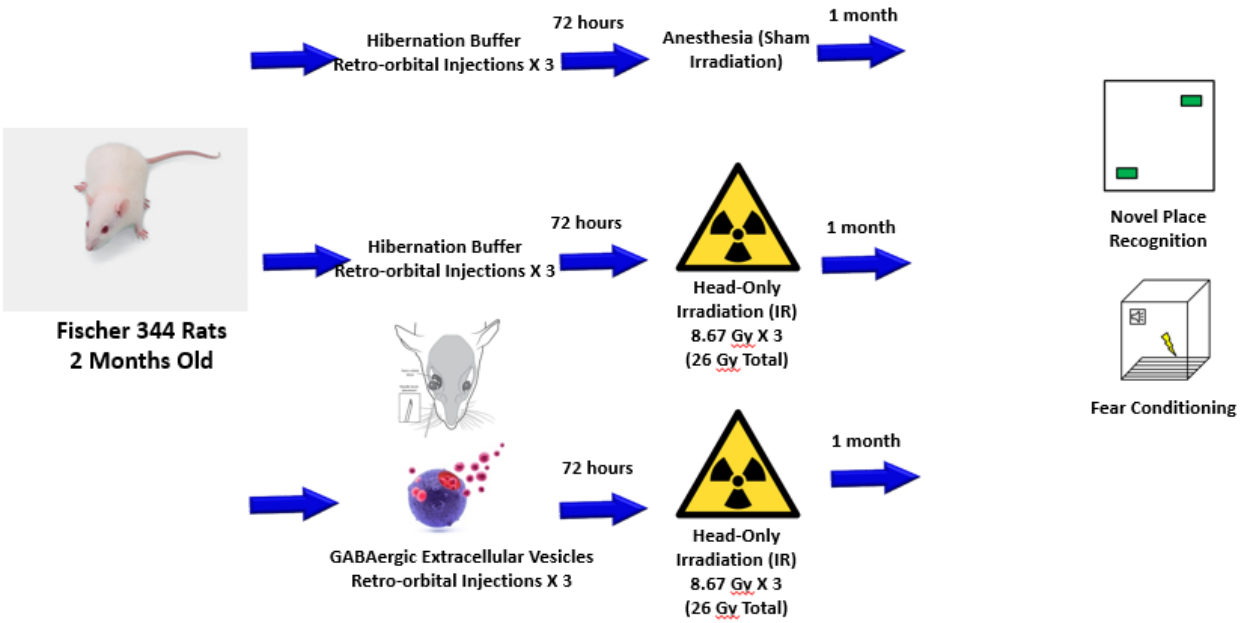

Figure 6.1: Experimental design

Materials and Methods

Animals and irradiation

All animal procedures are in accordance with NIH and approved by the University of California Institutional Animal Care and Use Committee. Eight-week-old male Fischer 344 rats (Crl:CD(Fischer 344), strain 002, Charles River Laboratories, Wilmington, MA) were maintained in standard housing conditions (20°C ± 1°C; 70% ± 10% humidity; 12 h:12 h light and dark cycle) and provided *ad libitum* access to food and water. The Fischer 344 rats were divided into three experimental groups (N = 16 animals per group): a control group that received sham irradiation (exposure to anesthesia) and vehicle (hibernation buffer) retro-orbital injections, a group that received 26 Gy total fractionated irradiation and vehicle injections, and a group that received 26 Gy total fractionated irradiation and injections of GABAergic neuron-derived extracellular vesicles. Rats were anesthetized using an isoflurane gas system (VWR Mobile RC2; induction=3.5% vol/vol isoflurane/oxygen) for irradiation, which was delivered using a self-shielded 320 kV X-irradiator (X-RAD320 irradiator, Precision X-Ray, North Branford, CT) and lead shielding to facilitate head-only irradiation over a 2 cm^2 area at a dose rate of 1 Gy/min. The irradiated experimental groups receiving three fractionated doses of whole-brain irradiation of 8.67 Gy x 3 (total 26 Gy) one week following the administration of the extracellular vesicles over the course of five days (i.e. delivered on days 8, 10, and 12). Control animals were anesthetized for the same amount of time as the irradiated animals to ensure corresponding isoflurane exposure, and handled identically to those undergoing irradiation.

Extracellular vesicle isolation

GABAergic neuron-derived extracellular vesicles were collected from conditioned culture media in which induced pluripotent stem (iPS) cell-derived GABAergic neurons (iCell GABANeurons, 01434, FUJIFILM Cellular Dynamics, Inc, Madison, WI) were cultured. The extracellular vesicles were

isolated and purified from the conditioned media by ultracentrifugation. The conditioned media was first centrifuged at 300 x g for 10 minutes to remove cells and cellular debris. The media was then centrifuged at 100,000 × g for 90 minutes and the extracellular vesicles were collected in hibernation buffer; the extracellular vesicles were pooled and purified in sterile Dulbecco's phosphate-buffered saline at 100,000 x g for 120 minutes, and collected in hibernation buffer. The extracellular vesicles were characterized using a ZetaView PMX 110 particle analyzer (Particle Metrix GmbH; Meerbusch Germany).

Retro-orbital injections

This study was initiated with retro-orbital injections of GABAergic neuron-derived EVs one week prior to the first dose of fractionated radiation, followed by a second retro-orbital injection two days later and a final EV injection administered two days following the second (e.g. injections on days 1, 3, and 5 of the experiment, with fractionated radiation doses of 8.67 G delivered on days 8, 10, and 12). The rats were anesthetized using an isoflurane gas system (VWR Mobile RC2; maintenance=3.5% vol/vol isoflurane/oxygen), and extracellular vesicles or vehicle (hibernation buffer) were delivered to the rats through circulation via the retro-orbital sinus. A 31-gauge needle with a 0.5 ml syringe attached (BD Veo™ insulin syringes with BD Ultra-Fine™ 6mm x 31G needle) was used to pierce 2 to 3 mm into the rat's orbital venous sinus with the bevel on the needle facing upward at a 45° angle before injecting the extracellular vesicles. The control and irradiated experimental groups received retro-orbital injections of 100 microliters hibernation buffer (vehicle). For the GABAergic extracellular vesicle group, 1.5 x 10^9 extracellular vesicles in 100 microliters hibernation buffer were delivered by retro-orbital injection.

	Protective Protocol						
	Day 1	Day 2	Day 3	Day 4	Day 5	Day 6	Day 7
Week 1	EV RO		EV RO		EV RO		
Week 2	IRR		IRR		IRR		

Table 6.1: Timeline of treatment for protective application of GABAergic extracellular vesicles prior to irradiation

Behavioral cognitive testing

Two weeks following the last retro-orbital injections, the rats underwent a battery of behavioral tasks designed to interrogate cognitive function. The animals were tested on spontaneous exploration tasks, namely Novel Place Recognition, which is sensitive to spatial cognitive impairments caused by hippocampal damage; and Novel Object Recognition, which assesses episodic memory retention dependent on the frontal and pre-frontal cortex. For the Novel Place Recognition and Novel Object Recognition tasks, the trials were scored for exploration time of the novel and familiar objects for each animal (n=16 per experimental group) and the discrimination index was calculated from the equation: [(Novel Object/Total Exploration Time) – (Familiar/Total Exploration Time)] × 100. A cognitively-intact animal is expected to exhibit a preference for novelty in each of these tasks. Statistical analysis was performed using a repeated measure ANOVA with Bonferroni correction in GraphPad Prism 6.0 Software (GraphPad Software Inc.), and data was plotted as mean ± SEM with significance set at $\alpha = 0.05$.

Extraction and ELISA for assessment of neurotrophins

Following the behavioral testing at approximately six weeks post-final retro-orbital injections, the rats were euthanized using isoflurane anesthesia. Brains were immediately extracted from the skull (N = 4-5 per group) and the hippocampus was dissected from each cerebral hemisphere. Each hippocampus was weighed and transferred into 300 µL ice-cold lysis buffer (N-PER Neuronal Protein Extraction Reagent, Thermo Scientific Product number 23225) containing sodium orthovanadate (0.5 mM), pheyl-methylsulfonyl fluoride (PMSF, 1 mM), aprotinin (10 µg/mL), and leupeptin (1 µg/mL; Santa Cruz Biotechnology, Santa Cruz, California). Tissues were sonicated individually, centrifuged at 4°C for 15 minutes at 13,200 rpm, and the supernatants were collected and diluted 1:5 with Dulbecco's phosphate-buffered saline. The supernatants were

acidified to pH 2.6 then neutralized to pH 7.6 to liberate the neurotrophic factors, and the BDNF and GDNF levels were assayed using E_{max} ImmunoAssay Systems from Promega (BDNF catalog number G7611, GDNF catalog number G7621) and uncoated ELISA plates (Biolegend Nunc MaxiSorp, catalog number 423501). All measurements were performed at a wavelength of 450 µm on a microplate reader (BioTek Synergy Mx).

Quantification of dendritic spine density

At approximately six weeks post-final retro-orbital injections, the rats were euthanized using isoflurane anesthesia and perfused with saline + heparin. Brains (N = 4 per group) were extracted from the skull and subjected to Golgi-Cox impregnation and staining of neurons according to the manufacturer's instructions (SuperGolgi kit, Bioenno Tech., Santa Ana, California). The brains were sectioned to 100 µm using a vibratome (need details on vibratome) and counterstained by nuclear fast red to visualize hippocampal subregions. The Stereoinvestigator program (v11, MicroBrightField) was used for the quantification of dendritic spines using four serial sections (every second) throughout the hippocampus to analyze potential differences in spine density between each of the experimental cohorts.

Results

Pre-emptive Retro-Orbital Application of GABAergic Extracellular Vesicles Allays Radiation-Induced Cognitive Dysfunction

Four weeks after the last dose of fractionated irradiation and five weeks following the last EV injection, the Fischer 344 rats (N = 16 rats per group) were subjected to a series behavioral tasks designed to interrogate cognitive function. The animals were habituated to the testing room and arena for three days before performing the Novel Object Recognition test to evaluate hippocampal function, in which they were exposed to two identical objects for five minutes, then

removed from the arena for five minutes, then returned to the arena with one of the same ("familiar") objects and a new ("novel") object. Control animals were able to discriminate between the novel and familiar objects and exhibited a preference for the novel objects as expected for cognitively-intact animals (mean discrimination index= 26.13%), while the animals that received fractionated irradiation showed no ability to discriminate between novel and familiar (mean discrimination index=-3.59%). The rats treated with GABAergic extracellular vesicles following irradiation demonstrated improvement in cognitive function on the Novel Object Recognition Task (mean discrimination index= 20.87%). Significant overall group effects were found ($F(2, 43) = 5.982$; $P=0.0488$), and the differences between the performance of the control group and the irradiated group ($F(2, 43) = 5.982$; $P=0.0393$) and that of the irradiated group and the extracellular vesicle-treated group ($F(2, 43) = 5.982$; $P=0.0450$) were statistically significant (Figure 6.2). In contrast, the mean discrimination index of the control group and the extracellular vesicle group were statistically indistinguishable ($F(2, 43) = 5.982$; $P>0.9999$).

The vitality of the function of the rats' pre-frontal and frontal cortices was next investigated via the Novel Place Recognition test. The animals were placed in an arena with two identical objects for five minutes, then returned to their housing for one hour, and finally placed back in the arena with one of the objects in its original position ("familiar") and the other object moved to a different position ("novel"). The Novel Place Recognition test detected an overall group effect ($F(2, 39) = 12.74$), with both the control (mean discrimination index=36.84%) and extracellular vesicle-treated (mean discrimination index= 23.06%) groups had higher mean discrimination indices than the irradiated group (mean discrimination index= -16.37%). Both of these differences, that between the control group and the irradiated group ($F(2, 39) = 12.74$; $P<0.0001$) and that between the irradiated group and the group that received protective

GABAergic extracellular vesicles before irradiation ($F(2, 39) = 12.74$; $P=0.0028$), were statistically significant (Figure 6.3). However, the control and GABAergic EV cohorts were statistically comparable ($F(2, 39) = 12.74$; $P=0.6063$)

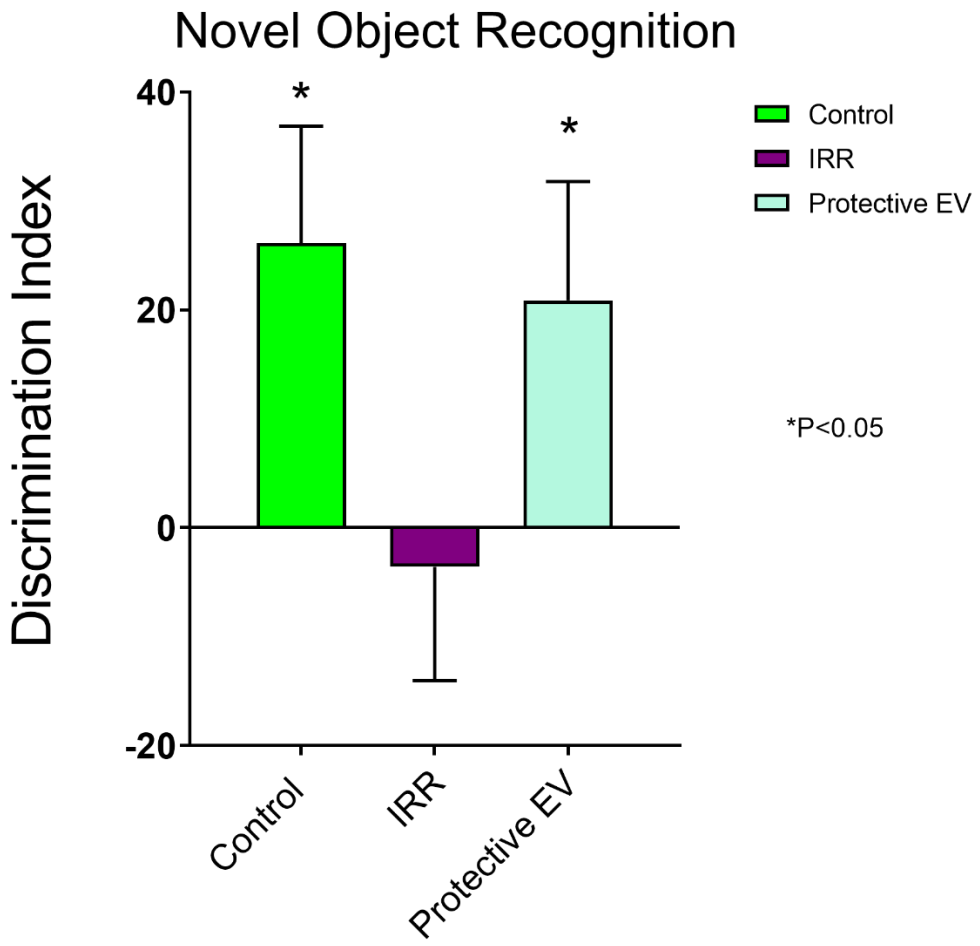

Figure 6.2: Protective application of GABAergic extracellular vesicles by retro-orbital injection mitigates radiation-induced performance decrements on the Novel Object Recognition task. Data are presented as the mean ± SEM (N = 16 animals/group). *P*-values are derived from analysis of variance and Bonferroni's multiple comparisons test. *, $P < .05$ all compared against the irradiated group

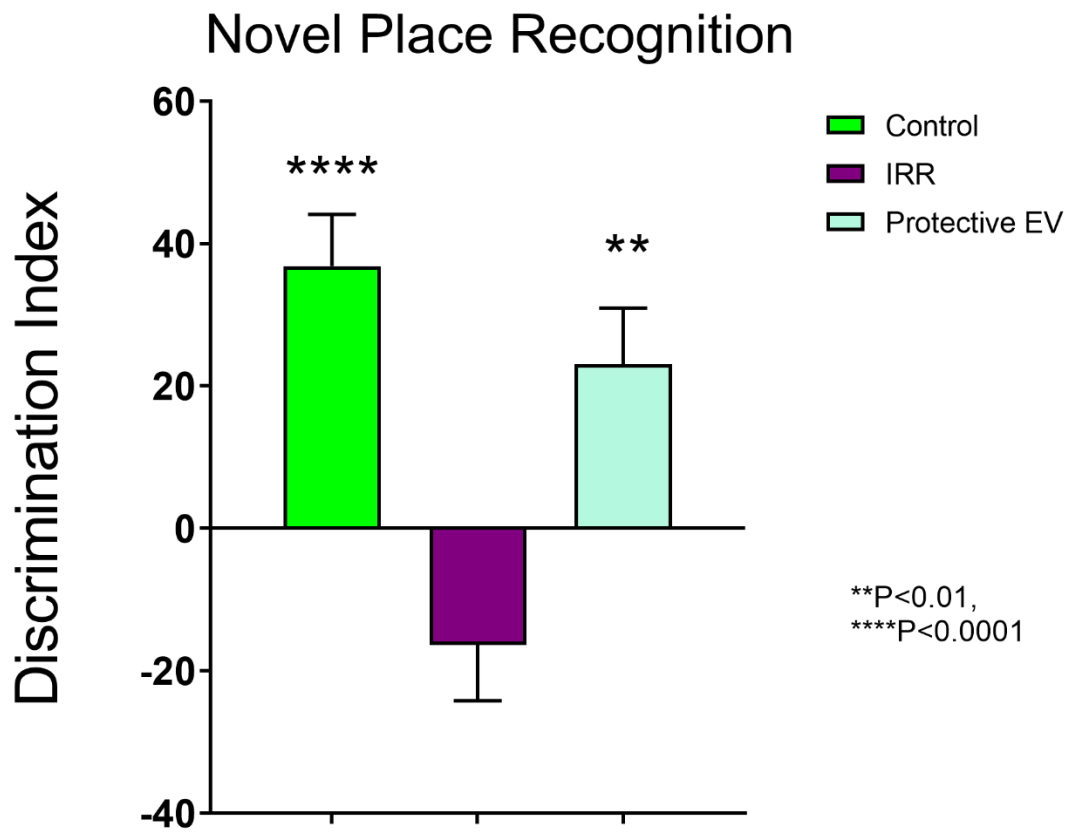

Figure 6.3: Pre-emptive administration of retro-orbital GABAergic extracellular vesicles prior to irradiation obliterates the inability to discriminate between novelty and familiarity on the Novel Place Recognition task. Data are presented as the mean ± SEM (N = 16 animals/group). *P*-values are derived from analysis of variance and Bonferroni's multiple comparisons test.

**, $P < .01$; ****, P<.0001 all compared against the irradiated group

Pre-emptive Injection of GABAergic Extracellular Vesicles Maintains Neurotrophin Levels After Irradiation

The effect of GABAergic extracellular vesicles on neurotrophin levels, specifically brain-derived neurotrophic factor and glial cell line-derived neurotrophic factor, in the hippocampus after fractionated irradiation was investigated by ELISA assay. The brain-derived neurotrophic factor (BDNF) analysis showed significant overall group effects ($F(2, 45) = 20.32$; $P<0.0001$); there was a significant decrease in hippocampal BDNF after fractionated irradiation ($F(2, 45) = 20.32$; $P <0.0001$) as compared to the control animals, but in the animals that first received injections of GABAergic extracellular vesicles before being irradiated, the BDNF levels were maintained, with a statistically significant increase in BDNF as compared to the irradiated rats ($F(2, 45) = 20.32$; $P <0.0001$). The BDNF levels in the control group and the group subjected to fractionated irradiation and protective GABAergic extracellular vesicles were highly similar, with no statistically significant difference between them ($F(2, 45) = 20.32$; $P=0.7855$).

Correspondingly, significant group effects ($F(2, 45) = 84.50$; $P<0.0001$) were detected in the glial cell line-derived neurotrophic factor (GDNF) assay. The irradiated animals experienced a statistically significant reduction in GDNF ($F(2, 45) = 84.50$; $P<0.0001$) relative to the control group; this reduction was mitigated by the protective application of GABAergic extracellular vesicles before undergoing irradiation, which caused a statistically significant increase in GDNF compared to the irradiated animals ($F(2, 45) = 84.50$; $P<0.0001$). Levels of GDNF in the control group and the extracellular vesicle-treated group were statistically equivalent, with no significant difference observed ($F(2, 45) = 84.50$; $P=0.4695$).

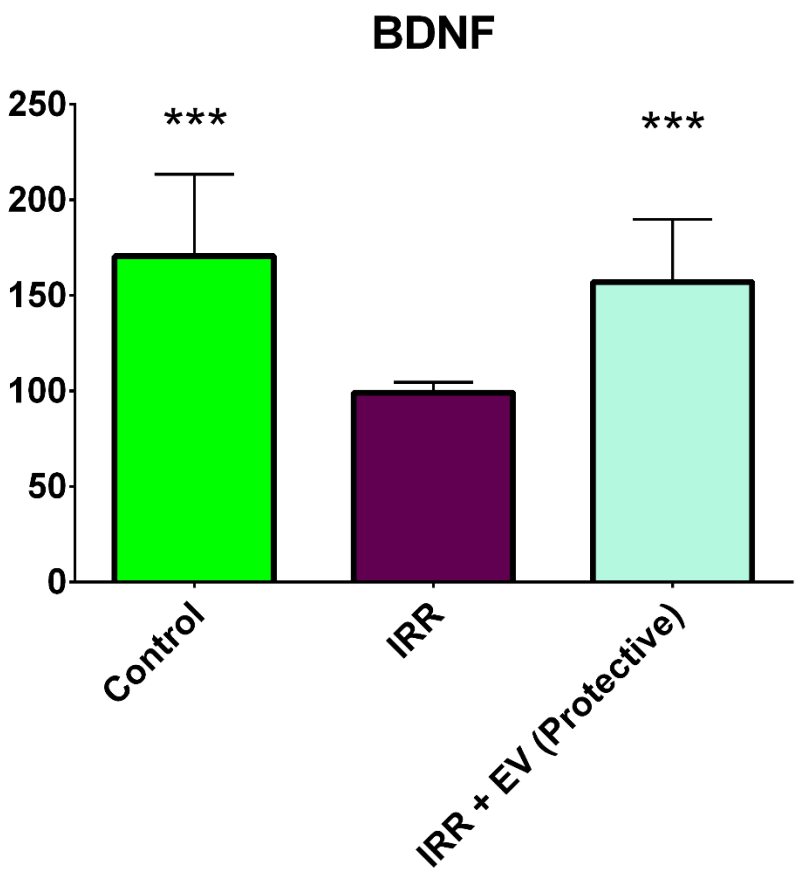

Figure 6.4: Reductions in brain-derived neurotrophic factor following 26 Gy fractionated irradiation are ameliorated by the protective application of GABAergic extracellular vesicles by retro-orbital injection before the doses of radiation. Data are presented as the mean ± SEM (N = 4-5 animals/group). P-values are derived from analysis of variance and Bonferroni's multiple comparisons test. ***, $P < .001$ all compared against the irradiated group

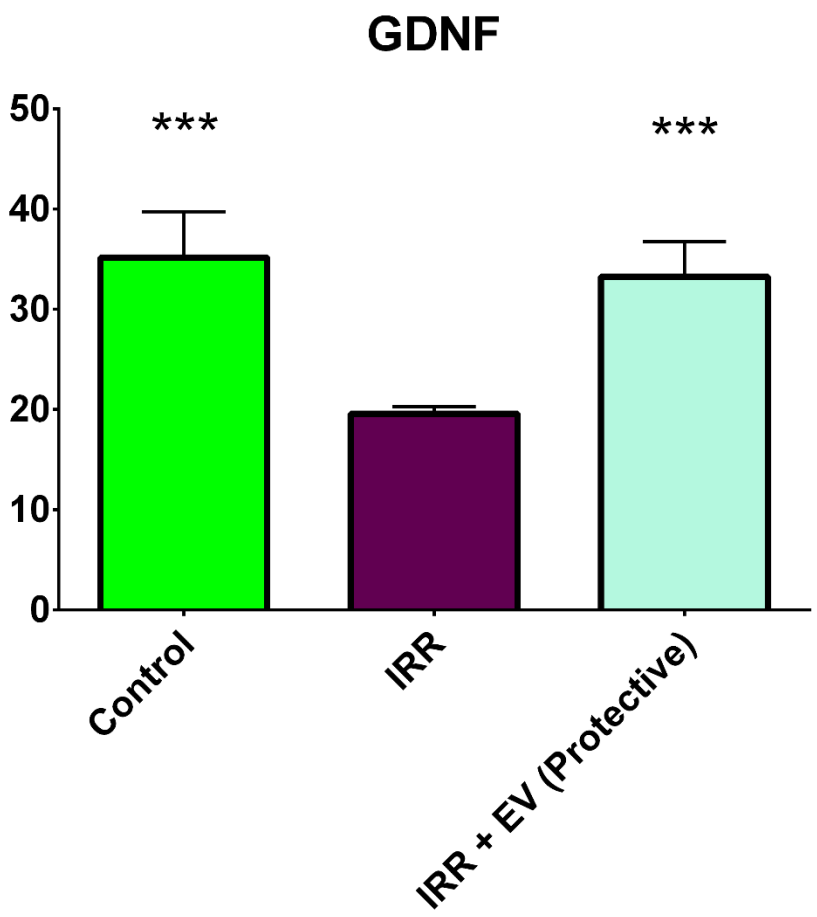

Figure 6.5: Glial cell-derived neurotrophic factor levels in the hippocampus are preserved in the irradiated brain if GABAergic extracellular treatment is applied by retro-orbital injection protectively prior to irradiation. Data are presented as the mean ± SEM (N = 4-5 animals/group). P-values are derived from analysis of variance and Bonferroni's multiple comparisons test. ***, $P < .001$ all compared against the irradiated group

Future Directions/ Studies in Progress

Again mirroring previous related studies described in this dissertation, brains from this experimental cohort have undergone Golgi-Cox staining, which will enable us to investigate dendritic spine density and host neuronal morphology throughout the hippocampus by employing spine counting and neuron tracing. Brains prepared for immunohistochemical analyses will be used to assess neuroinflammation, post-synaptic protein expression, microvasculature integrity, and serotonin receptor (5-HT_{1A}) density. To assess neuroinflammation, immunostaining for activated microglia (ED-1+ cells) will be carried out on serial sections, and the number of activated microglia within the DH, GCL and CA3/CA1 regions of the hippocampus will be analyzed by stereology. Immunostaining for post-synaptic density protein 95 will be executed to interrogate post-synaptic protein expression. The endothelium marker RECA will be employed to quantify the structural complexity and volume of the microvasculature, as immunostaining should proffer a vascular network to be imaged by confocal microscopy. Previous data has suggested that the volume of the capillary bed is reduced following chemotherapy, and thus this approach should prove informative in investigating the effects of a combined irradiation-chemotherapy treatment protocol on the neurovasculature. Lastly, utilizing immunohistochemical techniques to quantify 5-HT_{1A} receptor expression will explore how IRR exposure affects expression of this inhibitory G protein-coupled receptor, and perhaps more interestingly, whether the injection of GABA-derived EVs increases its expression.

REFERENCES

1. Cancer Stat Facts: Brain and Other Nervous System Cancer. National Cancer Institute Surveillance, Epidemiology, and End Results Program. https://seer.cancer.gov/statfacts/html/brain.html

2. Lee YW, Cho HJ, Lee WH, Sonntag WE. Whole brain radiation-induced cognitive impairment: pathophysiological mechanisms and therapeutic targets. Biomol Ther (Seoul). 2012; 20(4):357–70. DOI: 10.4062/biomolther.2012.20.4.357 [PubMed: 24009822]

3. Miller KD, Siegel RL, Lin CC, Mariotto AB, Kramer JL, Rowland JH, et al. Cancer treatment and survivorship statistics, 2016. CA Cancer J Clin. 2016; 66(4):271–89. DOI: 10.3322/caac.21349 [PubMed: 27253694]

4. Butler JM, Rapp SR, Shaw EG. Managing the cognitive effects of brain tumor radiation therapy. Curr Treat Options Oncol. 2006; 7(6):517–23. [PubMed: 17032563]

5. Meyers CA, Brown PD. Role and relevance of neurocognitive assessment in clinical trials of patients with CNS tumors. J Clin Oncol. 2006; 24(8):1305–9. 24/8/1305 [pii]. DOI: 10.1200/JCO.2005.04.6086 [PubMed: 16525186]

6. Roman DD, Sperduto PW. Neuropsychological effects of cranial radiation: current knowledge and future directions. Int J Radiat Oncol Biol Phys. 1995; 31(4):983–98. [PubMed: 7860415]

7. Duffner PK. Long-term effects of radiation therapy on cognitive and endocrine function in children with leukemia and brain tumors. Neurologist. 2004; 10(6):293–310. DOI: 10.1097/01.nrl.0000144287.35993.96 [PubMed: 15518596]

8. Sundgren PC, Cao Y. Brain irradiation: effects on normal brain parenchyma and radiation injury. Neuroimaging Clin N Am. 2009; 19(4):657–68. DOI: 10.1016/j.nic.2009.08.014 [PubMed: 19959011]

9. Greene-Schloesser D, Robbins ME. Radiation-induced cognitive impairment--from bench to bedside. Neuro-oncology. 2012; 14(Suppl 4):iv37–44. DOI: 10.1093/neuonc/nos196 [PubMed: 23095829]

10. Greene-Schloesser D, Robbins ME, Peiffer AM, Shaw EG, Wheeler KT, Chan MD. Radiation-induced brain injury: A review. Front Oncol. 2012; 2:73.doi: 10.3389/fonc.2012.00073 [PubMed: 22833841]

11. Parihar VK, Limoli CL. Cranial irradiation compromises neuronal architecture in the hippocampus. Proc Natl Acad Sci USA. 2013; 110(31):12822–7. DOI: 10.1073/pnas.1307301110 [PubMed: 23858442]

12. Greene-Schloesser D, Moore E, Robbins ME. Molecular pathways: radiation-induced cognitive impairment. Clin Cancer Res. 2013; 19(9):2294–300. DOI: 10.1158/1078-0432.CCR-11-2903 [PubMed: 23388505]

13. Tseng BP, Giedzinski E, Izadi A, Suarez T, Lan ML, Tran KK, et al. Functional consequences of radiation-induced oxidative stress in cultured neural stem cells and the brain exposed to charged particle irradiation. Antioxid Redox Signal. 2014; 20(9):1410–22. DOI: 10.1089/ars.2012.5134 [PubMed: 23802883]

14. Parihar VK, Acharya MM, Roa DE, Bosch O, Christie LA, Limoli CL. Defining functional changes in the brain caused by targeted stereotaxic radiosurgery. Transl Cancer Res. 2014; 3(2):124–37. DOI: 10.3978/j.issn.2218-676X.2013.06.02 [PubMed: 24904783]

15. Parihar VK, Allen BD, Tran KK, Chmielewski NN, Craver BM, Martirosian V, et al. Targeted overexpression of mitochondrial catalase prevents radiation-induced cognitive dysfunction. Antioxid Redox Signal. 2015; 22(1):78–91. DOI: 10.1089/ars.2014.5929 [PubMed: 24949841]

16. Acharya MM, Baulch JE, Lusardi TA, Allen BD, Chmielewski NN, Baddour AA, et al. Adenosine Kinase Inhibition Protects against Cranial Radiation-Induced Cognitive Dysfunction. Front Mol Neuroscience. 2016; 9:42.doi: 10.3389/fnmol.2016.00042

17. Liu R, Page M, Solheim K, Fox S, Chang SM. Quality of life in adults with brain tumors: current knowledge and future directions. Neuro-oncology. 2009; 11(3):330–9. DOI: 10.1215/15228517-2008-093 [PubMed: 19001097]

18. Benderitter M, Caviggioli F, Chapel A, Coppes RP, Guha C, Klinger M, et al. Stem cell therapies for the treatment of radiation-induced normal tissue side effects. Antioxid Redox Signal. 2014; 21(2):338–55. DOI: 10.1089/ars.2013.5652 [PubMed: 24147585]

19. Graves PR, Siddiqui F, Anscher MS, Movsas B. Radiation pulmonary toxicity: from mechanisms to management. Semin Radiat Oncol. 2010; 20(3):201–7. DOI: 10.1016/j.semradonc.2010.01.010 [PubMed: 20685583]

20. Tsoutsou PG, Koukourakis MI. Radiation pneumonitis and fibrosis: mechanisms underlying its pathogenesis and implications for future research. Int J Radiat Oncol Biol Phys. 2006; 66(5):1281–93. DOI: 10.1016/j.ijrobp.2006.08.058 [PubMed: 17126203]

21. Xue J, Li X, Lu Y, Gan L, Zhou L, Wang Y, et al. Gene-modified mesenchymal stem cells protect against radiation-induced lung injury. Mol Ther. 2013; 21(2):456–65. DOI: 10.1038/mt.2012.183 [PubMed: 23299797]

22. Kursova LV, Konoplyannikov AG, Pasov VV, Ivanova IN, Poluektova MV, Konoplyannikova OA. Possibilities for the use of autologous mesenchymal stem cells in the therapy of radiation-induced lung injuries. Bull Exp Biol Med. 2009; 147(4):542–6. [PubMed: 19704968]

23. Lombaert IM, Brunsting JF, Wierenga PK, Faber H, Stokman MA, Kok T, Visser WH, Kampinga HH, de Haan G, Coppes RP. Rescue of salivary gland function after stem cell transplantation in irradiated glands. PLoS One. 2008; 3(4):e2063. [PubMed: 18446241]

24. Nanduri LS, Lombaert IM, van der Zwaag M, Faber H, Brunsting JF, van Os RP, et al. Salisphere derived c-Kit+ cell transplantation restores tissue homeostasis in irradiated salivary gland. Radiother Oncol. 2013; 108(3):458–63. DOI: 10.1016/j.radonc.2013.05.020 [PubMed: 23769181]

25. Coppes RP, Stokman MA. Stem cells and the repair of radiation-induced salivary gland damage. Oral Dis. 2011; 17(2):143–53. DOI: 10.1111/j.1601-0825.2010.01723.x [PubMed: 20796229]

26. Nanduri LS, Maimets M, Pringle SA, van der Zwaag M, van Os RP, Coppes RP. Regeneration of irradiated salivary glands with stem cell marker expressing cells. Radiother Oncol. 2011; 99(3):367–72. DOI: 10.1016/j.radonc.2011.05.085 [PubMed: 21719134]

27. Porock D, Nikoletti S, Kristjanson L. Management of radiation skin reactions: literature review and clinical application. Plast Surg Nurs. 1999; 19(4):185–92. 223. quiz 191-2. [PubMed: 12024597]

28. Francois S, Mouiseddine M, Mathieu N, Semont A, Monti P, Dudoignon N, et al. Human mesenchymal stem cells favour healing of the cutaneous radiation syndrome in a xenogenic transplant model. Ann Hematol. 2007; 86(1):1–8. DOI: 10.1007/s00277-006-0166-5 [PubMed: 17043780]

29. Huang SP, Huang CH, Shyu JF, Lee HS, Chen SG, Chan JY, et al. Promotion of wound healing using adipose-derived stem cells in radiation ulcer of a rat model. J Biomed Sci. 2013; 20:51.doi: 10.1186/1423-0127-20-51 [PubMed: 23876213]

30. Ebrahimian TG, Pouzoulet F, Squiban C, Buard V, Andre M, Cousin B, et al. Cell therapy based on adipose tissue-derived stromal cells promotes physiological and pathological wound healing. Arterioscler Thromb Vasc Biol. 2009; 29(4):503–10. DOI: 10.1161/ATVBAHA.108.178962 [PubMed: 19201690]

31. Li N, Zhang L, Li H, Fang B. Human CD34+ cells mobilized by granulocyte colony-stimulating factor ameliorate radiation-induced liver damage in mice. Stem Cell Res Ther. 2010; 1(3):22.doi: 10.1186/scrt22 [PubMed: 20633298]

32. Gong W, Guo M, Han Z, Wang Y, Yang P, Xu C, et al. Mesenchymal stem cells stimulate intestinal stem cells to repair radiation-induced intestinal injury. Cell Death Dis. 2016; 7(9):e2387.doi: 10.1038/cddis.2016.276 [PubMed: 27685631]

33. Saha S, Bhanja P, Kabarriti R, Liu L, Alfieri AA, Guha C. Bone marrow stromal cell transplantation mitigates radiation-induced gastrointestinal syndrome in mice. PLoS One. 2011; 6(9):e24072.doi: 10.1371/journal.pone.0024072 [PubMed: 21935373]

34. Semont A, Francois S, Mouiseddine M, Francois A, Sache A, Frick J, et al. Mesenchymal stem cells increase self-renewal of small intestinal epithelium and accelerate structural recovery after radiation injury. Adv Exp Med Biol. 2006; 585:19–30. [PubMed: 17120774]

35. Kudo K, Liu Y, Takahashi K, Tarusawa K, Osanai M, Hu DL, et al. Transplantation of mesenchymal stem cells to prevent radiation-induced intestinal injury in mice. J Radiat Res. 2010; 51(1):73–9. [PubMed: 19851042]

36. Zheng K, Wu W, Yang S, Huang L, Chen J, Gong C, et al. Treatment of radiation-induced acute intestinal injury with bone marrow-derived mesenchymal stem cells. Exp Ther Med. 2016; 11(6):2425–31. DOI: 10.3892/etm.2016.3248 [PubMed: 27284330]

37. Chang PY, Qu YQ, Wang J, Dong LH. The potential of mesenchymal stem cells in the management of radiation enteropathy. Cell Death Dis. 2015; 6:e1840.doi: 10.1038/cddis.2015.189 [PubMed: 26247725]

38. Acharya MM, Martirosian V, Chmielewski NN, Hanna N, Tran KK, Liao AC, et al. Stem cell transplantation reverses chemotherapy-induced cognitive dysfunction. Cancer Res. 2015; 75(4):676–86. DOI: 10.1158/0008-5472.CAN-14-2237 [PubMed: 25687405]

39. Zickri MB, El Aziz DH, Metwally HG. Histological experimental study on the effect of stem cell therapy on adriamycin induced chemobrain. Int J Stem Cells. 2013; 6(2):104–12. [PubMed: 24386554]

40. Blurton-Jones M, et al. Neural stem cells improve cognition via BDNF in a transgenic model of Alzheimer disease. Proc Natl Acad Sci U S A 2009; 106(32):13594-13599.

41. Yamasaki TR, et al. Neural stem cells improve memory in an inducible mouse model of neuronal loss. J Neurosci 2007;27(44):11925-11933.

42. Acharya MM, Hattiangady B, & Shetty AK. Progress in neuroprotective strategies for preventing epilepsy. Prog Neurobiol 2008; 84(4):363-404.

43. Boison D. Engineered adenosine-releasing cells for epilepsy therapy: human mesenchymal stem cells and human embryonic stem cells. Neurotherapeutics 2009;6(2):278-283.

44. Maisano X, et al. Embryonic stem cell-derived neural precursor grafts for treatment of temporal lobe epilepsy. Neurotherapeutics 2009; 6(2):263-277.

45. Riess P, et al. Embryonic stem cell transplantation after experimental traumatic brain injury dramatically improves neurological outcome, but may cause tumors. J Neurotrauma 2007; 24(1):216-225.

46. Acharya MM, Christie LA, Lan ML, Donovan PJ, Cotman CW, Fike JR, et al. Rescue of radiation-induced cognitive impairment through cranial transplantation of human embryonic stem cells. Proc Natl Acad Sci U S A. 2009; 106(45):19150–5. DOI: 10.1073/pnas.0909293106 [PubMed: 19901336]

47. Acharya MM, Christie LA, Lan ML, Giedzinski E, Fike JR, Rosi S, et al. Human neural stem cell transplantation ameliorates radiation-induced cognitive dysfunction. Cancer Res. 2011; 71(14):4834–45. DOI: 10.1158/0008-5472.CAN-11-0027 [PubMed: 21757460]

48. Guzowski J, Setlow B, Wagner E, McGaugh J. Experience-dependent gene expression in the rat hippocampus after spatial learning: a comparison of the immediate-early genes Arc, c-fos, and zif268. J Neurosci. 2001; 21(14):5089–98. [PubMed: 11438584]

49. Guzowski JF, Timlin JA, Roysam B, McNaughton BL, Worley PF, Barnes CA. Mapping behaviorally relevant neural circuits with immediate-early gene expression. Curr Opin Neurobiol. 2005; 15(5):599–606. DOI: 10.1016/j.conb.2005.08.018 [PubMed: 16150584]

50. Acharya MM, Christie LA, Lan ML, Limoli CL. Comparing the functional consequences of human stem cell transplantation in the irradiated rat brain. Cell Transplant. 2013; 22(1):55–64. DOI: 10.3727/096368912X640565 [PubMed: 22546529]

51. Acharya MM, Martirosian V, Christie LA, Limoli CL. Long-term cognitive effects of human stem cell transplantation in the irradiated brain. Int J Radiat Biol. 2014; 90(9):816–20. DOI: 10.3109/09553002.2014.927934 [PubMed: 24882389]

52. Acharya MM, Rosi S, Jopson T, Limoli CL. Human neural stem cell transplantation provides long-term restoration of neuronal plasticity in the irradiated hippocampus. Cell Transplant. 2015; 24(4):691–702. DOI: 10.3727/096368914X684600 [PubMed: 25289634]

53. Acharya MM, Christie LA, Hazel TG, Johe KK, Limoli CL. Transplantation of human fetal-derived neural stem cells improves cognitive function following cranial irradiation. Cell Transplant. 2014; 23(10):1255–66. DOI: 10.3727/096368913X670200 [PubMed: 23866792]

54. Acharya MM, Martirosian V, Christie LA, Riparip L, Strnadel J, Parihar VK, et al. Defining the optimal window for cranial transplantation of human induced pluripotent stem cell-derived cells to ameliorate radiation-induced cognitive impairment. Stem Cell Transl Med. 2015; 4(1):74–83. DOI: 10.5966/sctm.2014-0063

55. Baulch JE, Acharya MM, Allen BD, Ru N, Chmielewski NN, Martirosian V, et al. Cranial grafting of stem cell-derived microvesicles improves cognition and reduces neuropathology in the irradiated brain. Proc Natl Acad Sci U S A. 2016; 113(17):4836–41. DOI: 10.1073/pnas.1521668113 [PubMed: 27044087]

56. Xin H, et al. Exosome-mediated transfer of miR-133b from multipotent mesenchymal stromal cells to neural cells contributes to neurite outgrowth. Stem Cells 2012;30(7):1556-1564.

57. Xin H, et al. Systemic administration of exosomes released from mesenchymal stromal cells promote functional recovery and neurovascular plasticity after stroke in rats. J Cereb Blood Flow Metab 2013;33(11):1711-1715.

58. Xiong Y, Zhang Y, Mahmood A, & Chopp M. Investigational agents for treatment of traumatic brain injury. Expert Opin Investig Drugs 2015;24(6):743-760.

59. Zhao C, Deng W, & Gage FH. Mechanisms and functional implications of adult neurogenesis. Cell 2008; 132(4):645-660.

60. Xin H, et al. MiR-133b Promotes Neural Plasticity and Functional Recovery After Treatment of Stroke with Multipotent Mesenchymal Stromal Cells in Rats Via Transfer of Exosome-Enriched Extracellular Particles. Stem Cells 32013;1(12):2737-2746.

61. Franklin RJ, Bayley SA, Blakemore WF. Transplanted CG4 cells (an oligodendrocyte progenitor cell line) survive, migrate, and contribute to repair of areas of demyelination in X-irradiated and damaged spinal cord but not in normal spinal cord. Exp Neurol. 1996; 137(2):263–76. DOI: 10.1006/exnr.1996.0025 [PubMed: 8635541]

62. Hinks GL, Chari DM, O'Leary MT, Zhao C, Keirstead HS, Blakemore WF, et al. Depletion of endogenous oligodendrocyte progenitors rather than increased availability of survival factors is a likely explanation for enhanced survival of transplanted oligodendrocyte progenitors in X-irradiated compared to normal CNS. Neuropathol Appl Neurobiol. 2001; 27(1):59–67. [PubMed: 11299003]

63. Niranjan A, Fellows W, Stauffer W, Burton EA, Hong CS, Lunsford LD, et al. Survival of transplanted neural progenitor cells enhanced by brain irradiation. J Neurosurg. 2007; 107(2):383–91. DOI: 10.3171/JNS-07/08/0383 [PubMed: 17695394]

64. Marshall GP 2nd, Scott EW, Zheng T, Laywell ED, Steindler DA. Ionizing radiation enhances the engraftment of transplanted in vitro-derived multipotent astrocytic stem cells. Stem Cells. 2005; 23(9):1276–85. DOI: 10.1634/stemcells.2005-0073 [PubMed: 16051984]

65. Rezvani M, Birds DA, Hodges H, Hopewell JW, Milledew K, Wilkinson JH. Modification of radiation myelopathy by the transplantation of neural stem cells in the rat. Radiat Res. 2001; 156(4):408–12. [PubMed: 11554852]

66. Chari DM, Gilson JM, Franklin RJ, Blakemore WF. Oligodendrocyte progenitor cell (OPC) transplantation is unlikely to offer a means of preventing X-irradiation induced damage in the

CNS. Exp Neurol. 2006; 198(1):145–53. S0014-4886(05)00426-7 [pii]. DOI: 10.1016/j.expneurol.2005.11.023 [PubMed: 16410004]

67. Piao J, Major T, Auyeung G, Policarpio E, Menon J, Droms L, et al. Human embryonic stem cell-derived oligodendrocyte progenitors remyelinate the brain and rescue behavioral deficits following radiation. Cell Stem Cell. 2015; 16(2):198–210. DOI: 10.1016/j.stem.2015.01.004 [PubMed: 25658373]

68. Joo KM, Jin J, Kang BG, Lee SJ, Kim KH, Yang H, et al. Trans-differentiation of neural stem cells: a therapeutic mechanism against the radiation induced brain damage. PLoS One. 2012; 7(2):e25936. DOI: 10.1371/journal.pone.0025936 [PubMed: 22347993]

69. Belkind-Gerson J, Hotta R, Whalen M, Nayyar N, Nagy N, Cheng L, et al. Engraftment of enteric neural progenitor cells into the injured adult brain. BMC Neurosci. 2016; 17:5.doi: 10.1186/s12868-016-0238-y [PubMed: 26810757]

70. Osman AM, Zhou K, Zhu C, Blomgren K. Transplantation of enteric neural stem/progenitor cells into the irradiated young mouse hippocampus. Cell Transplant. 2014; 23(12):1657–71. DOI: 10.3727/096368913X674648 [PubMed: 24152680]

71. Sato Y, Shinjyo N, Sato M, Osato K, Zhu C, Pekna M, et al. Grafting of neural stem and progenitor cells to the hippocampus of young, irradiated mice causes gliosis and disrupts the granule cell layer. Cell Death Dis. 2013; 4:e591.doi: 10.1038/cddis.2013.92 [PubMed: 23598403]

72. Makale MT, McDonald CR, Hattangadi-Gluth JA, Kesari S. Mechanisms of radiotherapy-associated cognitive disability in patients with brain tumours. Nat Rev Neurol. 2017;13:52-64.

73. Acharya MM, Lan ML, Kan VH, et al. Consequences of ionizing radiation-induced damage in human neural stem cells. Free Radic Biol Med. 2010;49:1846-1855.

74. Thery C, Amigorena S, Raposo G, Clayton A. Isolation and characterization of exosomes from cell culture supernatants and biological fluids. Curr Protoc Cell Biol. 2006;Chapter 3(Unit 3):22.

75. Parihar VK, Allen BD, Caressi C, et al. Cosmic radiation exposure and persistent cognitive dysfunction. Sci Rep. 2016;6:34774.

76. Parihar VK, Allen B, Tran KK, et al. What happens to your brain on the way to Mars. Sci Adv. 2015;1:e1400256.

77. Tofilon PJ, Fike JR. The radioresponse of the central nervous system: a dynamic process. Radiat Res. 2000;153:357-370.

78. Parihar VK, Pasha J, Tran KK, Craver BM, Acharya MM, Limoli CL. Persistent changes in neuronal structure and synaptic plasticity caused by proton irradiation. Brain Struct Funct. 2015;220:1161-1171.

79. Chakraborti A, Allen A, Allen B, Rosi S, Fike JR. Cranial irradiation alters dendritic spine density and morphology in the hippocampus. PLoS One. 2012;7:e40844.

80. Allen AR, Raber J, Chakraborti A, Sharma S, Fike JR. (56)Fe irradiation alters spine density and dendritic complexity in the mouse hippocampus. Radiat Res. 2015;184:586-594.

81. Chmielewski NN, Caressi C, Giedzinski E, Parihar VK, Limoli CL. Contrasting the effects of proton irradiation on dendritic complexity of subiculum neurons in wild type and MCAT mice. Environ Mol Mutagen. 2016;57:364-371.

82. Kalani A, Tyagi A, Tyagi N. Exosomes: mediators of neurodegeneration, neuroprotection and therapeutics. Mol Neurobiol. 2014;49:590-600.

83. Marsh SE, Blurton-Jones M. Neural stem cell therapy for neurodegenerative disorders: the role of neurotrophic support. Neurochem Int. 2017;106:94-100.

84. Kust N, Panteleev D, Mertsalov I, et al. Availability of pre- and proregions of transgenic GDNF affects the ability to induce axonal sprout growth. Mol Neurobiol. 2015;51:1195-1205.

85. Curcio M, Salazar IL, Inacio AR, Duarte EP, Canzoniero LM, Duarte CB. Brain ischemia downregulates the neuroprotective GDNF-Ret signaling by a calpain-dependent mechanism in cultured hippocampal neurons. Cell Death Dis. 2015;6:e1645.

86. Hofer HR, Tuan RS. Secreted trophic factors of mesenchymal stem cells support neurovascular and musculoskeletal therapies. Stem Cell Res Ther. 2016;7:131.

87. Zhao Y, Haney MJ, Gupta R, et al. GDNF-transfected macrophages produce potent neuroprotective effects in Parkinson's disease mouse model. PLoS One. 2014;9:e106867.

88. Berry KP, Nedivi E. Spine dynamics: Are they all the same? Neuron. 2017;96:43-55.

89. Ekdahl CT, Kokaia Z, Lindvall O. Brain inflammation and adult neurogenesis: the dual role ofmicroglia. Neuroscience. 2009;158:1021-1029.

90. Ransohoff RM, Brown MA. Innate immunity in the central nervous system. J Clin Invest. 2012;122:1164-1171.

91. Ransohoff RM. How neuroinflammation contributes to neurodegeneration. Science. 2016;353:777-783.

92. Chiang CS, Hong JH, Stalder A, Sun JR, Withers HR, McBride WH. Delayed molecular responses to brain irradiation. Int J Radiat Biol. 1997;72:45-53.

93. Schaue D, Micewicz ED, Ratikan JA, Xie MW, Cheng G, McBride WH. Radiation and inflammation. Semin Radiat Oncol. 2015;25:4-10.

94. Acharya MM, Green KN, Allen BD, et al. Elimination of microglia improves cognitive function following cranial irradiation. Sci Rep. 2016;6:31545.

95. Zhang J, Stevens MF, Bradshaw TD. Temozolomide: mechanisms of action, repair and resistance. Curr Mol Pharmacol. 2012 Jan;5(1):102-14. doi: 10.2174/1874467211205010102. PMID: 22122467.

96. Nguyen LD, Ehrlich BE. Cellular mechanisms and treatments for chemobrain: insight from aging and neurodegenerative diseases. EMBO Mol Med. 2020 Jun 8;12(6):e12075. doi: 10.15252/emmm.202012075. Epub 2020 Apr 29. PMID: 32346964; PMCID: PMC7278555.

97. Leavitt RJ, Acharya MM, Baulch JE, Limoli CL. Extracellular Vesicle-Derived miR-124 Resolves Radiation-Induced Brain Injury. Cancer Res. 2020 Oct 1;80(19):4266-4277. doi: 10.1158/0008-5472.CAN-20-1599. Epub 2020 Aug 19. PMID: 32816912; PMCID: PMC7541572.

98. Aznar S., Qian Z., Shah R., Rahbek B., Knudsen G. M. The 5-HT_{1A} serotonin receptor is located on calbindin- and parvalbumin-containing neurons in the rat brain. Brain Res. 2003;959 58–67. 10.1016/S0006-8993(02)03727-7.

99. Staroń J., Bugno R., Hogendorf A., Bojarski A. 5-HT_{1A} receptor ligands and their therapeutic applications: review of new patents. Expert Opinion on Therapeutic Patents. 2018; 28:9, 679-689, DOI: 10.1080/13543776.2018.1514011.

100. Colombo M, Raposo G, Théry C. Biogenesis, secretion, and intercellular interactions of exosomes and other extracellular vesicles. Annu Rev Cell Dev Biol. 2014;30:255–289.

101. Montay-Gruel P, Zhu Y, Petit B, Leavitt R, Warn M, Giedzinski E, Ollivier J, Sinclair DA, Vozenin MC, Limoli CL. Extracellular Vesicles for the Treatment of Radiation-Induced Normal Tissue Toxicity in the Lung. Front Oncol. 2021 Mar 2;10:602763. doi: 10.3389/fonc.2020.602763. PMID: 33738245; PMCID: PMC7962869.